THERMAL AND DIELECTRIC BEHAVIOUR OF POLYMER COMPOSITES WITH HYBRID FILLERS

A THESIS SUBMITTED IN PARTIAL FULFILLMENT OF THE REQUIREMENTS FOR THE DEGREE OF

Doctor of Philosophy

In

Mechanical Engineering

By

ALOK AGRAWAL

Roll No. 511 ME 124

Under the supervision of

Prof. Alok Satapathy

Department of Mechanical Engineering
National Institute of Technology
Rourkela

DEPARTMENT OF MECHANICAL ENGINEERING
National Institute of Technology
Rourkela (India)

2015

Dedicated To

My Beloved Grandmother

National Institute of Technology
Rourkela

C E R T I F I C A T E

This is to certify that the thesis entitled ***Thermal and Dielectric Behaviour of Polymer Composites with Hybrid Fillers*** submitted by **ALOK AGRAWAL** to National Institute of Technology, Rourkela for the award of the degree of **Doctor of Philosophy** in *Mechanical Engineering* is an authentic record of research work carried out by him under my guidance and supervision.

The work incorporated in this thesis has not been, to the best of my knowledge, submitted to any other University or Institute for the award of a degree or diploma.

Date:

Place: Rourkela

Prof. Alok Satapathy
Associate Professor
Department of Mechanical Engineering,
National Institute of Technology
Rourkela

ACKNOWLEDGEMENT

First of all, I would like to thank the almighty God, the Creator and the Guardian, to whom I owe my very existence. I am grateful to God for giving me strength that keeps me standing and for the hope that keeps me believe that this study would be possible. I thank God for reasons too numerous to mention.

My most earnest acknowledgment must go to my guide **Prof. Alok Satapathy** who has been instrumental in ensuring my academic, professional and moral well-being ever since. His profound knowledge and insights, dedication to research, enthusiasm for work, have been and will continue to be a great source of inspiration for me. Apart from the academic and technical training received from him, other important qualities and skills like self-motivation, time management and leadership will always benefit me in my future career and life. Above all, throughout my tenure, I got the much needed parental love from **Prof. Alok Satapathy** and **Mrs. Susmita Satapathy** who also taught me the most important lesson of my life to grow into a good human being.

I would like to express my sincere gratitude to the Head of the Department of Mechanical Engineering **Prof. S. S. Mahapatra** for his timely help during the entire course of my research work. I also sincerely thank **Prof. S.K. Sarangi**, honorable Director, NIT Rourkela for being a steady source of inspiration and encouragement for me.

I would also take this opportunity to thank my friend **Gaurav** who played a major role in this inning of my life right from the beginning. I owe a lot to my friend **Saurabh** who encouraged and supported me a lot during last three years. I am extremely thankful to my co-researchers **Abhishek, Vivek, Alok, Pravat, Debasmita, Madhusmita, Mimosha, Somen, Johan and Yagya** for helping me in every way they could and for making the past few years more delightful.

I would like to express my deepest gratitude to my family. My parents, my in-laws, brother and sisters, I thank you for the unparalleled love and care I always get from you and for being a constant source of endless inspiration and support for me in one way or the other. Last but not least, the most special thanks belong to my wife ***Rashi***, for her understanding about my leaving during all these years, selfless love and support all along and encouragement and company during the preparation of this thesis.

Date:

Place: Rourkela

Alok Agrawal
(Research Scholar)
Roll No. 511 ME 124
Dept. of Mechanical Engineering
National Institute of Technology
Rourkela

List of Figures

*****

List of Tables

*****

ABSTRACT

This thesis reports on the analytical and experimental study on thermal and dielectric behaviour of hybrid filler polymer composites. The objective is to explore the possibility of using multiple ceramic fillers in polymers to make composites suitable for microelectronic applications. The first part of the report is on the development of theoretical heat conduction models based on which mathematical correlations have been proposed for estimation of effective thermal conductivity of polymer composites with single as well as hybrid fillers. The second part has provided the description of the materials used, routes adopted to fabricate the various epoxy and polypropylene composites and the details of the experiments that are conducted during this research. It also presents the test results in regard to the physical, micro-structural and mechanical characteristics of all the epoxy and polypropylene based composites filled with single filler i.e. micro-sized Aluminium nitride (AlN)/ Aluminium oxide (Al_2O_3). A comparative evaluation of the effects of premixing of solid glass microspheres with micro-sized AlN/Al_2O_3 on the different physical and mechanical properties of composite systems is also reported. The last part has emphasized on the thermal and dielectric characteristics of the composites under this investigation. It includes an assessment of the effective thermal conductivity of these composites using the proposed theoretical models. Effects of inclusion of various combinations of single/hybrid fillers on the effective thermal conductivity (k_{eff}), glass transition temperature (T_g), coefficient of thermal expansion (CTE) and dielectric constant (ε_c) of the composites are presented.

Analytical models developed in this work for evaluating effective thermal conductivity of single/hybrid filler reinforced polymer composites are based on the principle of law of minimal thermal resistance and equal law of specific equivalent thermal conductivity. The values obtained from the theoretical model for single filler polymer composites are in close approximation with the corresponding measured values up to percolation threshold. For hybrid filler model, the calculated values are in good approximation for the entire range of filler content as no percolation is seen for hybrid composites. Percolation is the phenomenon which occurs when the content of conductive filler in matrix becomes substantially high so as to form thermal bridges across the planes throughout the system resulting in a sudden improvement of conductivity. The volume fraction of filler at which sudden jump in the composite effective thermal conductivity occurs is called the percolation threshold of that filler-matrix

combination. This phenomenon however has not occurred for hybrid filler composites.

The present research also shows that the selected aluminum based ceramic powders have the potential to be successfully used as functional filler materials in both thermoset and thermoplastic polymers. It is also noticed that the epoxy based composites have higher void fraction compared to that in the polypropylene based composites. Inclusion of spherical particles in these polymeric resins has not resulted in any improvement in the load bearing capacity (tensile strength). On the other hand, hardness and compressive strength values have been found to have improved invariably for all the composites.

Inclusion of single filler i.e. micro-sized AlN/Al_2O_3 appreciably enhances the effective thermal conductivity of polymers. Other thermal properties like CTE and Tg also get modified accordingly. But, with addition of these fillers, little increase in the value dielectric constant is noted. The polymer composite fabricated in present work must possess low dielectric constant which does not get completely fulfilled with single fillers. So SGM is introduced as a secondary filler to overcome this problem. With the addition of SGM in combination with AlN/Al_2O_3 modifies various physical, mechanical and thermal properties. But most importantly, a noticeable change is observed in case of dielectric constant value. With SGM as the secondary filler, much lower value of dielectric constant is obtained which is almost around that of the neat polymer. It is seen that apart from the effective thermal conductivity, all the other properties shows positive modification for hybrid filler composites as compared to single filler composites as far as their applications in microelectronics are concerned.

The particulate filled polymer composites developed for this investigation are expected to have adequate potential for a wide variety of applications particularly in microelectronic industries. With enhanced thermal conductivity, improved glass transition temperature, reduced thermal expansion coefficient and modified dielectric characteristics, the epoxy and polypropylene composites with appropriate proportions of fillers can be used in microelectronic applications like electronic packaging, encapsulations, printed circuit board substrates etc.

****

CONTENTS

*****

Chapter 1

Introduction

Chapter 1

INTRODUCTION

1.1 Preamble

Moore's Law, the famous prediction states that memory density in electronic components increases fourfold every three years [1]. Integration of large number of components on a single chip reduces the average distance between them which leads to compact devices with improved performance. However, this performance and functions of a chip have come with a hidden cost i.e. heat. The placement of more functions in a smaller package has an inevitable result of higher heat densities. Highly compact devices lead to the fast heating of chips, if not properly cooled. Such overheating reduces the reliability of integrated chips or sometimes may also cause permanent damage. With excessive working temperature, important electrical parameters such as gain, leakages and offset of a device also get changed. It is estimated that leakage currents in circuits often double every 10˚C. If the temperature of an active device increases too much, it will exceed the manufacturer's specifications and will usually fail [2]. The problem also aggravates as the power (voltage and current) increases and so the power gets to be restricted by the heat dissipation. The problem is further compounded by thermal fatigue, which results from cyclic heating and thermal expansion mismatches. Therefore, it is desired to keep the temperature of electronic components below its critical value to avoid any permanent damage. As it is known, the trend in packaging electronic systems has been to reduce size and increase performance. So the future of 3D integrated circuits crucially hinges on the development of practical solutions for heat removal which requires high priority to be given to thermal management in their design to maintain system performance and reliability. Since there is a need of high performance and small size of electronic components, installation of separate heat sinks is not an option anymore. In addition, materials with their coefficients of thermal expansion similar to those of ceramic substrates and semiconductors are

favourable to minimize the thermo-mechanical stresses. Hence, it is desired that the entire packaging of electronic devices must be made out of materials that can simultaneously provide signal distribution, heat dissipation, package protection and power distribution [3]. In other words, this prompts the need to develop advanced monolithic and composite materials that are tailored to meet the specific requirements of the microelectronic components, electronic packaging or other heat management solutions.

1.2 Composite Materials

Composite materials are combination of two or more materials differing in form or composition on a macro-scale. The combining constituents retain their identities i.e. they do not dissolve or merge into each other, although they act in concert. Normally, the components can be physically identified and exhibit an interface between each other. One constituent is called the reinforcing phase and the one in which the reinforcing phase is embedded is called the matrix phase. The primary functions of the matrix are to transfer stresses between the reinforcing fibers/particles and to protect them from mechanical and/or environmental damage whereas the presence of fibers/particles in a composite improves its various properties. A composite may also be defined as a material system composed of two or more physically distinct phases whose combination produces aggregate properties that are different from those of its constituents.The objective is to take advantage of the superior properties of both materials without compromising on the weakness of either [3].

Composites have successfully substituted the traditional materials in several light weight and high strength applications. The reasons why composites are selected for such applications are mainly their high strength-to-weight ratio, tensile strength at elevated temperatures, creep resistance and toughness. If the composite is designed and fabricated correctly it combines the strength of the reinforcement with the toughness of the matrix to achieve a combination of desirable properties not available in any single conventional material.

Classification of Composites

Composite materials are commonly classified at following two distinct levels:

a) The first level of classification is usually made with respect to the matrix constituent. The major composite classes include metal matrix composites (MMCs), ceramic matrix composites (CMCs) and polymer matrix composites (PMCs).
b) The second level of classification refers to the reinforcement form. The major classes in this level include fiber reinforced composites (FRP) and particulate reinforced composites (PRP).

Metal Matrix Composites:

Metal Matrix Composites have many advantages over monolithic metals like higher specific modulus, higher specific strength, better properties at elevated temperatures and lower coefficient of thermal expansion. Because of these attributes, metal matrix composites are under consideration for wide range of applications viz. combustion chamber nozzle (in rocket, space shuttle), housings, tubing, cables, heat exchangers, structural members etc.

Ceramic Matrix Composites:

Ceramics are materials which exhibit very strong ionic bonding and in few cases covalent bonding. High melting points, good corrosion resistance, stability at elevated temperatures and high compressive strength, render ceramic-based matrix materials a favourite for applications requiring a structural material. Also ceramic matrices are the obvious choice for high temperature applications that doesn't give way at temperatures above 1500ºC.

Polymer Matrix Composites:

Polymers make ideal materials as they possess lightweight. Most commonly used matrix materials are polymeric. The reasons for this are two-fold. In general, the mechanical properties of polymers are inadequate for many structural purposes; particularly their strength and stiffness compared to metals and ceramics. Also polymers possess very low value of thermal conductivity.

These difficulties are overcome by reinforcing other materials in polymers. Secondly, the processing of polymer matrix composites need not involve high pressure and temperature. Also, equipment required for manufacturing polymer matrix composites are simpler. They have a greater elastic modulus than the neat polymer and are not as brittle as ceramics.

Fiber Reinforced Composites:

Common fiber reinforced composites are composed of fibers and a matrix. Fibers are considered as important classes of reinforcement, as they satisfy the desired conditions and transfer strength to the matrix constituent influencing and enhancing their properties as desired. Fibers are the main source of strength while matrix glues all the fibers together in shape and transfers stresses between the reinforcing fibers. The performance of a fiber composite is judged by its length, shape, orientation and composition and the properties of the matrix.

Particle Reinforced Composites:

Microstructures of composites, which show particles of one phase strewn in the other, are known as particle reinforced composites. Particles are considered as another important class of reinforcement material. Particles include ceramics, small mineral particles, metal powders such as aluminium and amorphous materials including polymers and carbon black. These are used to increase the modulus and to decrease the ductility of the matrix and often the cost of the composites. The benefits offered by particulate fillers also include increased thermal resistance, stability, abrasion resistance etc. The filler particles may be irregular structures or have precise geometrical shapes.

1.3 Introduction to the Research Topic

From the beginning, composite materials are traditionally designed for making structural components. But with the rapid growth of the electronics industry, the composites start to find their electronic applications as well. The requirements of properties of composites for structural applications are different from those for electronic applications. So the criteria for designing these composites are also

entirely different. While structural composites concentrate on obtaining high strength value, electronic composites emphasize on obtaining high thermal conductivity, low coefficient of thermal expansion, low dielectric constant and high/low electrical conductivity depending on the application. Moreover the cost of materials tends to be of less concern for electronic composites due to small size of its parts than structural composites whose processability is mainly for large parts like panels, aerospace bodies etc. Apart from that, low density is very much desirable for both the above types of composite system.

Current research is being conducted on composite material that can be used for microelectronic applications. For these applications, high thermal conductivity and low dielectric constant are the most important requirements when selecting materials. Most metal matrix composites and ceramic matrix composites are thermally conductive but are electrically conductive as well, which may not be suitable for electronic packaging application due to the possibility of having short-circuits. So the present research has been focused on developing a third type of composites, which are polymer matrix composites, where polymers are embedded with thermally conductive and electrically insulative particulate fillers. PMCs have a number of advantages, including their low mass-density and the ability to be moulded into complex shapes with tight tolerances, eliminating the need for further machining that are often required with metal-cast parts.

The applications of polymer matrix composites in microelectronics include printed circuit boards, substrate, interconnection, interlayer dielectrics, die attach, encapsulations, lid, heat sinks, electrical contacts, connectors, thermal interface material and housings [4]. These require materials having high thermal conductivities, low coefficient of thermal expansion, light weight, lower dielectric constant, high compressive strength, increased reliability and good manufacturability.

Metallic and carbon-based fillers are highly conductive thermally, but they are electrically conductive as well. So they are not considered as an ideal reinforcing candidate for microelectronic applications. Ceramic powder reinforced polymer materials have been used extensively for such applications because of their high thermal and low electrical conductivity. Addition of ceramic filler successfully enhances the heat conduction in polymers but increase in dielectric constant of such composite is also reported [5]. Though this increase is very less as compared to the increase of heat conduction, but for microelectronic applications it may be hazardous. It seems that single filler alone cannot improve the thermal conductivity and decrease the dielectric constant of the composite simultaneously. So the incorporation of multiple fillers in terms of a combination of fillers with high thermal conductivity and low dielectric constant in polymer matrix is suggested which gives rise to the development of hybrid filler composites.

A hybrid composite is defined as a multi-component composite system, consisting of a matrix phase reinforced with more than one filler not similar in all respect. In other words, the use of two or more reinforcement in a polymeric matrix or the use of multiple matrices leads to the formation of hybrid polymeric matrix composites. Hybridization provides better tuning compatibility to get desired properties in comparison with their mono-reinforcement counterparts. This is expected as hybridization provides additional degrees of freedom to the designer in designing composite materials because of contrasting properties of additional filler material [6]. However, the characteristics of hybrid composites are governed by a more complex behaviour of the interfacial properties and lay-up design.

Against this background, an attempt has been made in this research work to develop a new class of composites which can be successfully used for microelectronic applications.

1.4 Thesis Outline

The remainder of this thesis is organized as follows:

Chapter 2

This chapter includes a literature review designed to provide a summary of the base of knowledge already available involving the issues of interest. It presents the research works on various analytical models as well as for particulate reinforced polymer composites with emphasis on their thermal and dielectric behaviour reported by previous investigators.

Chapter 3

This chapter presents the development of theoretical models for estimation of effective thermal conductivity of particulate filled polymer composites with single as well as multiple fillers.

Chapter 4

This chapter includes a description of the raw materials used and the test procedures followed. It presents the details of fabrication and characterization of the composites under investigation.

Chapter 5

This chapter presents the test results in regard to the physical, micro-structural and mechanical characteristics of the composites under study.

Chapter 6

This chapter presents the thermal and dielectric properties of epoxy based composites with single as well as with hybrid fillers.

Chapter 7

This chapter presents the thermal and dielectric properties of polypropylene based composites with single as well as with hybrid fillers.

Chapter 8

Provides summary of the research findings, outlines specific conclusions drawn from both the experimental and analytical efforts and suggests ideas and directions for future research.

*****

1. Development of theoretical models for estimation of effective thermal conductivity of polymer composites with single and hybrid fillers.
2. Fabrication of different sets of single filler epoxy and polypropylene composites filled with micro-sized AlN and Al_2O_3 particles.
3. Similar fabrication of different sets of hybrid filler epoxy and polypropylene composites filled with micro-sized AlN or Al_2O_3 particles premixed with SGM.
4. Validation of the proposed models by experimental determination of the effective thermal conductivities of all the fabricated samples.
5. Physical, mechanical and micro-structural characterization of all single and hybrid filler composites under this study.
6. Study the effects of fillers on properties like glass transition temperature, coefficient of thermal expansion and dielectric constant of these composites and exploring the possibility of their use in micro-electronics applications.

Chapter Summary

This chapter has provided

- An exhaustive review of research works on various aspects of particulate filled polymer composites reported by previous investigators
- The knowledge gap in earlier investigations
- The objectives of the present work

The next chapter presents the development of two theoretical models to estimate the effective thermal conductivity of polymer composites filled with single and hybrid fillers.

*****

Chapter 3

Development of Theoretical Models for Effective Thermal Conductivity of Polymer Composites

Chapter 3

DEVELOPMENT OF THEORETICAL MODELS FOR EFFECTIVE THERMAL CONDUCTIVITY OF POLYMER COMPOSITES

This chapter presents the development of theoretical models for estimating the effective thermal conductivity of polymer composites filled with one and more than one type of particulate fillers. It also gives an overview of the principles used for deriving the correlation for estimating the effective thermal conductivity of particulate filled polymer composites.

3.1 Basic principles

Law of minimal thermal resistance and equal law of specific equivalent thermal conductivity:

In a heterogeneous system, heat conduction takes place along the path that offers minimum thermal resistance. On the basis of law of minimal thermal resistance and equal law of specific equivalent thermal conductivity, when only one mode of heat transfer is considered, i.e. heat conduction, and specific equivalent thermal resistance of single element of the composite is considered equal to the total thermal resistance of the composite. And the equivalent thermal conductivity of that single element is considered equal to the total thermal conductivity of the composite. So by following the above laws, once the equivalent thermal conductivity of small single element is calculated, the effective thermal conductivity of the complete system can be estimated.

3.2 Development of theoretical model: for single filler

3.2.1 Nomenclature

The following symbols are used for the development of theoretical model for estimation of effective thermal conductivity of single filler reinforced polymer composites:

H	side length of the cubical element under study
R	radius of the spherical filler
k_p	intrinsic thermal conductivity of polymer phase
k_f	intrinsic thermal conductivity of filler phase
S	cross-sectional area of element under study in the direction of heat flow
S_p	cross-sectional area of polymer phase in the direction of heat flow
S_f	cross-sectional area of filler phase in the direction of heat flow
Q	quantity of heat flow through the cross sectional area of the element under
Q_p	quantity of heat flow through the cross sectional area of polymer phase
Q_f	quantity of heat flow through the cross sectional area of filler phase
V_c	volume of element under study
V_p	volume of polymer phase
V_f	volume of filler phase
h_1,h_2,h_3	height of part 1,2 and 3 respectively of the element under study
k_1, k_2,k_3	thermal conductivity of part 1,2 and 3 respectively of the element under study
R	total thermal resistance of the element under study
R_1, R_2,R_3	thermal resistance of part 1, 2 and 3 respectively of the element under study
Φ_f	volume fraction of the filler in the matrix
ΔT	temperature difference along the direction of heat flow
k_{eff}	effective thermal conductivity of element under study

3.2.2 Model development

From the literature, it is clear that the most effective way to enhance heat conduction behaviour of a polymer is by incorporating thermally conductive fillers into it. Inclusion of insoluble solid particles in a polymer gives rise to the formation of a heterogeneous material system i.e. a composite. Study on analytical evaluation of effective thermal conductivity of such composite material is less compared to its experimental counterparts. However, as stated, the factors affecting the effective thermal conductivity and heat transfer in polymer composites are relatively more, such as nature of resin, the shape, size and content of particles as well as the dispersion and distribution pattern of the fillers in the matrix. Therefore, a thorough research into the heat transfer process, mechanisms and their quantitative description is mandatory. The proposed model addresses these in an effective manner for estimating the effective thermal conductivity of composite material with a wide range of filler concentration. The development of the model proceeds as follows:

Heat transfer element

Figure 3.1 shows the three-dimensional depiction of particulate filled composite where spherical filler particles are embedded inside a cubical arrangement and a single element with a single filler surrounded by matrix as shown in Figure 3.2 is chosen from it for further analysis of heat transfer mechanism. Figure 3.3 shows the front view of the element under study in which heat flow enters into the element from top of the square.

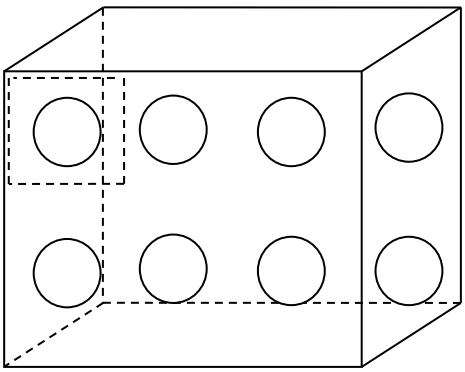

Fig 3.1 3-Dimensional view of single filler composite

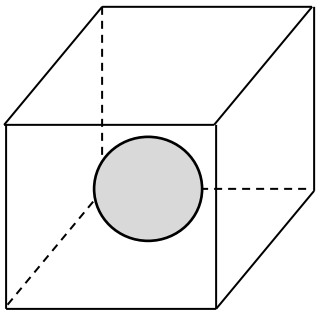

Fig 3.2 3-Dimensional view of anelement under study

As the filler material is spherical in shape, for convenience, only the case of spherical inclusions is considered in the matrix. From the element under study, expression for filler volume fraction can be expressed as follows:

$$\phi_f = \frac{V_f}{V_S} = \frac{4\pi r^3}{3H^3} \tag{3.1}$$

In present study, theoretical analysis of heat transfer in composite material is based on the following assumptions:

(a) The solid spherical fillers are evenly distributed in the polymer matrix;

(b) Locally both the matrix and fillers are homogeneous and isotropic;

(c) The thermal contact resistance between the filler and the matrix is negligible;

(d) The composite body is free from voids and

(e) The temperature distribution along the direction of heat flow is linear.

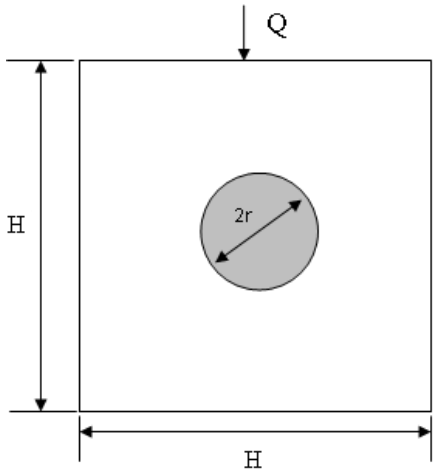

Fig 3.3 Front view of heat transfer model for single filler composite

Heat transfer modelling

The thermal property of a body depends on the path followed by the heat while getting transferred in the materials. A series model of heat conduction through the unit cell of particulate filled polymer composite is considered as shown in Figure 3.4. The element is divided into three parts, part I and part III represents the neat polymer while part II represent the combination of polymer matrix and filler particle. k_1, k_2 and k_3 are the mean conductivity coefficient of respective parts. The thicknesses of part I and part III are h_1 and h_3 respectively and that of part II is h_2. For simplicity, thicknesses of part I and part III are considered to be equal i.e. $h_1 = h_3$. To determine the effective thermal conductivity of the entire element, the law of minimum thermal resistance and the equal law of specific thermal conductivity are followed.

The heat transport in solid micro-sphere particle filled polymer composites has two mechanisms: (i) solid thermal conduction and (ii) heat radiation on the surface between neighbouring particles. The heat transfer is occurred mainly by the mode of conduction. The temperature changes more quickly inside the sphere than outside the sphere. Polymer composite works usually under lower temperature conditions where the proportion of the thermal radiation in the total heat transfer is very small, hence the thermal radiation effect is neglected.

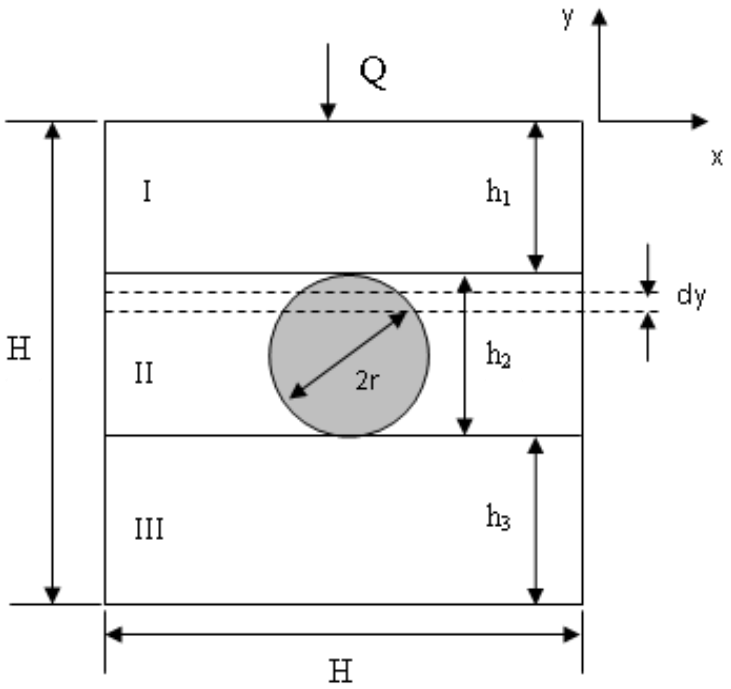

Fig 3.4 A series model of heat transfer for single filler composite

From the Fourier law of heat conduction, heat quantity can be expressed as:

$$Q = kS\frac{\Delta T}{dx} = \frac{\Delta T}{dx/kS} \tag{3.2}$$

And the thermal resistance is expressed as:

$$R = \frac{dx}{kS} \tag{3.3}$$

where *dx* is the length of path followed by heat quantity.

As already assumed that the temperature distribution along the direction of heat flow will be linear, thermal conductivity of each section can be calculated as:

For part I and III:

Since, no filler particle is there in this region, thermal conductivity of this region will be the same as that of polymer matrix i.e.

$$k_1 = k_3 = \int_{h_{11}} k_p \frac{dy}{h_1} = k_p \tag{3.4}$$

For part II:

As this section consists of both the phases, its equivalent thermal conductivity is the result of the combined effect of matrix and filler material. Taking a thin elemental piece of thickness *dy* and applying Fourier's law of heat conduction, k_2 is given as:

$$k_2 = \frac{Q_p + Q_f}{\left(\frac{dT}{dy}\right)S} = \frac{k_p S_p}{S} + \frac{k_f S_f}{S} \tag{3.5}$$

Now integrating it over the complete thickness, we get

$$k_2 = \int_{h_2} \frac{\left(k_p S_p / S + k_f S_f / S\right)dy}{h_2} = \frac{1}{h_2 S}\left(k_p V_p + S_f V_f\right) \tag{3.6}$$

Similarly, thermal resistances of the three parts are given as:

$$R_1 = R_3 = \frac{h_1}{k_p S} \tag{3.7}$$

$$R_2 = \frac{h_2}{\frac{1}{h_2 S}\left(k_p V_p + k_f V_f\right)S} = \frac{h_2^2}{k_p V_p + k_f V_f} \tag{3.8}$$

As the series model is considered for heat transfer in the element, the effective thermal conductivity of composites is given by:

$$k_{eff} = \frac{H}{RS} = \frac{H}{\left(R_1 + R_2 + R_3\right)S} \tag{3.9}$$

Substituting equation (3.7) and (3.8) into equation (3.9), we get,

$$k_{eff} = \frac{H}{\left(\frac{h_1}{k_p S} + \frac{h_2^2}{k_p V_p + k_f V_f} + \frac{h_1}{k_p S}\right)S} \tag{3.10}$$

which can be written as:

$$k_{eff} = \frac{H}{\left(\frac{2h_1}{k_p} + \frac{h_2^2 S}{k_p V_p + k_f V_f} \right)} \tag{3.11}$$

From Figure 3.4 it is clear that,

$$h_1 = \frac{H - 2r}{2} \quad , \qquad h_2 = 2r \tag{3.12}$$

Substituting equation (3.12) in equation (3.11), we get

$$k_{eff} = \frac{H}{\frac{2}{k_p}\frac{(H - 2r)}{2} + \frac{4r^2 S}{k_p V_p + k_f V_f}} \tag{3.13}$$

From equation (3.1), H can be written as:

$$H = r\left(\frac{4\pi}{3\phi_f} \right)^{\frac{1}{3}} \tag{3.14}$$

Substituting equation (3.14) in equation (3.13), we get

$$k_{eff} = \frac{r\left(\frac{4\pi}{3\phi_f} \right)^{\frac{1}{3}}}{\frac{r\left(\frac{4\pi}{3\phi_f} \right)^{\frac{1}{3}}}{k_p} - \frac{2r}{k_p} + \frac{4r^2 S}{k_p V_p + k_f V_f}} \tag{3.15}$$

which otherwise can be written as:

$$k_{eff} = \frac{1}{\frac{1}{k_p} - \frac{2}{k_p}\left(\frac{3\phi_f}{4\pi} \right)^{\frac{1}{3}} + \frac{4rS}{\left(\frac{4\pi}{3\phi_f} \right)^{\frac{1}{3}} (k_p V_p + k_f V_f)}} \tag{3.16}$$

As per the assumption that the composite is free from voids,

$$V_c = V_p + V_f \tag{3.17}$$

Deducing it further in known terms, we get,

$$k_{eff} = \frac{1}{\frac{1}{k_p} - \frac{1}{k_p}\left(\frac{6\phi_f}{\pi}\right)^{\frac{1}{3}} + \frac{4rH^2}{\left(\frac{4\pi}{3\phi_f}\right)^{\frac{1}{3}}\left(k_p V_c + V_f\left(k_f - k_p\right)\right)}} \tag{3.18}$$

This can further be written as:

$$k_{eff} = \frac{1}{\frac{1}{k_p} - \frac{1}{k_p}\left(\frac{6\phi_f}{\pi}\right)^{\frac{1}{3}} + \frac{4r^3\left(\frac{4\pi}{3\phi_f}\right)^{\frac{2}{3}}}{\left(\frac{4\pi}{3\phi_f}\right)^{\frac{1}{3}}\left(k_p V_c + V_f\left(k_f - k_p\right)\right)}} \tag{3.19}$$

Putting the expression of respective volume in above equation and rearranging it, the final expression can be written as:

$$k_{eff} = \frac{1}{\frac{1}{k_p} - \frac{1}{k_p}\left(\frac{6\phi_f}{\pi}\right)^{\frac{1}{3}} + \frac{4}{\left(k_p\left(\frac{4\pi}{3\phi_f}\right)^{\frac{2}{3}} + \left(\frac{2\phi_f}{9\pi}\right)^{\frac{1}{3}} 2\pi\left(k_f - k_p\right)\right)}} \tag{3.20}$$

The correlation given in equation (3.20) gives the value of the effective thermal conductivity of the composite material filled with single filler (spherical inclusion) in terms of the volume fraction of the filler, its intrinsic thermal conductivity and the conductivity of base matrix. This correlation can be used for estimation of k_{eff} of any single filler polymer composite with similar structural arrangement.

3.3 Development of theoretical model: for hybrid fillers

3.3.1 Nomenclature

The following symbols are used for the development of a theoretical model for estimation of effective thermal conductivity of multi filler reinforced polymer composites:

H	side length of the cuboidal element perpendicular to the direction of heat flow
$2H$	side length of the cuboidal element in the direction of heat flow
r_a , r_b	radius of the spherical filler 1 and 2 respectively
k_p	thermal conductivity of polymer phase
k_a , k_b	thermal conductivity of filler 1 and 2 respectively
S	cross-sectional area of element under study in the direction of heat flow
S_p	cross-sectional area of polymer phase in the direction of heat flow
S_a, S_b	cross-sectional area of filler 1 and 2 respectively in the direction of heat flow
Q	heat quantity flow through the cross sectional area of the element under study
Q_p	heat quantity flow through the cross sectional area of polymer phase
Q_a, Q_b	heat quantity flow through the cross sectional area of filler 1 and 2 respectively
V_c	volume of element under study
V_p	volume of polymer phase
V_a, V_b	volume of filler 1 and 2 respectively
h_1,h_2,h_4,h_4	height of part 1,2 and 3 respectively of the element under study
k_1,k_2,k_3, k_4	thermal conductivity of part 1,2 and 3 respectively of the element under study
R	total thermal resistance of the element under study
R_1, R_2,R_3, R_4	thermal resistance of part 1, 2 and 3 respectively of the element under study
Φ_a, Φ_b	volume fraction of the filler 1 and 2 respectively in the matrix
ΔT	temperature difference along the direction of heat flow
k_{eff}	effective thermal conductivity of the element under study

3.3.2 Model development

From the literature it is clear that all the models proposed in the past are applicable for determination of effective thermal conductivity of polymer based composites with single filler only and no work has so far been reported on developing a theoretical model for hybrid filler composites. It has been seen earlier that incorporation of single filler will not always be able to fulfill the desired property for some applications which necessitates reinforcing of more

than one filler (hybrid fillers) into the matrix body. Consequently, it becomes mandatory to make a thorough research into the heat conduction mechanism within such hybrid composites. The proposed model addresses these in an effective manner for estimating the effective thermal conductivity of composite material for a wide range of hybrid filler concentration.

Heat transfer element

Figure 3.5 shows the three-dimensional view of a particulate filled composite where two spherical filler particles are embedded inside a cubical arrangement and a single cuboidal element with two different fillers surrounded by matrix as shown in Figure 3.6 is chosen from it for further analysis of heat transfer mechanism. Figure 3.7 shows the front view of the element under study in which heat flows into the element from top of the element as indicated by arrow.

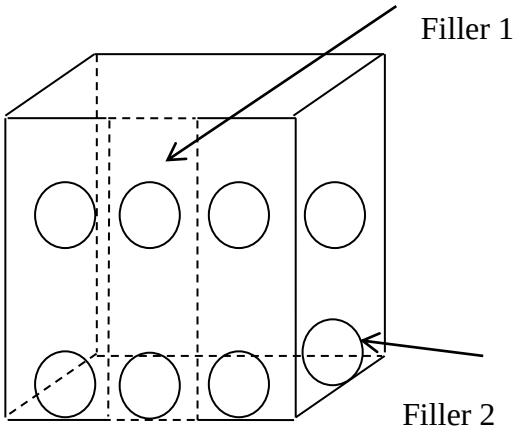

Fig 3.5 3-Dimensional view of hybrid filler composite

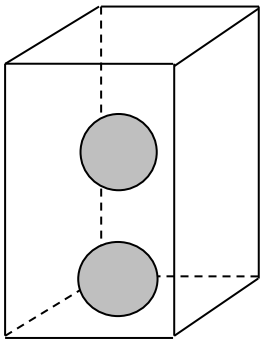

Fig 3.6 3-Dimensional view of anelement under study

From the element under study, expression for filler volume fraction can be expressed as follows:

For filler 1:

$$\phi_a = \frac{V_a}{V_S} = \frac{4\pi r_a^{\,3}}{3 \times 2H^{\,3}} \qquad (3.21)$$

For filler 2:

$$\phi_b = \frac{V_b}{V_S} = \frac{4\pi r_b^{\,3}}{3 \times 2H^{\,3}} \tag{3.22}$$

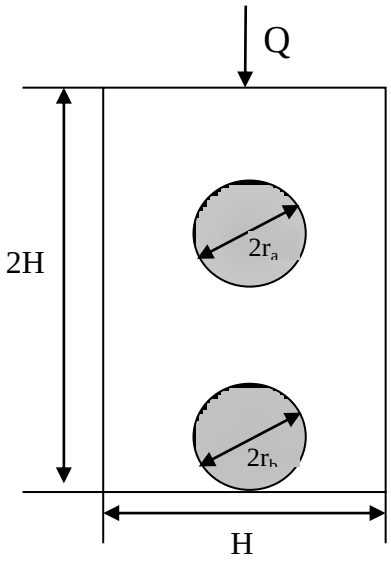

Fig 3.7 Front view of heat transfer model for hybrid filler composite

The assumptions taken to derive the mathematical correlation for estimating the effective thermal conductivity for hybrid filler reinforced polymer composite are same as those taken for single filler reinforced polymer composites.

Heat transfer modelling

A series model of heat conduction through the unit cell of hybrid particulate filled polymer composite is considered as shown in Figure 3.8. The element is divided into four parts, part I and part III represent the neat polymer while part II and part IV represent the combination of polymer matrix and two different spherical filler in section A and B respectively. k_1, k_2, $k_3$and k_4 are the mean conductivity coefficients of the respective parts. The thicknesses of part I and part III are h_1 and h_3 respectively, where $h_1=H-2r_a$and $h_3 = H-2r_b$. Part II and Part IV are having thicknesses of $h_2 = 2r_a$and $h_4 = 2r_b$ respectively. To determine the effective thermal conductivity of the entire element, law of minimum thermal resistance and the equal law of specific thermal conductivity are followed.

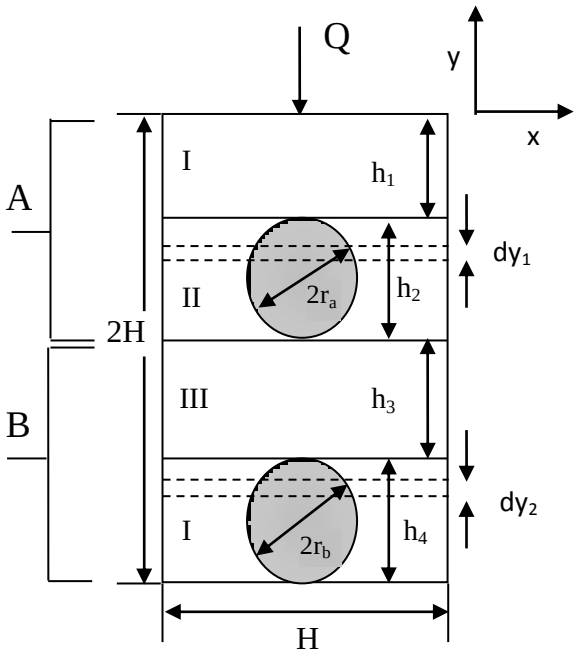

Fig 3.8 A series model of heat transfer in hybrid filler composite

Again, the thermal radiation effect is neglected and heat transport is considered only because of solid thermal conduction. Also, based on the assumptions, thermal conductivity of each section can be calculated as follows:

For part I and III:

Since there is no filler present, thermal conductivity of these parts will be same as that of polymer matrix i.e.

$$k_1 = k_3 = \int_{h1} k_p \frac{dy}{h_1} = k_p \qquad (3.23)$$

For part II and IV:

Taking a thin piece of thickness dy_1 and dy_2, applying Fourier's law of heat conduction, $k_2$and $k_4$are given as:

For Part II

$$k_2 = \frac{Q_p + Q_a}{\left(\frac{dT}{dy}\right)S} = \frac{k_p S_p}{S} + \frac{k_a S_a}{S} \qquad (3.24)$$

For Part IV

$$k_4 = \frac{Q_p + Q_b}{\left(\frac{dT}{dy}\right)S} = \frac{k_p S_p}{S} + \frac{k_b S_b}{S} \tag{3.25}$$

Integrating equation (3.24) and (3.25) over the complete thickness, we get

For Part II

$$k_2 = \int_{h_2} \frac{\left(k_p S_p / S + k_a S_a / S\right) dy_1}{h_2} = \frac{1}{h_2 S}\left(k_p V_p + k_a V_a\right) \tag{3.26}$$

For Part IV

$$k_4 = \int_{h_4} \frac{\left(k_p S_p / S + k_b S_b / S\right) dy_2}{h_4} = \frac{1}{h_4 S}\left(k_p V_p + k_b V_b\right) \tag{3.27}$$

Similarly, thermal resistances of the four parts are given as:

$$R_1 = \frac{h_1}{k_p S} \tag{3.28}$$

$$R_2 = \frac{h_2}{\frac{1}{h_2 S}\left(k_p V_p + k_a V_a\right)S} = \frac{h_2^2}{k_p V_p + k_a V_a} \tag{3.29}$$

$$R_3 = \frac{h_3}{k_p S} \tag{3.30}$$

$$R_4 = \frac{h_4}{\frac{1}{h_4 S}\left(k_p V_p + k_b V_b\right)S} = \frac{h_4^2}{k_p V_p + k_b V_b} \tag{3.31}$$

As the series model is considered for heat transfer in the element, the effective thermal conductivity of composite is given by dividing the element into two parts and calculating its thermal conductivity individually and then combining them assuming a series connection.

For part A:

$$k_{eff\ 1} = \frac{H}{RS} = \frac{H}{(R_1 + R_2)S} \tag{3.32}$$

For part B:

$$k_{eff\ 2} = \frac{H}{RS} = \frac{H}{(R_3 + R_4)S} \tag{3.33}$$

The effective thermal conductivity of the complete composite system would then be given by:

$$k_{eff} = 2 \times \left(\frac{1}{k_{eff\ 1}} + \frac{1}{k_{eff\ 2}} \right)^{-1} \tag{3.34}$$

For part A:

Substituting equations 3.28 and 3.29 in equation 3.32,

$$k_{eff\ 1} = \frac{H}{\left(\frac{h_1}{k_p S} + \frac{h_2^2}{k_p V_p + k_a V_a} \right) S} \tag{3.35}$$

which can be written as,

$$k_{eff\ 1} = \frac{H}{\left(\frac{h_1}{k_p} + \frac{h_2^2 S}{k_p V_p + k_a V_a} \right)} \tag{3.36}$$

From Figure 3.8 it is clear that,

$$h_1 = \frac{H - 2r_a}{2}, \qquad h_2 = 2r_a \tag{3.37}$$

Substituting equation 3.37 in equation 3.36,

$$k_{eff\ 1} = \frac{H}{\left(\frac{1}{k_p}(H - 2r_a) + \frac{4r_a^2 S}{k_p V_p + k_a V_a} \right)} \tag{3.38}$$

From equation 3.21, H can be written as:

$$H = r_a \left(\frac{2\pi}{3\phi_a} \right)^{\frac{1}{3}} \tag{3.39}$$

Now, substituting equation 3.39 in equation 3.38,

$$k_{eff\ 1} = \frac{r_a \left(\frac{2\pi}{3\phi_a} \right)^{\frac{1}{3}}}{\left(\frac{1}{k_p} r_a \left(\frac{2\pi}{3\phi_a} \right)^{\frac{1}{3}} - \frac{2r_a}{k_p} + \frac{4r_a^2 S}{k_p V_p + k_a V_a} \right)} \tag{3.40}$$

which otherwise can be written as,

$$k_{eff\ 1} = \frac{1}{\left(\frac{1}{k_p} - \frac{2}{k_p} \left(\frac{3\phi_a}{2\pi} \right)^{\frac{1}{3}} + \frac{4r_a S}{\left(\frac{2\pi}{3\phi_a} \right)^{\frac{1}{3}} \left(k_p V_p + k_a V_a \right)} \right)} \tag{3.41}$$

Going by the earlier assumption that the composite is free from voids,

$$V_c = V_p + V_a + V_b \tag{3.42}$$

Deducing it in known terms, we get,

$$k_{eff\ 1} = \frac{1}{\left(\frac{1}{k_p} - \frac{1}{k_p} \left(\frac{12\phi_a}{\pi} \right)^{\frac{1}{3}} + \frac{4r_a H^2}{\left(\frac{2\pi}{3\phi_a} \right)^{\frac{1}{3}} \left(k_p V_{Sa} + V_a \left(k_a - k_p \right) \right)} \right)} \tag{3.43}$$

This can further be written as:

$$k_{eff\ 1} = \frac{1}{\left(\frac{1}{k_p} - \frac{1}{k_p}\left(\frac{12\,\phi_a}{\pi}\right)^{\frac{1}{3}} + \frac{4\,r_a^{\,3}\left(\frac{2\pi}{3\phi_a}\right)^{\frac{2}{3}}}{\left(\frac{2\pi}{3\phi_a}\right)^{\frac{1}{3}}\left(k_p \times V_{sa} + V_a\left(k_a - k_p\right)\right)} \right)} \quad (3.44)$$

Putting the expressions for the respective volume terms in above equation and rearranging it, the final expression for part A can be written as:

$$k_{eff\ 1} = \frac{1}{\left(\frac{1}{k_p} - \frac{1}{k_p}\left(\frac{12\,\phi_a}{\pi}\right)^{\frac{1}{3}} + \frac{2}{\left(k_p\left(\frac{2\pi}{3\phi_a}\right)^{\frac{2}{3}} + \left(\frac{4\phi_a}{9\pi}\right)^{\frac{1}{3}}\pi\left(k_a - k_p\right)\right)} \right)} \quad (3.45)$$

For part B:

By following similar procedure as for part A, the expression for the thermal conductivity of part B can be written as:

$$k_{eff\ 2} = \frac{1}{\left(\frac{1}{k_p} - \frac{1}{k_p}\left(\frac{12\,\phi_b}{\pi}\right)^{\frac{1}{3}} + \frac{2}{\left(k_p\left(\frac{2\pi}{3\phi_b}\right)^{\frac{1}{3}} + \left(\frac{4\phi_b}{9\pi}\right)^{\frac{1}{3}}\pi\left(k_b - k_p\right)\right)} \right)} \quad (3.46)$$

Finally substituting equations 3.45 and 3.46 in equation 3.34,

$$k_{eff} = 2\left[\left(\frac{1}{k_p} - \frac{1}{k_p}\left(\frac{12\phi_a}{\pi}\right)^{\frac{1}{3}} + \frac{2}{\left(k_p\left(\frac{2\pi}{3\phi_a}\right)^{\frac{1}{3}} + \left(\frac{4\phi_a}{9\pi}\right)^{\frac{1}{3}}\pi\left(k_a - k_p\right)\right)}\right) + \left(\frac{1}{k_p} - \frac{1}{k_p}\left(\frac{12\phi_b}{\pi}\right)^{\frac{1}{3}} + \frac{2}{\left(k_p\left(\frac{2\pi}{3\phi_b}\right)^{\frac{1}{3}} + \left(\frac{4\phi_b}{9\pi}\right)^{\frac{1}{3}}\pi\left(k_b - k_p\right)\right)}\right)\right]^{-1}$$

(3.47)

The correlation given in equation (3.47) is thus an expression for k_{eff} of hybrid filler polymer composites in terms of the volume fraction of individual fillers, their respective intrinsic thermal conductivities and the thermal conductivity of the base matrix.

Chapter Summary

This chapter has presented the development of a theoretical model for estimating the effective thermal conductivities of polymer composites filled with one and more than one type of particulate fillers but since, heat transfer within a filled polymer involves complex mechanisms; a simplified theoretical model for such a process may appear inadequate unless its assessment against experimental results is made. So, for the validation of the proposed models, thermal conductivity tests on the composites with various filler concentrations are to be conducted.

The next chapter presents a description of materials used for fabricating various composites under this study and the details of various characterization tests carried out on them.

*****

Chapter 4

Materials and Experimental Details

Chapter 4

MATERIALS AND EXPERIMENTAL DETAILS

This chapter describes the materials used for processing and characterizing the composites under this investigation. It presents the details of the tests related to the physical, micro-structural, mechanical, thermal and dielectric characterization of the prepared particulate filled polymer composite specimens.

4.1 MATERIALS

4.1.1 Matrix Materials

Polymers are widely employed in our everyday life due to their unique characteristics, such as low density, ease of forming, chemical inertness, low cost and often ductile nature. Polymers are broadly classified into two basic types, namely thermoplastics and thermosets [286]. Each of them has its own individual chemical characteristics based on its molecular structure.

The makeover process from pre-polymer to final polymer represents the line of demarcation separating the thermosets from the thermoplastic polymers. Thermosetting materials are polymers that will undergo, or have undergone, a chemical reaction by the action of heat, a catalyst, leading to a relatively infusible state that will not re-melt after setting. It means that the thermosets can't be recycled. The solidification process of these plastics is known as curing. During the complete process of curing, the small molecules are chemically linked together to form complex inter-connected network structures as shown in Figure 4.1 (a). This cross-linking makes them rigid and prevents the slippage of individual chains making them generally stronger than the thermoplastics. Contrary to this, thermoplastic materials are polymers which are capable of being repeatedly softened or melted by increasing the temperature and solidified by decreasing the temperature. These changes are physical rather than chemical. The molecules are joined end-to-end into a series of long chains, each chain being independent of the other as shown in Figure 4.1 (b). The matrix material

used in present research work is a thermoset i.e. epoxy and a thermoplastic i.e. polypropylene.

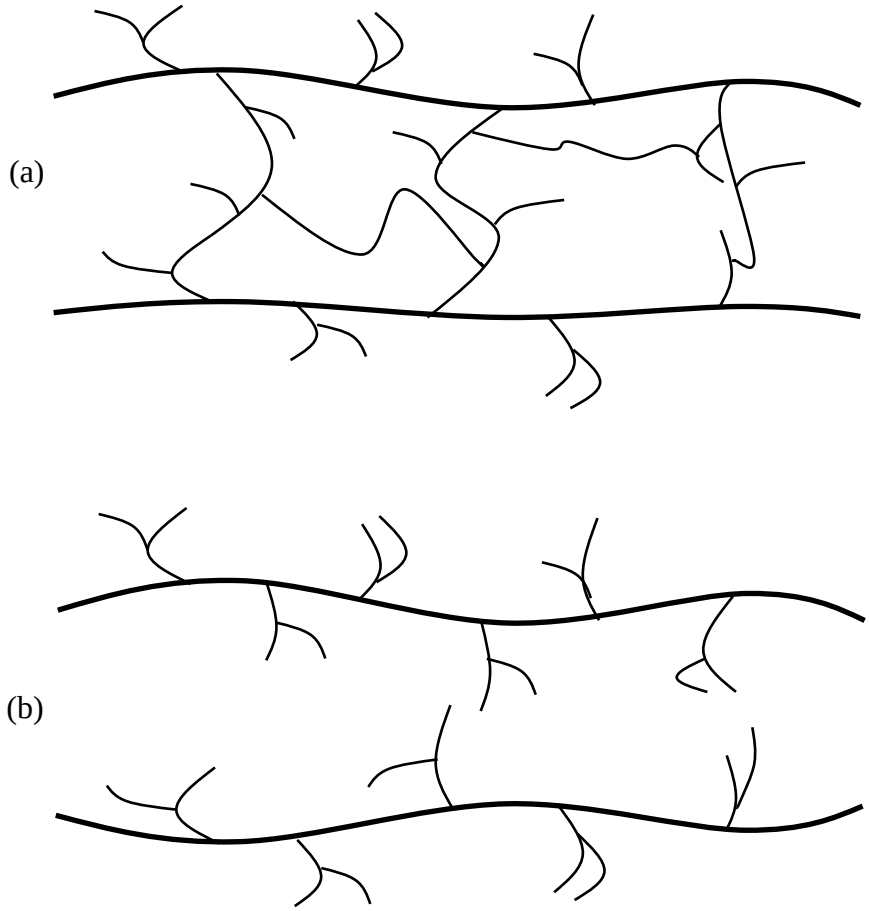

Fig 4.1 Molecular structures (a) thermoset polymer (b) thermoplastics polymer

Matrix Material - 1 :(Epoxy)

The history of epoxy began in 1947 when United States based Devoe-Raynolds company made commercial debut of epoxy by making first product out of it [287] From then, it is being used in wide variety of applications which includes electrical, automotive, marine, aerospace, civil infrastructure, pipes and vessels in the chemical industry, food packing, building material etc. Due to their low density and good adhesive and mechanical properties, over the years epoxy and its composites have become promising materials for high performance applications in the transportation industry. In addition, they have low shrinkage upon curing and good chemical resistance.

Due to several advantages over other thermoset polymers, epoxy (LY 556) is chosen as one of the matrix materials for the present research work. It chemically belongs to the 'epoxide' family. Its common name is Bisphenol-A-Diglycidyl-Ether (commonly abbreviated to DGEBA or BADGE) and its molecular chain structure is shown in Figure 4.2. It provides a solvent free room temperature curing system when it is combined with the hardener tri-ethylene-tetramine (TETA) which is an aliphatic primary amine with commercial designation HY 951 (Figure 4.3).The system was chosen because of low viscosity before curing and the widespread use in the high voltage industry.

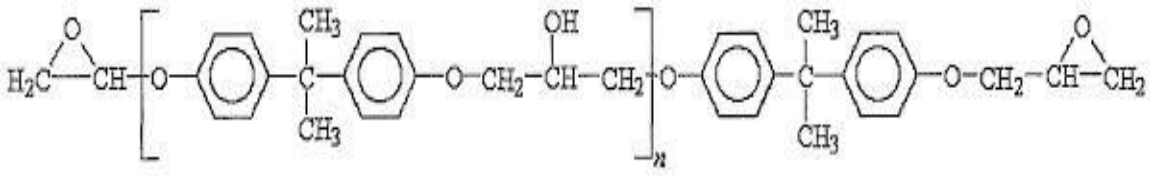

Fig 4.2 Unmodified epoxy resin chain ('**n**' denotes number of polymerized unit)

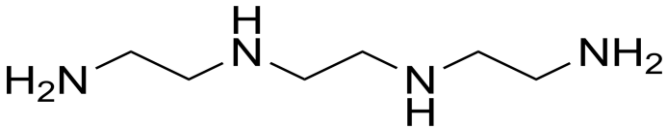

Fig 4.3 Tri-ethylene-tetramine chain

The term "epoxy resin" refers to both the pre-polymer and its cured resin/hardener system. Before the epoxy gets cured, the resin has indefinite shelf life. Ability to transform from liquid state to hard thermoset solids is one of the valuable properties of epoxy resins. The solidification is accomplished by the addition of a chemical reagent known as a curing agent or hardener. The polymerization reaction may be accomplished at room temperature, with heat produced by an exothermic reaction or may require external heat [288]. A schematic representation of the curing process of a thermoset polymer is shown in Figure 4.4.

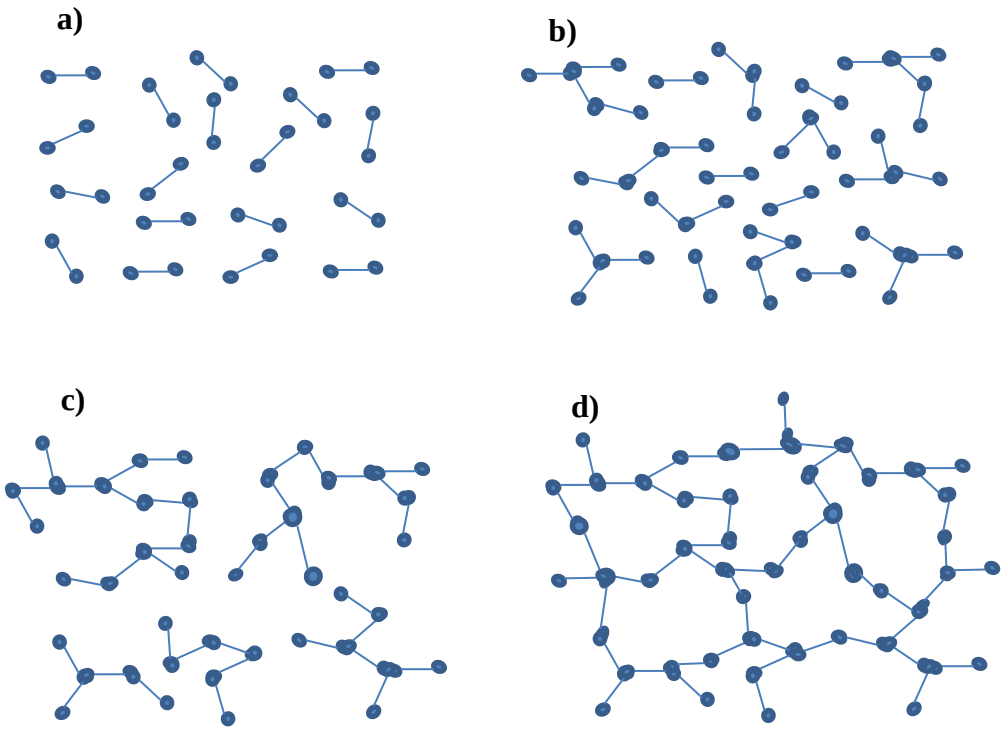

Fig 4.4 Schematic curing of epoxy matrix (a) Cure begins with monomers; (b) proceeds via linear growth; (c) continues with formation of incompletely crosslinked network; (d) finishes as fully cured thermoset.

Fig 4.5 Epoxy resin and corresponding hardener

The LY 556 epoxy resin and the corresponding hardener HY-951 are procured from Ciba Geigy Ltd, India (Figure 4.5). Table 4.1 provides some of the important properties of epoxy.

Table 4.1 Some important properties of epoxy resin

Characteristic Property	Values	Units
Density	1.1	g/cm^3
Compressive strength	114	MPa
Tensile strength	59	MPa
Micro-hardness	0.087	GPa
Thermal conductivity	0.363	W/m-K
Glass transition temperature	98	$^{\circ}C$
Coefficient of thermal expansion	66.0	$ppm/^{\circ}C$
Dielectric constant	4.3	at 1MHz

Matrix Material - 2 :(Polypropylene)

A German chemist named Karl Rehn and an Italian chemist named Giulio Natta were the first who polymerized polypropylene in 1954. The first industrially produced polypropylene resins were introduced around three years later of that which led to a large commercial production of its product. Polypropylene (PP), also known as polypropene, is used in a wide variety of applications including packaging and labeling, textiles, stationery, laboratory equipment, loudspeakers, automotive components and polymer banknotes. This most widely used thermoplastic polymer, is another matrix material used in the present investigation. PP of homo-polymer M110 grade shown in Figure 4.6 is used presently. Its molecular formula is $(C_3H_6)_n$, where n is the number of polymerized unit (Figure 4.7). It is used for its balanceamong strength, modulus and chemical resistance and its aesthetics, cost effectiveness and stability to heat and recyclability. PP used in the present work is procured from Reliance Industries Limited located in Mumbai, India.Table 4.2 provides some important properties of polypropylene.

4.1.2 Filler Materials

Filler Material -1: (Aluminium Nitride)

Aluminium nitride,an aluminium based ceramic material is used as one of the filler materials and has been procured from M/s Alfa Aesar Limited-Beijing, China.

Fig 4.6 Polypropylene of grade homo-polymer M110

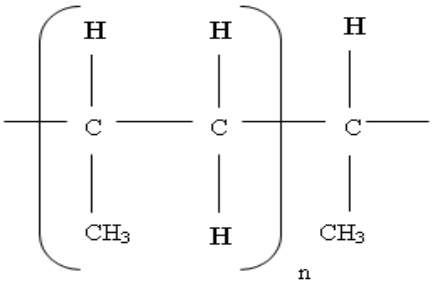

Fig 4.7 Polypropylene Chain (n is the number of polymerized unit)

Table 4.2 Some important properties of polypropylene resin

Characteristic Property	Values	Units
Density	0.92	g/cm^3
Compressive strength	83	MPa
Tensile strength	45	MPa
Micro-hardness	0.059	MPa
Thermal conductivity	0.11	W/m-K
Glass transition temperature	-14.93	$^{\circ}C$
Coefficient of thermal expansion	111.5	$ppm/^{\circ}C$
Dielectric constant	2.25	at 1MHz

The average size of AlN used is about 60-70 microns.AlN is a relatively newer material in the familyof technical ceramics. While its discovery occurred over 100 years ago, it has been developed into a commercially viable product with controlled and reproducible properties within the last 25 years. AlN powder with hexagonal structure is chosen as ceramic filler because of its unique

combination of high thermal conductivity, good dielectric properties, low thermal expansion coefficient, moderate strength and non-reactive with normal semiconductor process chemicals and gases.A pictorial view of AlN used in the present work as the particulate filler is given in Figure 4.8.

Filler Material -2: (Aluminium Oxide)

Aluminium oxide (Al_2O_3)is the other aluminium based ceramic material that has been used as a filler in the present work. It is an inorganic material that can exist in severalcrystalline phases which all revert to the most stable hexagonal alpha phase at elevated temperatures.Al_2O_3 is the most cost effective and widely used material in the family of engineering ceramics. It is hard, resistant to strong acid and alkali attack at elevated temperatures,wear resistant and has good dielectric properties, high strength and stiffness. With an excellent combination of properties and a reasonable price, it is no surprise that fine grain technical grade Al_2O_3 has a very wide range of applications.Al_2O_3in the form of micro and nano-filler in polymers has been studied by many research groups in the past. Al_2O_3 is therefore chosen as the second primary filler material with an average size of 90-100 micron which is procured from Rankem Corporation Limited located at New Delhi, India.A pictorial view of Al_2O_3particles used in the present work is given in Figure 4.9.

Filler Material -3: (Solid glass microspheres)

Solid glass microspheres (SGMs) withan average size of 100 μm procured from NICEN Limited located at Bangalore, Indiaare used as the secondary filler material in the present research. These microspheres are normally obtained by heating tiny droplets of dissolved sodium meta-silicate (Na_2SiO_3, commonly referred to as water glass or liquid glass) during ultrasonic spray pyrolysis process.These are made of high grade soda lime silica glass containing around 70% of SiO_2 and are usually free from lead and iron.They havelower CTE, low dielectric constant, high compressive strength, improved surface hardness and smoothness.

Fig 4.8 Micro-sized aluminium nitride particles

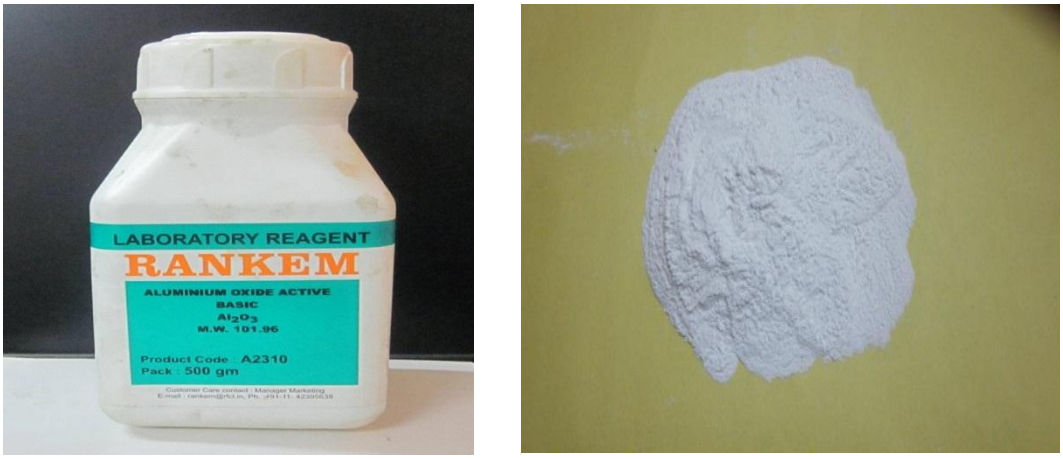

Fig 4.9 Micro-sized aluminium oxide particles

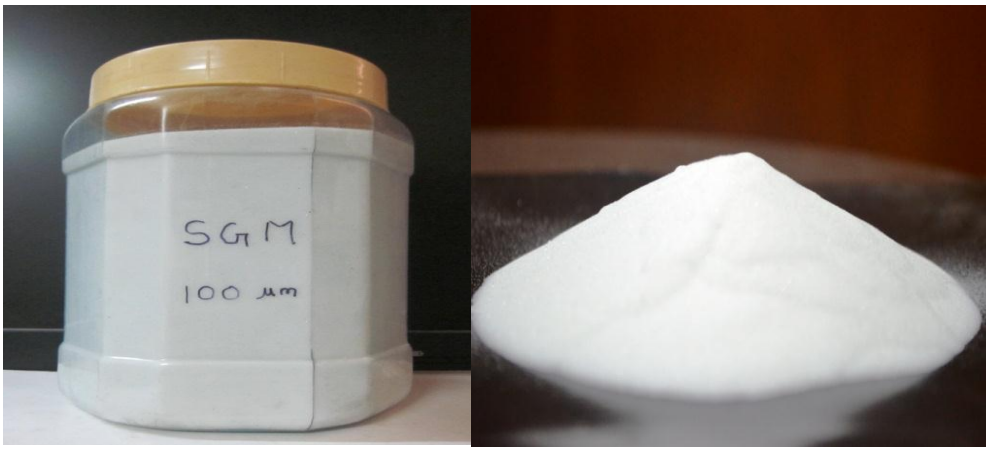

Fig 4.10 Solid glass microspheres

Table 4.3 Some important properties of fillers under investigation

Characteristic Property	AlN	Al_2O_3	SGM	Units
Density	3.3	3.89	1.5	gm/cm^3
Compressive strength	2100	2600	330	MPa
Tensile strength	345	394	97	MPa
Micro-hardness	10.78	14.12	16.84	GPa
Thermal conductivity	160	35	0.238	W/m-K
Coefficient of thermal expansion	4.5	8.1	7.5	ppm/°C
Dielectric constant	8.9	9.8	2.25	at 1MHz

A pictorial view of glass microspheres used in the present work as the particulate filler is given in Figure 4.10. Some important properties of these fillers, used in present investigation, are presented in Table 4.3.

4.2 COMPOSITE FABRICATION

4.2.1 Epoxy based composites - Hand lay-up route

Hand lay-up technique is the oldest and simplest open moulding method of composite processing. The infrastructural requirement for this method is minimal and the processing steps are also quite simple. All the epoxy based composite samples of various compositions with different fillers are prepared by this hand lay-up technique in the following steps:

1) The low temperature curing epoxy resin (LY556) and corresponding hardener (HY 951) are mixed in a ratio 10:1 by weight as recommended.
2) Micro-sized particles are then added to the epoxy-hardener combination and mixed thoroughly by hand stirring.
3) Before pouring the epoxy/filler mixture in the mould, a silicon spray (Figure 4.11 a) is done over the mould reliving sheet (Figure 4.11 b). The use of relieving sheet and silicon spray enables the easy removal of composites from the mould after curing. The uniformly mixed dough is then slowly decanted into the moulds (Figure 4.12) so as to get disc type specimens of three different dimensions (dia50 mm and thickness 3 mm, dia 20 mm and thickness 1 mm and dia 12.7 mm and thickness 25.4 mm) and rectangular slab specimens (200×200 in area and thickness 3 mm).

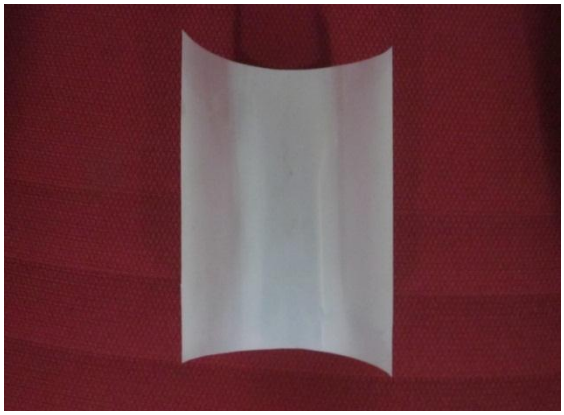

Fig 4.11 (a) Silicon spray, (b) Mould relieving sheet

Fig 4.12 Different moulds used to fabricate epoxy based composites

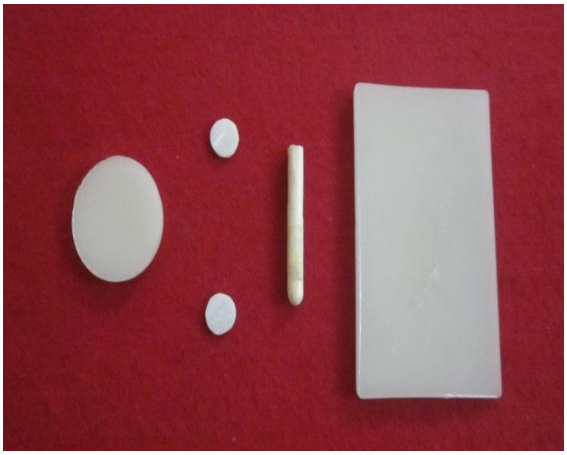

Fig 4.13 Fabricated epoxy based composites from various moulds

Fig 4.14 Particulate filled epoxy composite fabrication by hand lay-up process

4) The cast of each composite is cured for 24 hours before it is removed from the mould. Disc type specimens are used for evaluating effective thermal conductivity, dielectric constant and compressive strength whereas, for rest of the characterization tests, specimens of required dimensions are cut from the rectangular composite slabs.

Figure 4.13 shows some of these composite samples prepared through hand-layup technique. A pictorial representation of fabrication process using hand-layup technique for particulate filled epoxy composites is shown in Figure 4.14.The compositions of various composites fabricated using epoxy as the base matrices are presented in Table 4.4.

Table 4.4 Epoxy based composites filled with different inorganic fillers

S.No.	Set I	Set II	Set III	Set IV
1	EP + 2.5 vol% AlN	EP + 2.5 vol% Al_2O_3	EP + 5.0 vol% AlN + 5.0 vol% SGM	EP + 5.0 vol% Al_2O_3 + 5.0 vol% SGM
2	EP + 5.0 vol% AlN	EP + 5.0 vol% Al_2O_3	EP + 10.0 vol% AlN + 10.0 vol% SGM	EP + 10.0 vol% Al_2O_3 + 10.0 vol% SGM
3	EP + 7.5 vol% AlN	EP + 7.5 vol% Al_2O_3		
4	EP + 10.0 vol% AlN	EP + 10.0 vol% Al_2O_3	EP + 15.0 vol% AlN + 15.0 vol% SGM	EP + 15.0 vol% Al_2O_3 + 15.0 vol% SGM
5	EP + 12.5 vol% AlN	EP + 12.5 vol% Al_2O_3		
6	EP + 15.0 vol% AlN	EP + 15.0 vol% Al_2O_3	EP + 5.0 vol% AlN + 10.0 vol% SGM	EP + 5.0 vol% Al_2O_3 + 10.0 vol% SGM
7	EP + 17.5 vol% AlN	EP + 17.5 vol% Al_2O_3		
8	EP + 20.0 vol% AlN	EP + 20.0 vol% Al_2O_3	EP + 15.0 vol% AlN + 10.0 vol% SGM	EP + 15.0 vol% Al_2O_3 + 10.0 vol% SGM
9	EP + 22.5 vol% AlN	EP + 22.5 vol% Al_2O_3		
10	EP + 25.0 vol% AlN	EP + 25.0 vol% Al_2O_3	EP + 20.0 vol% AlN + 10.0 vol% SGM	EP + 20.0 vol% Al_2O_3 + 10.0 vol% SGM

** EP: Epoxy, SGM: Solid Glass Micro-spheres*

4.3.2 Polypropylene based composites - *Compression moulding route*

In present study, PP based composites are fabricated by compression moulding route, but prior to that, proper mixing of filler with resin is necessary. Most of the melt compounding is performed using a miniaturized internal batch mixer (Haake Rheomix 600), a pictorial view of which is given in Figure 4.15. It consists of a mixing head with a pair of sigma blades for mixing the materials.

The mixing head consists of three important components used for mixing:
1) A small feed port that is used for feeding the materials,
2) A mixing chamber for mixing the batch,
3) The blades that shear the material.

The blades are mainly designed for mixing and homogenizing highly viscous materials. These blades rotate in opposite directions which cause the materials to shear. The rated maximum volume of this batch mixer is 70 cm^3. In practice, a batch of about 50 cm^3 can be loaded into the mixing head to avoid overloading. Haake Rheomix 600 is controlled by software called Polylab^{TM}, which records the torque, temperature and time during mixing as well as the speed of the rotating blades. Torque vs time graph typically shows that the torque increases as the material is sheared and it gradually decreases once the required amount of mixing is attained within the specified time. The temperature of the mixing chamber is set to 190°C and time of the mixing is 12 minutes in the present case. The shearing action provides the major portion of heating to the mixing chamber. Once the mixing time is reached, the mixer is stopped. The mixing head is then removed and the batch is scraped off and collected. These mixtures are again oven dried at 130°C for 1 hour to remove any moisture. These small pieces of materials are then taken out from the hot air oven and kept in compression moulding die. The pictorial view and specifications of compression moulding machine are presented in Figure 4.16 and Table 4.5 respectively. The dimension of the sheet produced from the die is of 3 mm thickness and 180×180 mm in area. By using a hydraulic press (Figure 4.16), the material is pressed with a pressure of 150 kg/cm^2 for around three minutes.

Fig 4.15 Haake Rheomix 600 batch mixer

Fig 4.16 Compression moulding machine

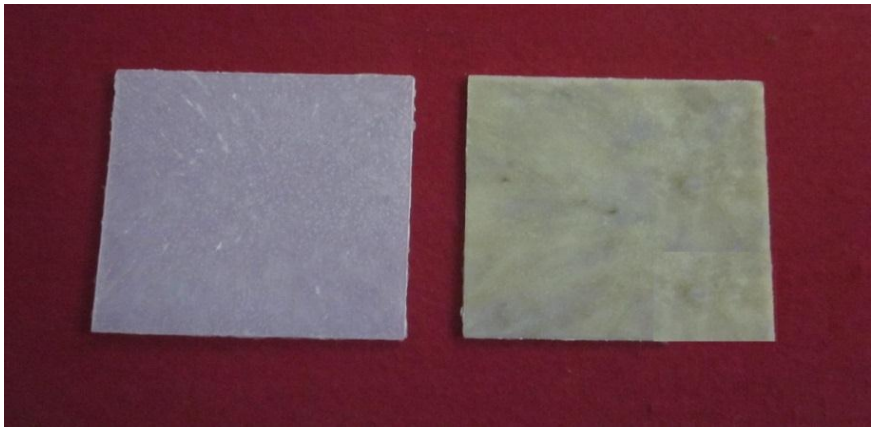

Fig 4.17 Composite sheets prepared by compression moulding machine

During the process, the temperature of the compression moulding die is maintained at 190°C with the help of heaters. After that it gets water cooled and the sheet (Figure 4.17) is taken out from the die. From this sheet, specimens of required dimensions for various mechanical, thermal and dielectric characterizations are obtained through machining. The compositions of various composites fabricated using polypropylene as the base matrices are presented in Table 4.6.

Table 4.5 COMPRESSION MOULDING (Hydraulic press) Instruments details

Make:	M/S Neoplast Engineering Pvt. Ltd., India
Model No.:	HP 80 T
Test methods:	ASTM-D 695
Specification:	
Capacity:	80 Ton to develop pressure upto 150 kg/cm^2
Temperature:	Ambient to 450°C
Timer:	LED 0.01 sec, 999 hours (digital)
Heat plate area:	320 mm × 320 mm (mild steel)
Specimen plate area:	180 mm × 180 mm (SS)
Cooling method:	Water circulation
Power supply:	440V AC, 3 Phase
Specimen frame:	1mm, 3mm, 1.5mm, SS304, Cooling/heating in mould
Accuracy:	Temperature: + 0.10C, Sheet thickness + 0.01mm
Application:	Powder/granules compaction, To prepare plastic sheet

Table 4.6 Polypropylene based composites filled with different inorganic fillers

S.No.	Set I	Set II	Set III	Set IV
1	PP + 2.5 vol% AlN	PP + 2.5 vol% Al_2O_3	PP+ 5.0 vol% AlN + 5.0 vol% SGM	PP+ 5.0 vol% Al_2O_3 + 5.0 vol% SGM
2	PP + 5.0 vol% AlN	PP + 5.0 vol% Al_2O_3	PP+ 10.0 vol% AlN + 10.0 vol% SGM	PP+ 10.0 vol% Al_2O_3 + 10.0 vol% SGM
3	PP + 7.5 vol% AlN	PP + 7.5 vol% Al_2O_3		
4	PP + 10.0 vol% AlN	PP + 10.0 vol% Al_2O_3	PP+ 15.0 vol% AlN + 15.0 vol% SGM	PP+ 15.0 vol% Al_2O_3 + 15.0 vol% SGM
5	PP + 12.5 vol% AlN	PP + 12.5 vol% Al_2O_3		
6	PP + 15.0 vol% AlN	PP + 15.0 vol% Al_2O_3	PP+ 5.0 vol% AlN + 10.0 vol% SGM	PP+ 5.0 vol% Al_2O_3 + 10.0 vol% SGM
7	PP + 17.5 vol% AlN	PP + 17.5 vol% Al_2O_3		
8	PP + 20.0 vol% AlN	PP + 20.0 vol% Al_2O_3	PP+ 15.0 vol% AlN + 10.0 vol% SGM	PP+ 15.0 vol% Al_2O_3 + 10.0 vol% SGM
9	PP + 22.5 vol% AlN	PP + 22.5 vol% Al_2O_3		
10	PP + 25.0 vol% AlN	PP + 25.0 vol% Al_2O_3	PP+ 20.0 vol% AlN + 10.0 vol% SGM	PP+ 20.0 vol% Al_2O_3 + 10.0 vol% SGM

**PP: Polypropylene, SGM: Solid Glass Micro-spheres*

4.3 PHYSICAL CHARACTERIZATION

4.3.1 Density and volume fraction of voids

Polymers are well known for their low density and high strength to weight ratio. The addition of filler into polymer improves many useful properties, but at the same time it gives rise to certain complex phenomena as well, like percentage of voids present and/or changes in weight of the filled product, which ultimately influence its density. As in the present case, the densities of all the fillers are higher than those of the polymers used, it becomes imperative to make an assessment of the increase in the overall densities of the composites.

The actual density (ρ_{ce}) of composites is determined by the Archimedes principle using distilled water as a medium (ASTM D 792-91). According to this principle, when an object is immersed in a liquid the apparent loss of weight of an object is equal to the upthrust and this is also equal to the weight of the liquid displaced. Therefore if density of the liquid is known and the volume of the liquid displaced is measured, the apparent loss of weight is calculated and hence density of the composite is obtained by using equation 4.1,

$$\rho_{ce} = \frac{\rho_w W_a}{W_a - W_w} \tag{4.1}$$

Here ρ_{ce} is the actual/measured density of composite, ρ_w is the density of distilled water, W_a is weight of sample in air and W_w is weight of sample in water. The theoretical density (ρ_{ct}) of composite materials in terms of volume fractions of different constituents can easily be obtained using rule of mixture [118].

$$\rho_{ct} = \phi_f \rho_f + (1 - \phi_f)\rho_p \tag{4.2}$$

where, Φ and ρ represent the volume fraction and density respectively. The suffixes f and p stand for the filler and polymer respectively in a composite reinforced with single filler.

For hybrid filler composite, the above expression for density has been modified as:

$$\rho_{ct} = \phi_a \rho_a + \phi_b \rho_b + [1 - (\phi_a + \phi_b)]\rho_p \quad (4.3)$$

where, the suffix *a* and *b* stand for the first and second filler respectively.

The volume fraction of voids (V_v) in the composites is calculated by using the following equation:

$$V_v = (\rho_{ct} - \rho_{ce})/\rho_{ct} \quad (4.4)$$

4.3.2 Scanning Electron Microscopy

The surface morphology of the particulate reinforced composites together with the dispersion characteristics of the fillers in the matrix body have been studied using a scanning electron microscope JEOL JSM-6480LV (Figure 4.18). The composite samples are mounted on stubs with silver paste. To improve the penetration of light and for better surface micrographs, thermal conductivity of the samples are enhanced by vacuum-evaporated a thin film of platinum onto them before the photomicrographs are taken.

4.4 MECHANICAL CHARACTERIZATION

4.4.1Micro-hardness

Micro-hardness measurement is done using a Leitz micro-hardness tester (Figure 4.19). A diamond indenter, in the form of a right pyramid with a square base and an angle 136° between opposite faces, is forced into the material under a load *F*. The two diagonals *X* and *Y* of the indentation left on the surface of the material after removal of the load are measured and their arithmetic mean is calculated. In the present study, the load considered *F*= 0.2454 N and micro-hardness value is calculated using the following equation.

$$H_v = 0.1889 \frac{F}{L^2} \quad (4.5)$$

where, $L = \frac{X + Y}{2}$

where, *F* is the applied load (N), *L* is the diagonal of square impression (mm), *X* is the horizontal length (mm) and *Y* is the vertical length (mm).

Fig 4.18 Scanning electron microscope (JEOL JSM-6480LV)

Fig 4.19 Leitz micro-hardness tester

4.4.2Tensile strength

One of the most important and widely measured properties of any composite material is its tensile strength i.e., the ability of a material to resist breaking under tensile load. The tensile strength of the composites is measured with a computerized Instron 1195 universal testing machine (Figure 4.20) in accordance with ASTM D 3039-76 procedure by applying uni-axial load through both the ends at a cross head speed of 10mm/min.

Fig 4.20 Instron 1195 universal testing machine

Figure 4.21 Composite samples for tensile test and its loading arrangement

Figure 4.22 Composite samples for compression test and its loading arrangement

The specimens used in present investigation to perform all the tensile tests are of dog-bone shape (length 150mm, end width 20mm and mid width 12 mm) having both the surface flat and its loading arrangement is shown in Figure 4.21. Bluehill material testing software is used which allows setting the desired test control, to automatically calculate the desired results and statistics, and to produce a test report. Tests are repeated three times for each composition and the mean value is reported as the tensile strength of that composite.

4.4.3 Compressive strength

In addition to tensile testing, another common form of determining the material properties of plastic (both unreinforced and reinforced) is by compression testing. This test is useful for determining the modulus of elasticity, yield stress, compressive strength, and the deformation beyond yield point. Static uni-axial compression tests on specimens are carried out using the same Universal Testing Machine *Instron 1195* (Figure 4.20). For performing the test, two 50mm diameter hardened-steel compression platens are mounted on this testing machine with compression fixture and a strain measuring device such as extensometer is attached directly to the specimen. Bluehill material testing software is used again. The method by which the compression test is conducted is in accordance with ASTM D695 [289].Specimens used for this testing can either be blocks or cylinders. The typical cylinder blocks used for these tests are 12.7 mm in diameter and 25.4 mm in length. The standard requires that the specimen is compressively loaded at a rate of 5 mm/min until fracture. Prior to testing, it is ensured that all specimens are made to the sizes specified in the standard and are free from visible surface flaws. The specimens used in present investigation to perform the compressive tests and its loading arrangement are shown in Figure 4.22. Three identical specimens are tested for each composition and the average test result is recorded as the compressive strength of the composite.

4.5 THERMAL CHARACTERIZATION

4.5.1 Effective thermal conductivity

Equipment used:

Unitherm Model 2022 thermal conductivity tester (Figure 4.23).

Scope:

Thermal conductivity values are used to measure heat flow through a material. It is the measure of resistance of materials to thermal transmission. The test method is utilized for various materials of a representative thickness, which include polymers, glasses, ceramics, rubbers, composites, few metals and other materials with medium to low thermal conductivity.

Test procedure:

The specimen is placed in the thermal conductivity equipment at a specified temperature and a compressive load is applied. The lower surface is part of a calibrated heat flow transducer. The heat flows from the upper surface, through the sample, to the lower surface, establishing an axial temperature gradient in the stack. After certain time, thermal equilibrium is obtained. The temperature and output of the heat flux transducer are recorded. Testing is performed following ASTM E1530 standards for evaluating the resistance to thermal transmission of materials by the guarded heat flow meter technique.

Specimen size:

For solid plastic materials, normally 50 mm diameter disks are required. The thickness range is 0.5mm to 25mm using the standard setup and below 0.5mm using thin film stacking method as per ASTM E1530. In present case, the sample is in solid state and so discs of 50 mm diameter and 3 mm thickness are used.

Operating Principle of Unitherm^{TM}Model 2022

For one-dimension heat flow, the equation is given as:

$$Q = kA \frac{T_1 - T_2}{x} \tag{4.6}$$

where, Q is the heat flux (W), A is the cross-sectional area (m^2), k is thermal conductivity (W/m-K), x is the sample thickness (m), $T_1 - T_2$ is the temperature difference between surfaces (°C or K).

Fig 4.23 Thermal conductivity tester *Unitherm™ 2022*

Fig 4.24 Perkin Elmer DSC-7 Thermal Mechanical Analyzer

The thermal resistance of the sample is given as:

$$R = \frac{T_1 - T_2}{Q} \tag{4.7}$$

where, R is sample resistance between hot and cold surfaces (K / W)

From the former equation, we can write:

$$k = \frac{x}{RA} \tag{4.8}$$

In Unitherm™ 2022, transducers are employed to measure the heat flux Q and temperature difference between upper and lower plate. Thus, thermal resistance between surfaces can be evaluated. Providing thickness and cross-sectional area as input parameters, the sample thermal conductivity can then be calculated.

4.5.2 Thermal Mechanical Analyzer

Glass transition temperature (T_g) is the temperature at which the mechanical properties of amorphous polymer changes from the brittle state to a rubbery state. The most important property change at the T_g of the printed circuit board (PCB) materials is the thermal expansion, which is a swift from a relative low value to a very high value. This kind of change is not desirable as it imposes stress on the PCBs when they experience high-temperatures during manufacturing, assembly or during their service-life. Similarly, coefficient of thermal expansion (CTE) is another vital property which needs proper understanding. A material with high CTE will induce stress within the component. A low CTE is therefore preferable. In the present work, T_g and CTE of the composites are measured with a *Perkin Elmer DSC-7 Thermal Mechanical Analyzer* (Figure 4.24). At first, the thermal mechanical analyzer sample stage is purged with nitrogen gas. The sample length is set between 6-8 mm and the width and thickness is about 2-3 mm. During the measurement, the specimen is heated from 30 to 150°C at a heating rate of 5°C/min. For each measurement, two heating scans are used. The first heating scan is used to eliminate any possible internal stress and moisture in the sample which is likely to be generated during the curing and sample preparation processes. The second heating scan is used to determine the T_g and CTE of the material.

4.6 DIELECTRIC CHARACTERIZATION

A dielectric is an electrical insulator that can be polarized by an applied electric field. When a dielectric is placed in an electric field, electric charges do not flow through the material as they do in a conductor, but only slightly shift from their average equilibrium positions causing dielectric polarization. Because of this polarization, positive charges are displaced towards the field and negative charges shift in the opposite direction. This creates an internal electric field which reduces the overall field within the dielectric itself. The term insulator is generally used to indicate electrical obstruction while the term dielectric is used to indicate the energy storing capacity of the material.

Using *Hioki 3532-50 Hi - Tester LCR Analyzer* with applied voltage of 500 mV, the dielectric constant (ε_c), in frequency range 1 kHz – 1 MHz can be calculated from capacitance by:

$$\varepsilon_c = \frac{Ct}{\varepsilon_0 A} \tag{4.9}$$

where, C is the capacitance, t is the thickness of disc, $\varepsilon_0$is the electrical permittivity of free space and A is the disc area.

Fig 4.25 Hioki 3532-50 LCR Hi tester

Fig 4.26 Aluminium foil wrapped test samples for dielectric test

Figure 4.25 gives the pictorial view of *Hioki 3532-50 Hi - Tester LCR Analyzer* used in the present work for the measurement of dielectric constant. Disc type samples (Figure 4.26) with both surfaces wrapped with aluminium foil are used for this purpose.

Chapter Summary

This chapter has provided:

- The descriptions of materials (matrices and fillers) used in this research.
- The details of fabrication of the composites.
- The details of physical, mechanical, thermal and dielectric characterization tests.

The next chapter presents the test results related to the physical and mechanical properties of the polymer composites under this study.

*****

Chapter 5

Results and Discussion – I

Physical and Mechanical Characteristics of the Composites

Chapter 5

Results and Discussion – I

PHYSICAL AND MECHANICAL CHARACTERISTICS OF THE COMPOSITES

This chapter presents the measured values of various physical and mechanical properties of the epoxy and polypropylene based single and hybrid filler composites. The relative effects of different filler materials on composite properties have been discussed. This part of the thesis also presents the scanning electron micrographs showing some typical micro-structural features of the composites under study.

5.1 PHYSICAL CHARACTERISTICS

Evaluation of the physical properties of any new composite system is essential both from the viewpoints of scientific understanding and practical applications. In the present work, a property data has been generated by conducting characterization tests under controlled laboratory conditions to evaluate physical property i.e. density and also the morphology of fabricated composites.

5.1.1 Density and void content

The densities of unfilled epoxy and PP resins measured by Archimedes method are found to be 1.1 g/cm^3 and 0.92 g/cm^3 respectively. Further, the densities of their composites are also measured by the same principle. The test results and the theoretical density along with the corresponding void content for single filler reinforced epoxy and polypropylene based composites are presented in Tables 5.1 and 5.2 respectively and for hybrid filler reinforced epoxy and polypropylene based composites are presented in Tables 5.3 and 5.4 respectively. It is seen that the density of all the sets of composites increases with increase in filler content as expected due to the fact that the densities of fillers used in this work are higher than those of the base matrices. It can also be noted from all the tables that the theoretically calculated density values are higher as compared to the

measured values. The reason for this is, while calculating the density using equation 4.2; it has been presumed that the composites are free from voids and defects, while in actual practice, fabrication of composites inevitably gives rise to a certain amount of voids/pores within the composite body.

Table 5.1 Measured and theoretical densities of the composites (Epoxy filled with single filler)

Filler content (Vol%)	Epoxy/AlN			Epoxy/Al_2O_3		
	Density (g/cm^3)		Void content (%)	Density (g/cm^3)		Void content (%)
	Theoretical	Measured		Theoretical	Measured	
5	1.21	1.17	3.30	1.239	1.20	3.15
10	1.32	1.27	3.78	1.379	1.33	3.55
15	1.43	1.37	4.19	1.518	1.46	3.82
20	1.54	1.43	7.14	1.658	1.57	5.30
25	1.65	1.50	9.09	1.797	1.68	6.51

Table 5.2 Measured and theoretical densities of the composites (Polypropylene filled with single filler)

Filler content (Vol%)	Polypropylene/AlN			Polypropylene/Al_2O_3		
	Density (g/cm^3)		Void content (%)	Density (g/cm^3)		Void content (%)
	Theoretical	Measured		Theoretical	Measured	
5	1.039	1.03	0.86	1.068	1.06	0.75
10	1.158	1.14	1.55	1.217	1.19	2.21
15	1.277	1.25	2.12	1.365	1.33	2.56
20	1.396	1.35	3.29	1.514	1.46	3.56
25	1.515	1.44	4.95	1.662	1.59	4.33

It is found that with the increase in micro-sized AlN content in epoxy resin from 0 to 25 vol% (Set I Epoxy composites), there is an increase in density of the composite by 36.36% and simultaneous increase in porosity by 9.09%. Similarly, for Set II epoxy composites, rise in composite density by about 52.7% is recorded as the Al_2O_3 content in epoxy increased from 0 to 25 vol% whereas

void content reaches 6.51% (Table 5.1). For the PP-AlN (Set I PP composites) and PP-Al_2O_3 (Set II PP composites) composites with filler content of 25 vol%, the density increases by 56.52% and 72.82% respectively whereas void contents are restricted to 4.95% and 4.33% respectively (Table 5.2).

Table 5.3 Measured and theoretical densities of the composites (Epoxy filled with hybrid filler)

Epoxy + AlN + SGM				Epoxy + Al_2O_3 + SGM			
Compositions	Density (g/cm^3)		Void content (%)	Compositions	Density (g/cm^3)		Void content (%)
	Theoretical	Measured			Theoretical	Measured	
EP + 5 vol %AlN + 5 vol % SGM	1.23	1.21	1.62	EP + 5 vol %Al_2O_3 + 5 vol %SGM	1.26	1.24	1.58
EP + 10 vol %AlN + 10 vol % SGM	1.36	1.32	2.94	EP + 10 vol %Al_2O_3 + 10 vol % SGM	1.42	1.39	2.11
EP + 15 vol % AlN + 15 vol % SGM	1.49	1.43	4.02	EP + 15 vol % Al_2O_3 + 15 vol % SGM	1.578	1.53	3.04
EP + 5 vol % AlN +10 vol % SGM	1.25	1.23	1.60	EP + 5 vol % Al_2O_3 +10 vol % SGM	1.279	1.26	1.48
EP + 15 vol % AlN + 10 vol %SGM	1.47	1.42	3.40	EP + 15 vol % Al_2O_3 + 10 vol %SGM	1.558	1.52	2.44
EP + 20 vol % AlN + 10 vol % SGM	1.58	1.49	5.69	EP + 20 vol % Al_2O_3 + 10 vol % SGM	1.698	1.62	4.59

** EP: Epoxy, SGM: Solid Glass Micro-spheres*

For multi filler composites, when AlN or Al_2O_3 is premixed with SGM and reinforced in matrix body, density of matrix increases with the volume fraction of either of the filler. For Epoxy Set III composites, when epoxy is reinforced with AlN and SGM, the maximum density reaches 1.49 g/cm^3 with a void content of 5.69 % for 20 vol% of AlN and 10 vol% of SGM. For Epoxy Set IV composites, with 20 vol% Al_2O_3 and 10 vol% SGM, density of epoxy reaches to still higher value of 1.62 g/cm^3 whereas, void becomes 4.59 % (Table 5.3).

Similar is the case with PP based hybrid composites. As for PP Set III composites, reinforcement of 20 vol% AlN and 10 vol% SGM enhances the

density of PP to 1.41 g/cm^3 and void content to 3.02 %, whereas for PP Set IV composites, 20 vol % of Al_2O_3 and 10 vol % SGM enhances the density to 1.53 g/cm^3, though void content remains relatively lower i.e. 2.67 % (Table 5.4). It is interesting to note that the volume fraction of voids decreases appreciably for hybrid composites as compared to the single filler composites. This may be attributed to the inclusion of glass microspheres which fill the voids created by the ceramics to a great extent.

Table 5.4 Measured and theoretical densities of the composites (Polypropylene filled with hybrid filler)

PP + AlN + SGM				PP + Al_2O_3 + SGM			
Compositions	Density (g/cm^3)		Void content (%)	Compositions	Density (g/cm^3)		Void content (%)
	Theoretical	Measured			Theoretical	Measured	
PP + 5 vol %AlN + 5 vol % SGM	1.068	1.06	0.74	PP + 5 vol %Al_2O_3 + 5 vol %SGM	1.097	1.09	0.63
PP + 10 vol %AlN + 10 vol % SGM	1.216	1.20	1.31	PP + 10 vol %Al_2O_3 + 10 vol % SGM	1.275	1.26	1.17
PP + 15 vol % AlN + 15 vol % SGM	1.364	1.34	1.75	PP + 15 vol % Al_2O_3 + 15 vol % SGM	1.45	1.43	1.37
PP + 5 vol % AlN +10 vol % SGM	1.097	1.09	0.63	PP + 5 vol % Al_2O_3 +10 vol % SGM	1.126	1.12	0.53
PP + 15 vol % AlN + 10 vol % SGM	1.335	1.31	1.87	PP + 15 vol % Al_2O_3 + 10 vol %SGM	1.423	1.40	1.61
PP + 20 vol % AlN + 10 vol % SGM	1.454	1.41	3.02	PP + 20 vol % Al_2O_3 + 10 vol % SGM	1.572	1.53	2.67

** PP: Polypropylene, SGM: Solid Glass Micro-spheres*

It is well-known that the voids are the cause for the difference between the measured density and the theoretically calculated ones. The voids significantly affect some of the mechanical properties and even the performance of composites in the workplace. Higher void content usually means lower fatigue resistance and greater susceptibility to water penetration. It is understandable that a good composite should have fewer voids. It can also be seen from the tables that for low volume fraction of filler, the calculated density and the

measured density are in good agreement with each other, but as the filler content is increasing, the deviation between the theoretical and experimental value increases. Also, for same volume fraction of filler, composite with AlN as filler contain more percentage of voids as compare to Al_2O_3 as filler.The possible reason is that AlN is having affinity towards moisture, so because of this, AlN particles try to form clusters in few parts of composites, due to which non-uniform distribution of particle inside the matrix occurs and often gives rise to greater percentage of voids.

It is again noteworthy that the volume fractions of voids in the thermoset composites are more than those in the thermoplastic composites irrespective of the filler content. This can be attributed to the routes adopted for fabricating these two different classes of composites. Compression moulding has always been more effective than hand lay-up technique as far as the uniformity of particle dispersion and void formation are concerned. In hand lay-up route, formation of pores and voids becomes inevitable whereas in compression moulding the possibility of voids is usually much less.

5.1.2 Morphology

It is well known that the properties of the composites are strongly affected by the compatibility between the organic matrix and inorganic filler phase. In order to assess this filler-matrix interaction, geometry of the filler particles and their dispersion in the matrix body, the particulates and the composites are observed under scanning electron microscope (SEM). Figure 5.1 shows typical SEM images of various fillers used in the present work. These micrographs confirm the spherical shape of the fillers used as reinforcement in the matrix body. It is clear from the image that the average particle size of AlN particle is 60-80 micron, Al_2O_3 is around of 90-100micron and that of SGM is of 100 microns.

Figure 5.2 shows the morphologies of cross-section of composites reinforced with single fillers i.e AlN/Al_2O_3. Figure 5.2 (a) and 5.2 (b) are for epoxy/AlN and epoxy/Al_2O_3 composites respectively whereas; Figure 5.2 (c) and 5.2 (d) are

for PP/AlN and PP/Al_2O_3 composites respectively. All the micrographs are taken for composites with filler content of 25 vol%.

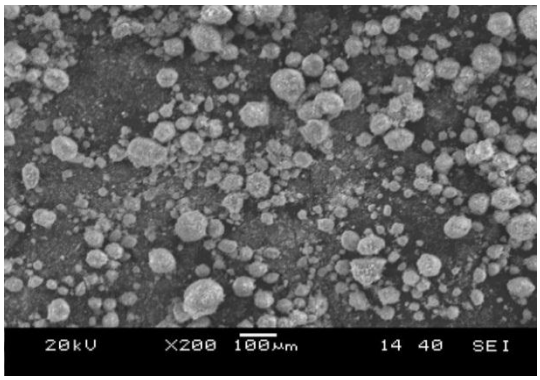

(a)

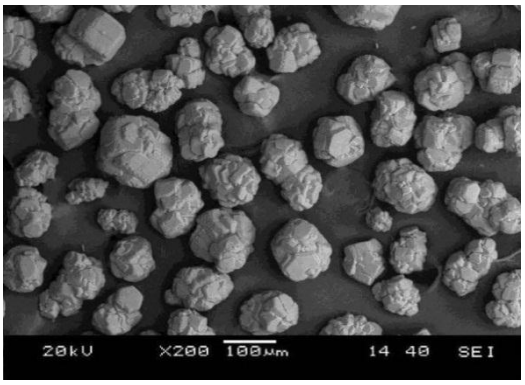

(b)

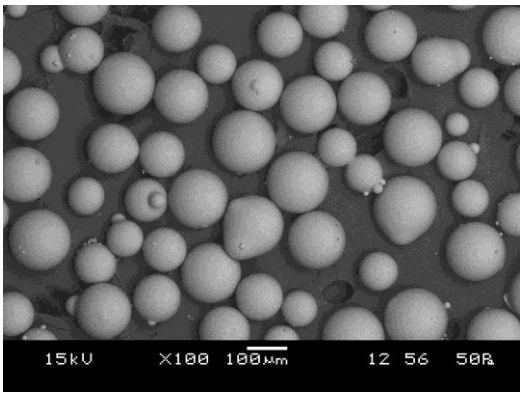

(c)

Fig. 5.1 SEM images of fillers (a) micro-sized aluminium nitride, (b) micro-sized aluminium oxide (c) solid glass microspheres

From the figures it is clear that the distributions of micro size particles in epoxy and PP resin for the fabricated samples are more of less uniform. It can also be observed from SEM images that further increase of filler content in matrix material beyond 25% volume fraction is quite difficult task, as increase in filler content reduces the inter particle distance upto the limit that particles start to interfere with each other, which may degrade the properties of filler as well as of the composite. Increasing filler content beyond this may raise a problem of improper wetting which would make the composite formation near impossible. Also, the degree of particle dispersion is different for composites of epoxy and PP because of the difference in their respective fabrication routes. PP composites are fabricated by compression moulding technique in which the mixing is done

by batch-mixer Rheomix 600 whereas epoxy composites are fabricated by hand lay-up technique.

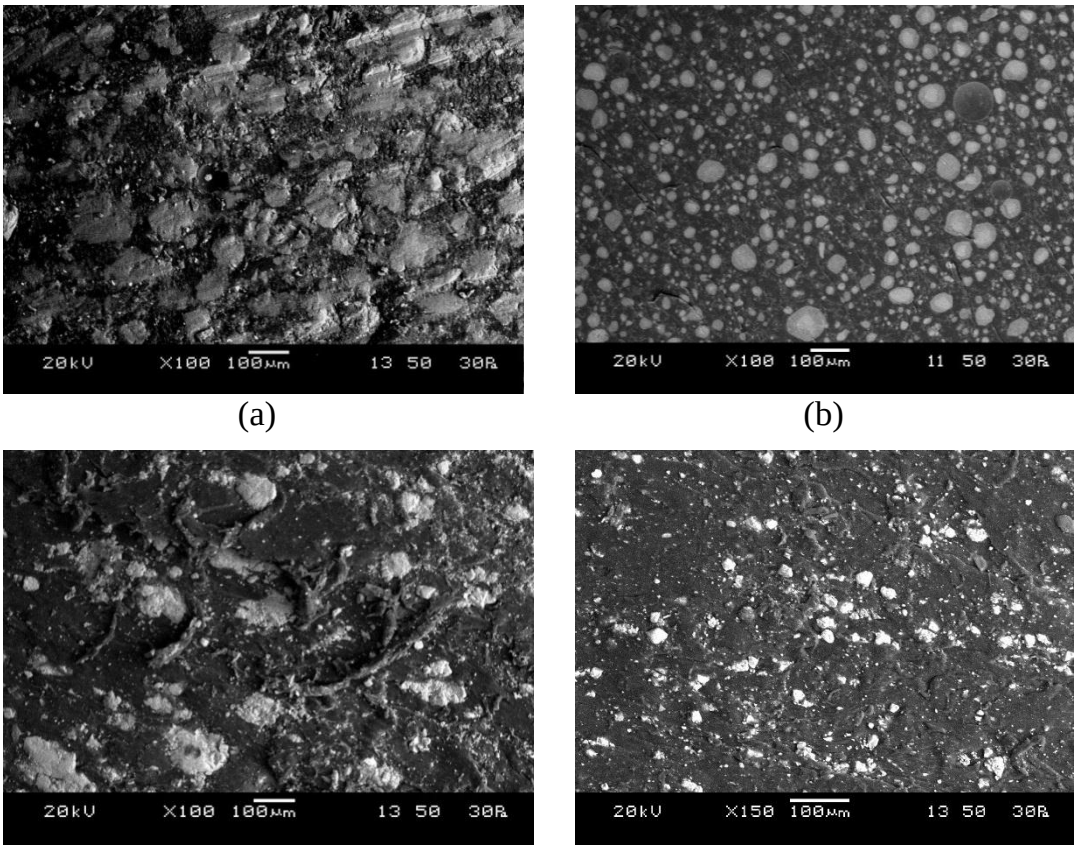

Fig. 5.2 Typical SEM images of single filler polymer composites (a) Epoxy/AlN, (b) Epoxy/Al_2O_3, (c) Polypropylene/AlN, (d) Polypropylene/Al_2O_3

5.2 MECHANICAL CHARACTERISTICS

Evaluation of strength and other mechanical properties of any new composites are essential from research as well as functionality point of view. In the present work, a wealth of property data has been generated by conducting different characterization tests under controlled laboratory conditions to evaluate some of the mechanical characteristics of composites fabricated for this work. The property values of single as well as hybrid filler composites are presented below.

5.2.1 Micro-hardness

Hardness is the ability of the material to resist indentation and is considered as one of the most important characteristic features of any multi-component

composite system. In the present work, micro-hardness values are measured and the test results for all the fabricated epoxy and PP based composites are presented in Tables 5.5 and 5.6 respectively. It is evident from the tables that with addition of fillers, micro-hardness of the composites improved irrespective of the matrix and filler type and this improvement is mainly a function of the filler content. For Set I epoxy composites, with addition of 25 vol% of AlN, the micro-hardness of epoxy improves from 0.087 GPa to 0.278 GPa which indicates an enhancement of about 220 % whereas, for Set II epoxy composites, 25 vol% of Al_2O_3 improves the micro-hardness of epoxy by about 280 % i.e. to 0.331 GPa. It can be seen that, with Al_2O_3 as the filler material, hardness of the polymers increases to greater extent as compared to its counterpart AlN which can be attributed to the obvious reason that Al_2O_3 is harder than AlN.

As far as the hybrid filler composites considered in this work are concerned, the mean micro-hardness values of the epoxy composites exhibit improved hardness not only with the increase in the content of AlN/Al_2O_3, but also with increasing SGM content. In fact, it is seen that the incorporation of SGM with either of the fillers in epoxy results in sharp increase in its micro-hardness value which is obvious because of very high hardness value of SGM. For the Set III epoxy composites, the maximum hardness is obtained for reinforcement of 15 vol% AlN and 15 vol% SGM. In this case, the hardness value reaches 0.385 GPa which is around 342 % more than that of neat epoxy. For the Set IV epoxy composites, this value goes further high and an improvement of about 380% is obtained i.e. micro-hardness value reaches 0.419 GPa, when 15 vol % $Al_2O_3$and 15 vol% SGM are reinforced in epoxy matrix (Table 5.5).

Similarly, for the Set I PP composites, micro-hardness of PP (0.059 GPa) is found to be increased by about 250% and reach a value of 0.208 GPa when 25 vol% of AlN is added. This increment is about 325% i.e. hardness reaches 0.252 GPa when 25 vol% of Al_2O_3 is added (Set II PP composites). Likewise, for the Set III PP composites the maximum micro-hardness value is obtained when a mixture of 15 vol% AlN and 15 vol% SGM is reinforced. In this case, the

composite micro-hardness value reaches 0.319GPa which is around 440% higher than that of neat PP.

Table 5.5 Micro-hardness of epoxy based composites

Single Filler			**Hybrid Filler**			
Filler content (vol %)	Micro hardness (GPa)		Composition	Micro hardness (GPa)	Composition	Micro hardness (GPa)
	EP/AlN	EP/Al_2O_3				
0	0.087	0.087	EP + 5 vol % AlN + 5 vol % SGM	0.167	EP + 5 vol % Al_2O_3 + 5 vol % SGM	0.186
5	0.118	0.138	EP + 10 vol % AlN + 10 vol % SGM	0.274	EP + 10 vol % Al_2O_3 + 10 vol % SGM	0.298
10	0.146	0.179	EP + 15 vol % AlN + 15 vol % SGM	0.385	EP + 15 vol % Al_2O_3 + 15 vol % SGM	0.419
15	0.182	0.218	EP + 5 vol % AlN + 10 vol % SGM	0.246	EP + 5 vol % Al_2O_3 + 10 vol % SGM	0.271
20	0.226	0.274	EP + 15 vol % AlN + 10 vol % SGM	0.318	EP + 15 vol % Al_2O_3 + 10 vol % SGM	0.343
25	0.278	0.331	EP + 10 vol % AlN + 10 vol % SGM	0.362	EP + 20 vol % Al_2O_3 + 10 vol % SGM	0.391

** EP: Epoxy, SGM: Solid Glass Micro-spheres*

Table 5.6 Micro-hardness of polypropylene based composites

Single Filler			**Hybrid Filler**			
Filler content (vol %)	Micro hardness (GPa)		Composition	Micro hardness (GPa)	Composition	Micro hardness (GPa)
	PP/AlN	PP/Al_2O_3				
0	0.059	0.059	PP + 5 vol % AlN + 5 vol % SGM	0.128	PP + 5 vol % Al_2O_3 + 5 vol % SGM	0.161
5	0.082	0.095	PP + 10 vol % AlN + 10 vol % SGM	0.203	PP + 10 vol % Al_2O_3 + 10 vol % SGM	0.243
10	0.112	0.137	PP + 15 vol % AlN + 15 vol % SGM	0.346	PP + 15 vol % Al_2O_3 + 15 vol % SGM	0.382
15	0.141	0.176	PP + 5 vol % AlN + 10 vol % SGM	0.182	PP + 5 vol % Al_2O_3 + 10 vol % SGM	0.223
20	0.179	0.216	PP + 15 vol % AlN + 10 vol % SGM	0.255	PP + 15 vol % Al_2O_3 + 10 vol % SGM	0.297
25	0.208	0.252	PP + 10 vol % AlN + 10 vol % SGM	0.319	PP + 20 vol % Al_2O_3 + 10 vol % SGM	0.348

** PP: Polypropylene, SGM: Solid Glass Micro-spheres*

For the Set IV PP composites, this value becomes even higher and an improvement of about 490% is obtained i.e. micro-hardness value reaches 0.348GPa, when 15 vol % $Al_2O_3$and 15 vol % SGM are reinforced in PP matrix (Table 5.6). Few reports are also available in the past on similar increasing trend in the value of micro-hardness for different filler-matrix combinations for both single filler and multi-filler systems [38, 41, 196].

As far as the comparison between the epoxy and PP based composites is concerned, the former ones are found to be always harder than the later ones. But for the same filler composition, the rate of increase in composite micro hardness is always found to be higher in case of PP composites as compared to epoxy composites. This may be primarily because of the better uniformity in distribution of fillers in PP composites than the epoxy composites as different techniques have been employed for the fabrication of these two classes of composite systems. The other possible reason might be the fact that the difference in intrinsic hardness values of fillers and PP is more than that between the fillers and epoxy.

5.2.2 Tensile Strength

Tensile strengths of the fabricated composite specimens are evaluated and the test results for all the epoxy and PP composites are presented in Tables 5.7 and 5.8 respectively. It is noticed that with addition of different fillers, tensile strength of both the polymers decreases and this decrement is a function of the filler loading. However, the rates of decrease for both the resins are quite marginal. While the tensile strength of neat epoxy is 59 MPa, it decreases by about 14.7% and reaches 50.3 MPa with the incorporation of 25 vol% of AlN (Set I epoxy composites). For the epoxy/Al_2O_3 composites (Set II epoxy composites), the tensile strength is found to be decreasing by about 12.9% when it attains a value 51.4 MPa with a filler content of 25 vol% (Table 5.7). Similarly, the tensile strength of PP reduces by 13.8% and 10.8% with inclusion

of 25 vol% of AlN (Set I PP composites) and Al_2O_3 (Set II PP composites) respectively.

Table 5.7 Tensile strength of epoxy based composites

Single Filler			**Hybrid Filler**			
Filler content (vol %)	Tensile strength (MPa)		Composition	Tensile strength (MPa)	Composition	Tensile strength (MPa)
	EP/AlN	EP/Al_2O_3				
0	59.0	59.0	EP + 5 vol % AlN + 5 vol % SGM	56.8	EP + 5 vol % Al_2O_3 + 5 vol % SGM	57.5
5	57.1	57.7	EP + 10 vol % AlN + 10 vol % SGM	55.1	EP + 10 vol % Al_2O_3 + 10 vol % SGM	56.3
10	55.8	56.9	EP + 15 vol % AlN + 15 vol % SGM	54.2	EP + 15 vol % Al_2O_3 + 15 vol % SGM	55.1
15	53.9	55.8	EP + 5 vol % AlN + 10 vol % SGM	56.4	EP + 5 vol % Al_2O_3 + 10 vol % SGM	57
20	52.4	53.3	EP + 15 vol % AlN + 10 vol % SGM	53.6	EP + 15 vol % Al_2O_3 + 10 vol % SGM	54.6
25	50.3	51.4	EP + 20 vol % AlN + 10 vol % SGM	51.2	EP + 20 vol % Al_2O_3 + 10 vol % SGM	52.3

** EP: Epoxy, SGM: Solid Glass Micro-spheres*

Table 5.8 Tensile strength of polypropylene based composites

Single Filler			**Hybrid Filler**			
Filler content (vol %)	Tensile strength (MPa)		Composition	Tensile strength (MPa)	Composition	Tensile strength (MPa)
	PP/AlN	PP/Al_2O_3				
0	45.0	45.0	PP + 5 vol % AlN + 5 vol % SGM	43.4	PP + 5 vol % Al_2O_3 + 5 vol % SGM	43.8
5	43.8	44.1	PP + 10 vol % AlN + 10 vol % SGM	41.6	PP + 10 vol % Al_2O_3 + 10 vol % SGM	42.9
10	42.1	43.5	PP + 15 vol % AlN + 15 vol % SGM	40.8	PP + 15 vol % Al_2O_3 + 15 vol % SGM	41.6
15	41.4	42.2	PP + 5 vol % AlN + 10 vol % SGM	42.9	PP + 5 vol % Al_2O_3 + 10 vol % SGM	43.5
20	40.2	41.3	PP + 15 vol % AlN + 10 vol % SGM	41.2	PP + 15 vol % Al_2O_3 + 10 vol % SGM	42.1
25	38.8	40.1	PP + 20 vol % AlN + 10 vol % SGM	39.9	PP + 20 vol % Al_2O_3 + 10 vol % SGM	40.8

** PP: Polypropylene, SGM: Solid Glass Micro-spheres*

It means the tensile strength which is 45 MPa for neat PP resin is reduced to 38.8 MPa and 40.1 MPa with incorporation of AlN and Al_2O_3 respectively (Table 5.8). This reduction in tensile strength with filler addition may be due to the fact that chemical bond strength between filler particles and the matrix body is not adequately strong to transfer the tensile load and due to the increase in void percentage in the composites with increase in filler content. Similar behaviour of variation in tensile strength has been reported previously by various researchers as well for a number of similar matrix-filler combinations [175, 202, 223]. Also, when the filler is Al_2O_3, decrease in tensile strength of both the resins are less compared to when AlN is filler material which is because of the obvious reason that Al_2O_3possesses higher strength value than its counterpart AlN. Again compression moulding is coming out to be a more efficient way to fabricate composite as compared to hand lay-up method as the percentage reduction in tensile strength of PP composite is less compared to epoxy composites.

It is further seen that the rate of decrease of tensile strength reduces when AlN/Al_2O_3 particles are premixed with SGM and are incorporated in resins mainly because of the perfect spherical shape of the SGM which reduces stress concentration inside the composite body. Among the various hybrid composites fabricated, for the Set III epoxy composites, highest reduction of 13.2 % is observed for 20 vol% AlN and 10 vol% SGM combination where tensile strength goes down to 51.2 MPa. Likewise, for the Set IV epoxy composites, maximum reduction of 11.4% is noticed for 20 vol% Al_2O_3 and 10 vol% SGM with tensile strength of 52.3 MPa (Table 5.7). Similar is the case when matrix material is changed from epoxy to PP, where for the Set III PP composites, 20 vol% AlN and 10 vol% SGM reduce PP tensile strength value to 39.9 MPa i.e. by 11.3 % and for the Set IV PP composites, 20 vol% Al_2O_3 and 10 vol% SGM reduce its tensile strength value to 40.8 MPa i.e. by 9.3 % (Table 5.8).

5.2.3 Compressive Strength

Compressive strengths of the fabricated specimens are evaluated and the test results for all the epoxy and PP composites are presented in Tables 5.9 and 5.10 respectively. It is noticed that with addition of fillers, compressive strength of both the polymers increases and this improvement is found to be more for increased filler content.

While the compressive strength of neat epoxy is 114 MPa, it increases by 34.5 % and reaches 153.4 MPa with the incorporation of 25 vol% of AlN (Set I epoxy composites) and with the incorporation of 25 vol% of Al_2O_3 (Set II epoxy composites) it increasesby39.8 % and reaches159.4 MPa (Table 5.9). Similarly, the compressive strength of PP which is 83 MPa increases to 116.4 MPa and 124.2 MPa with the incorporation of 25 vol% of AlN (Set I PP composites) and 25 vol% of Al_2O_3(Set II PP composites) respectively which is an enhancement of 40.2% and 49.6% respectively(Table 5.10). The improvement in compressive strength with filler addition is mainly because of the high compressive strength of filler material. Also, the increase in compressive strength with increased filler content is due to the favorable deformation processes facilitated by the presence of fillers in the matrix. Under a compressive loading situation, the fillers apparently aid the load bearing capability of a composite, rather than acting as stress raiser as is the case in tensile loading. Further, the fact that in a compression test, any crack or flaw introduced by dispersion of the filler will, if at all, get healed (closed) and made ineffective, contrary to the crack opening mechanism occurring in a tensile loading situation. Similar trend in regard to variation of compressive strength with filler content has been reported previously by few researchers for particulate filled polymer composites [19, 290]. Also, with Al_2O_3 as filler, increase in compressive strength of both the resins is more compared to AlN as filler which is possibly because Al_2O_3 possesses higher compressive strength than AlN. Here also, compression moulding is coming out to be a more efficient way to fabricate composite as

compared to hand lay-up method as the percentage improvement is more for PP composites compared to epoxy composites.

Table 5.9 Compressive strength of epoxy based composites

Single Filler			**Hybrid Filler**			
Filler content (vol %)	Compressive strength (MPa)		Composition	Compressive strength (MPa)	Composition	Compressive strength (MPa)
	EP/AlN	EP/Al_2O_3				
0	114.0	114.0	EP + 5 vol % AlN + 5 vol % SGM	125.3	EP + 5 vol % Al_2O_3 + 5 vol % SGM	129.2
5	120.8	123.7	EP + 10 vol % AlN + 10 vol % SGM	138.7	EP + 10 vol % Al_2O_3 + 10 vol % SGM	145.6
10	127.4	132.3	EP + 15 vol % AlN + 15 vol % SGM	154.2	EP + 15 vol % Al_2O_3 + 15 vol % SGM	160.9
15	136.8	141.9	EP + 5 vol % AlN + 10 vol % SGM	129.4	EP + 5 vol % Al_2O_3 + 10 vol % SGM	133.8
20	144.5	151.4	EP + 15 vol % AlN + 10 vol % SGM	150.5	EP + 15 vol % Al_2O_3 + 10 vol % SGM	155.4
25	153.4	159.4	EP + 20 vol % AlN + 10 vol % SGM	156.7	EP + 20 vol % Al_2O_3 + 10 vol % SGM	163.5

** EP: Epoxy, SGM: Solid Glass Micro-spheres*

Table 5.10 Compressive strength of polypropylene based composites

Single Filler			**Hybrid Filler**			
Filler content (vol %)	Compressive strength (MPa)		Composition	Compressive strength (MPa)	Composition	Compressive strength (MPa)
	PP/AlN	PP/Al_2O_3				
0	83.0	83.0	PP + 5 vol % AlN + 5 vol % SGM	92.1	PP + 5 vol % Al_2O_3 + 5 vol % SGM	96.8
5	88.7	91.8	PP + 10 vol % AlN + 10 vol % SGM	102.9	PP + 10 vol % Al_2O_3 + 10 vol % SGM	108.7
10	94.2	99.4	PP + 15 vol % AlN + 15 vol % SGM	118.7	PP + 15 vol % Al_2O_3 + 15 vol % SGM	126.5
15	100.5	106.5	PP + 5 vol % AlN + 10 vol % SGM	95.8	PP + 5 vol % Al_2O_3 + 10 vol % SGM	99.2
20	108.3	115.7	PP + 15 vol % AlN + 10 vol % SGM	114.3	PP + 15 vol % Al_2O_3 + 10 vol % SGM	123.4
25	116.4	124.2	PP + 20 vol % AlN + 10 vol % SGM	121.2	PP + 20 vol % Al_2O_3 + 10 vol % SGM	129.9

** PP: Polypropylene, SGM: Solid Glass Micro-spheres*

Among the various hybrid composites fabricated, for the Set III epoxy composites, a maximum enhancement of 37.4 % is observed for 20 vol% AlN and 10 vol% SGM where compressive strength valuereaches156.7 MPa. Likewise, for the Set IV epoxy composites, highest improvement of 43.4 % is noticed for 20 vol% Al_2O_3 and 10 vol% SGM with compressive strength value of 163.5 MPa (Table 5.9). Similar is the case when matrix material is changed from epoxy to PP, where for the Set III PP composites, 20 vol% AlN and 10 vol% SGM combination enhances the compressive strength of PP to 121.2 MPa i.e. by 46 % and where for the Set IV PP composites, 20 vol% Al_2O_3 and 10 vol% SGM combination enhances its compressive strength to 129.9 MPa i.e. by 56.5 % (Table 5.10).

Chapter Summary

Several important conclusions emerge from the extensive results obtained in these studies carried out on epoxy composites with single and hybrid filler systems and polypropylene composites with similar fillers, with regard to their physical, mechanical and micro-structural behaviour. The results presented in this chapter clearly indicate a trendy characterization in the behaviour of different particulate composites studied and they provide a very important criterion for the choice of the composites for specific needs.

The next chapter presents the test results related to the thermal and dielectric characteristics of all the epoxy based composites considered in the present work.

*****

Chapter 6

Results and Discussion – II

Thermal and Dielectric Characteristics of Epoxy Based Composites

Chapter 6

Results and Discussion – II

THERMAL AND DIELECTRIC CHARACTERISTICS OF EPOXY BASED COMPOSITES

This chapter presents the calculated and measured values of thermal and dielectric properties of the epoxy based composites filled with different fillers. The relative effects of different filler materials on various thermal and dielectric properties of the composites have also been discussed. It also presents the experimental validation of the proposed models (Chapter 3) related to the effective thermal conductivity of the composites.

6.1 THERMAL CHARACTERISTICS

6.1.1 Effective thermal conductivity (k_{eff})

Effective thermal conductivity of epoxy based composites reinforced with single filler:

The thermal conductivities of epoxy composites filled with micro-sized AlN particles (Set I epoxy composites) with filler volume fraction ranging from 0 % to 25 % are shown in Figure 6.1, whereas for micro-sized Al_2O_3 particles (Set II epoxy composites) as filler are shown in Figure 6.2. The figures show comparisons among the values of thermal conductivity calculated from some well-established theoretical models [127, 129, 132, 141], those obtained from the proposed mathematical model (Equation 3.20) and the measured values. It may be noted that, while the intrinsic thermal conductivity of thermoset polymer epoxy is 0.363 W/m-K, that of aluminium nitride is 160 W/m-K and of aluminium oxide is 35 W/m-K. Thus the conductivities of both the aluminium based ceramic fillers used in this work are much greater than that of the neat polymer. Therefore, the addition of either of the fillers to epoxy is expected to improve the k_{eff} of composites and this is reflected in Figures 6.1 and 6.2. It is but obvious that as the filler content in the matrix increases, there will be monotonic improvement in the effective conductivity.

This can be explained as follows; since the polymer is less conductive, the resistance to heat flow within an unfilled polymer body is quite high. But when the particulate fillers are added to it and the filler content in the polymer gradually increases, the space filled with epoxy resin between consecutive conductive filler particles reduces. As a result of which the overall resistance offered to heat flow becomes relatively less and subsequently the thermal conductivity of the composite system increases.

It is also observed that the proposed model is in good agreement with measured data whereas other established models are underestimating the value of effective thermal conductivity. The deviation of values obtained from the existing models with the measured ones might be attributed to the assumptions taken for the respective models most of which are often unrealistic. Further, for low volume fraction of filler particles, a marginal increase in the value of thermal conductivity is observed as they can disperse randomly in the epoxy matrix and has weak interaction with one another. As the volume fraction of filler increases, the particles begin to touch each other, resulting in the formation of conductive path, due to which a sudden jump in the value of thermal conductivity is observed. The limiting filler content (volume fraction) at which such sudden rise in k_{eff} of the composite is noticed is called the percolation threshold of that particular filler in the resin. For epoxy/AlN composites, the percolation threshold reaches when filler content increases beyond 17.5 vol% and for epoxy/Al_2O_3 composites, the percolation threshold reaches when filler content increases beyond 15 vol%. Beyond this, no theoretical model including the proposed model is able to estimate the conductivity value correctly. This can be attributed to the fact that, while deriving the present correlation, the inter-connectivity between the filler particles which are built up at high filler concentrations in the real composite have not taken care of.

Some more obvious observations are seen from Figure 6.1 and 6.2. For example, the experimentally measured values are less than the values obtained from proposed model up to the percolation threshold for each sample.

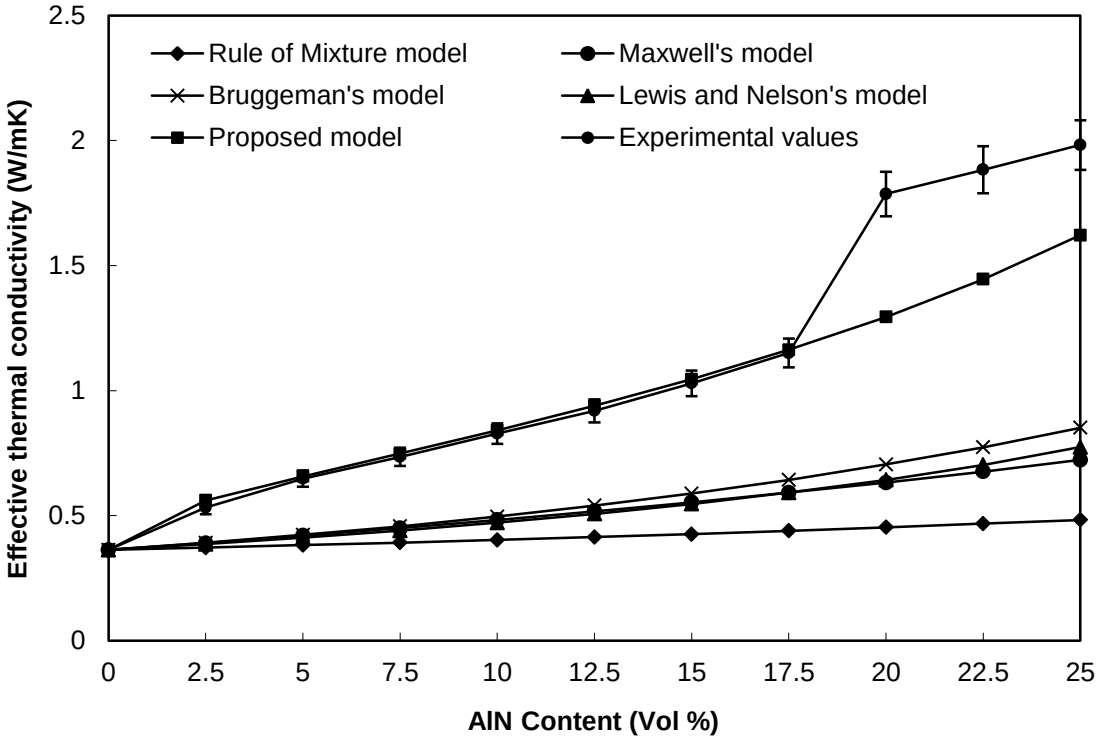

Fig 6.1 Effective thermal conductivity of Set I epoxy composites

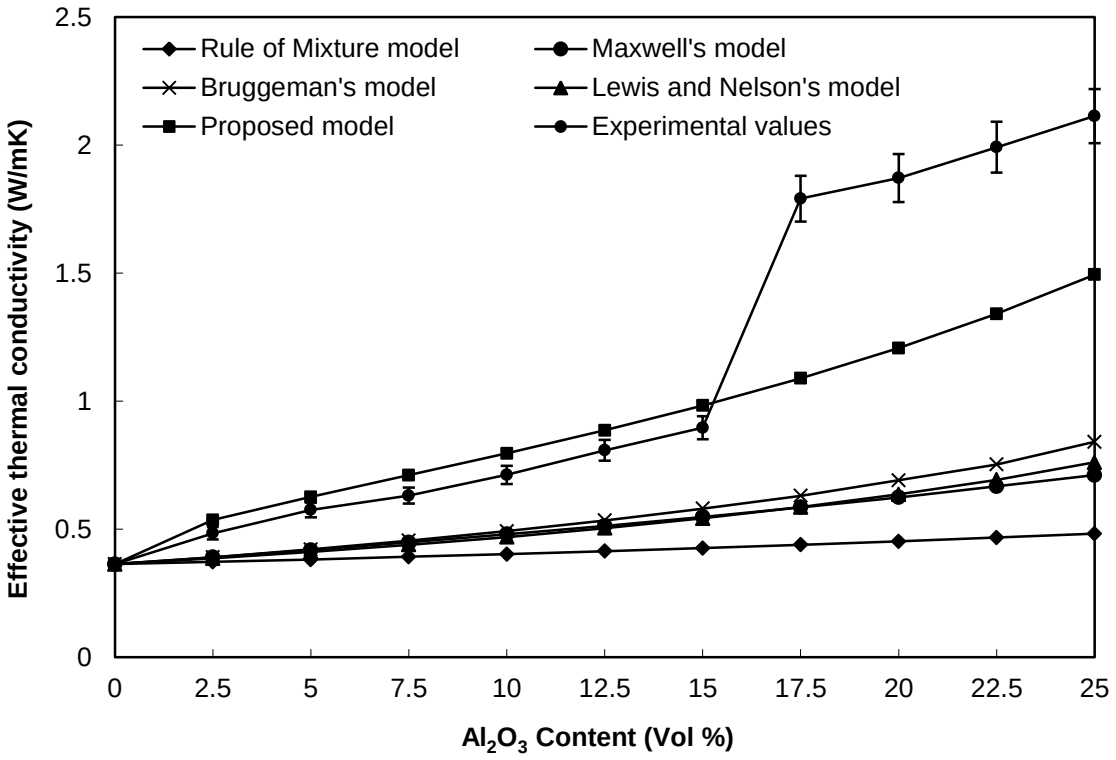

Fig 6.2 Effective thermal conductivity of Set II epoxy composites

It is because, some actual factors are not considered while deriving the theoretical model, such as thermal resistance between matrix and filler material and voids present. The volume fraction of air present in the composite material is a very important factor which affects its thermal conductivity, though the volume fraction and density of air is very small compared to the filler and matrix material but because of its very low thermal conductivity, its effect is noticeable.

Table 6.1 Comparison of proposed model and measured values along with associated error (For single filler epoxy composites)

Filler content (Vol%)	**Epoxy/AlN**			**Epoxy/Al_2O_3**		
	Effective thermal conductivity (W/m-K)		Absolute error (%)	Effective thermal Conductivity (W/m-K)		Absolute error (%)
	Proposed model	Measured value		Proposed model	Measured value	
2.5	0.560	0.532	5.26	0.536	0.484	10.74
5	0.657	0.648	1.39	0.626	0.575	8.86
7.5	0.748	0.735	1.77	0.711	0.631	12.6
10	0.841	0.828	1.57	0.796	0.712	11.8
12.5	0.939	0.919	2.18	0.886	0.808	9.65
15	1.045	1.029	1.55	0.983	0.896	9.71
17.5	1.163	1.150	1.13	1.089	1.791	39.2
20	1.294	1.786	27.55	1.207	1.872	35.5
22.5	1.445	1.883	23.26	1.341	1.992	32.7
25	1.621	1.982	18.21	1.494	2.114	29.3

With 25 vol% of filler content, the k_{eff} of epoxy/AlN composites reaches 1.982 W/m-K which is an improvement of around 446% as compared to virgin epoxy and with same amount of filler loading the k_{eff} of epoxy/Al_2O_3 composites improved by around 482 % and reaches 2.114 W/m-K. It can be observed that the rate of increase in thermal conductivity beyond percolation is more when Al_2O_3 is reinforced in epoxy as compared to when AlN as filler. It is because,

once the particles begin to touch each other, Al_2O_3 with its uniform distribution and low porosity of its composites form well organized conductive chains which shoot the thermal conductivity value to a higher side. Also it is discussed by Bigg [291] that when intrinsic thermal conductivity of the filler material is greater than 100 times that of the polymer matrix, there is no significant improvement in the composite effective thermal conductivity and the rate of increase in conductivity becomes stagnant. In the present case, Al_2O_3 possesses a thermal conductivity of about 100 times that of epoxy whereas conductivity of AlN is around 400 times, but the difference between k_{eff} of their composites is very less.

Table 6.1 presents the comparison between the measured values of k_{eff} and those obtained from the proposed model for composites with different filler content. The absolute error percentages associated with each set of readings are also given. It can be seen from the error column that there is a better agreement between the experimental value and the theoretical value up to the percolation threshold and the errors are well within an acceptable range (0-12%).

Effective thermal conductivity of epoxy based composites reinforced with hybrid fillers:

For multi filler composites, the effective thermal conductivity values of epoxy filled with AlN in different proportions with SGM (Set III epoxy composites) are shown in Figure 6.3 and those of epoxy filled with Al_2O_3 in different proportions with SGM (Set IV epoxy composites) are shown in Figure 6.4. The figures show comparisons among the values of thermal conductivity calculated from the proposed theoretical model (Equation 3.47) and the measured values. It can be seen from both the figures that the values obtained from the proposed model are in close approximation with the measured values for the entire range of filler content. Table 6.2 presents the model values and measured values together with the absolute errors associated with them. From the table it is clear that the deviations between the two values are in the narrow range of 8-11%. The reason

for this marginal deviation is because of the assumptions taken while deriving the correlation.

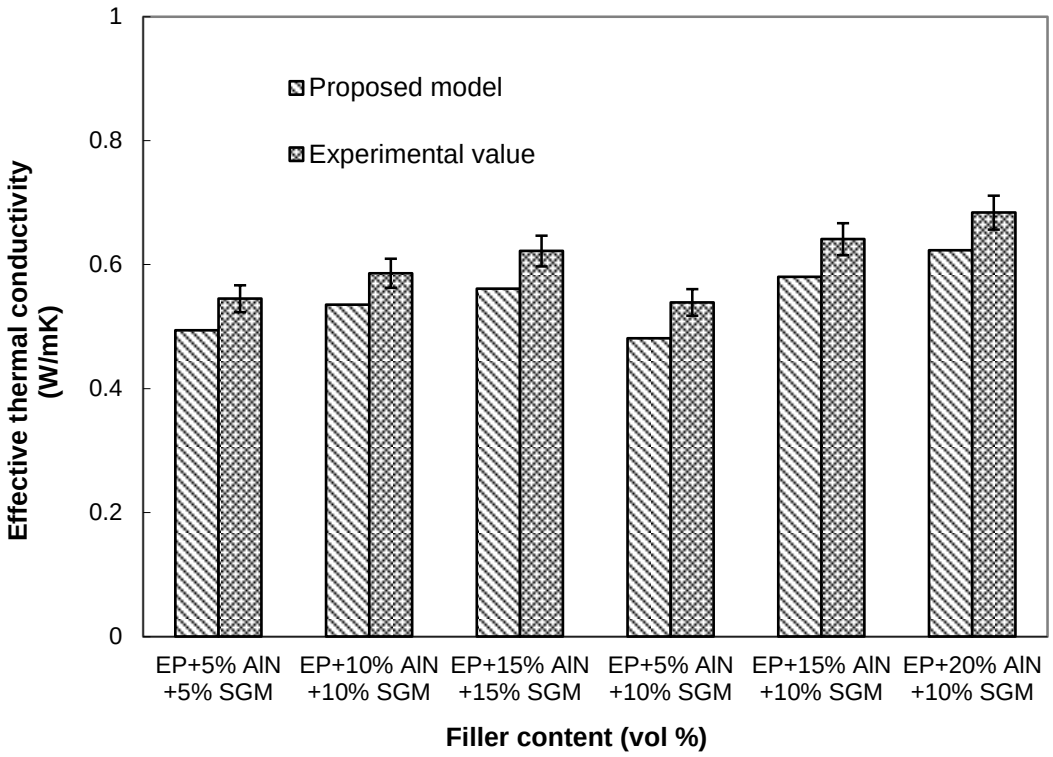

Fig 6.3 Effective thermal conductivity of Set III epoxy composites

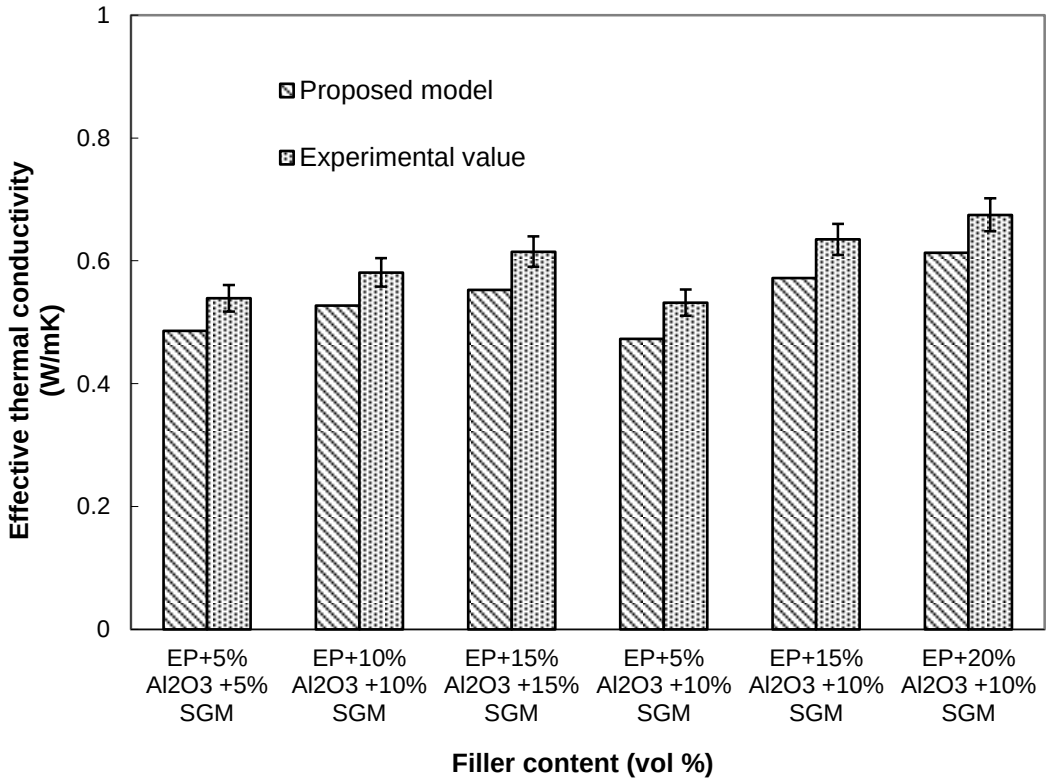

Fig 6.4 Effective thermal conductivity of Set IV epoxy composites

Table 6.2 Comparison of proposed model and measured values along with associated error (For hybrid filler epoxy composites)

Epoxy + AlN + SGM				Epoxy + Al_2O_3 + SGM			
Compositions	Effective thermal conductivity		Absolute error (%)	Compositions	Effective thermal conductivity		Absolute error (%)
	Proposed model	Measured value			Proposed model	Measured value	
Epoxy + 5 vol % AlN + 5 vol % SGM	0.494	0.545	9.35	Epoxy + 5 vol % Al_2O_3 + 5 vol %SGM	0.486	0.539	9.83
Epoxy + 10 vol % AlN + 10 vol % SGM	0.535	0.586	8.71	Epoxy + 10 vol % Al_2O_3 + 10 vol % SGM	0.527	0.581	9.29
Epoxy + 15 vol % AlN + 15 vol % SGM	0.561	0.622	9.81	Epoxy + 15 vol % Al_2O_3 + 15 vol % SGM	0.553	0.615	10.08
Epoxy + 5 vol % AlN +10 vol % SGM	0.481	0.539	10.76	Epoxy + 5 vol % Al_2O_3 +10 vol % SGM	0.473	0.532	11.09
Epoxy + 15 vol % AlN + 10 vol %SGM	0.58	0.641	9.51	Epoxy + 15 vol % Al_2O_3 + 10 vol %SGM	0.572	0.635	9.92
Epoxy + 20 vol % AlN + 10 vol % SGM	0.623	0.684	8.91	Epoxy + 20 vol % Al_2O_3 + 10 vol % SGM	0.613	0.675	9.18

Incorporation of SGM with either of the AlN/Al_2O_3 fillers in epoxy gives lesser value of thermal conductivity as compared to when AlN/Al_2O_3 are alone reinforced in matrix body which is mainly because of the insulative nature of SGM filler. The maximum k_{eff} among the various fabricated samples is obtained when 20 vol% AlN premixed with 10 vol% SGM is reinforced in epoxy resin for the Set III epoxy composites. The k_{eff} values goes up to 0.684 W/mK which is an improvement of 88.5% compared to neat epoxy (Figure 6.3). Similarly, among the Set IV epoxy composites, a maximum k_{eff} value of 0.675 W/mK is obtained for the composite filled with 20 vol% Al_2O_3 and 10 vol% SGM. This improvement in k_{eff} amounts to about 86% compared to the neat epoxy (Figure 6.4).

Interestingly, it can be seen that contrary to the single filler reinforced composites where experimental values are less compared to the values obtained from the proposed correlation; for hybrid filler composites, experimental values

are found to be higher. The main reason for lower values (measured) of conductivity below percolation threshold in case of single filler reinforced polymer composites is the presence of greater amount of voids in the composites. The volume fractions of voids for composites with hybrid fillers are relatively less as can be seen in chapter 5 (Tables 5.1, 5.2, 5.3 and 5.4). Further it can be seen that, unlike single filler reinforced composites, there is no phenomenon of percolation occurring for hybrid composites. This is solely because of the presence of insulative SGM particles which deter AlN/Al_2O_3 particles to form conductive chains inside the polymer matrix.

6.1.2 Glass transition temperature (T_g)

Glass transition temperatureof epoxy based composites reinforced with single filler:

The glass transition temperatures of the epoxy/AlN composites (Set I epoxy composites) and epoxy/Al_2O_3 composites (Set II epoxy composites) are shown in Figure 6.5 and 6.6 respectively. Glass transition temperature of neat epoxy is measured to be 98°C which gradually increases to 112^{o}C when AlN is reinforced in epoxy and to 116°C in case of Al_2O_3 reinforcement as the respective filler content is increased from 0 to 25 vol%.

Usually, addition of such filler increases the T_g of the composites, which results from the interaction between a filler and a polymer by forming a network structure between them. Because of this network structure, the movement of molecular segment is limited in it and hence the glass transition temperature increases [244].

The glass transition temperature of the polymer matrix depends on the free volume of the polymer, which is related to the affinity between the filler and the polymer matrix [175]. The filler which shows better affinity with matrix will result in higher glass transition temperature of composite. It is clear from the graphs that Al_2O_3 particles possess better affinity for epoxy matrix as compared to AlN particles. Similar trends regarding the glass transition temperature of

particulate filled polymer composites have also been reported by some other investigators earlier [208, 244].

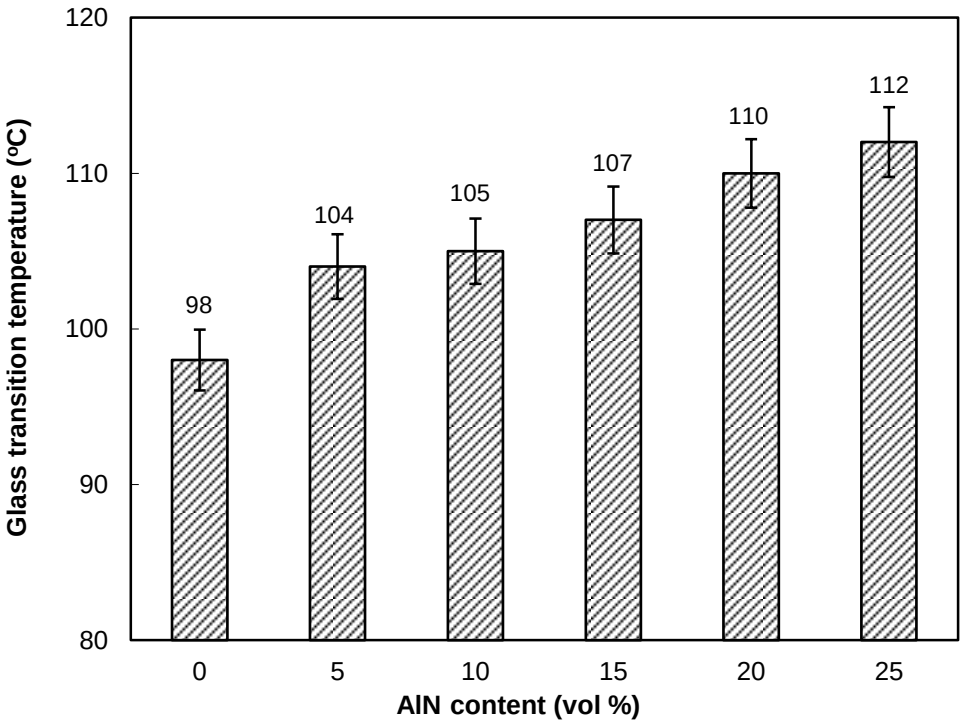

Fig 6.5 Glass transition temperatures of Set I epoxy composites

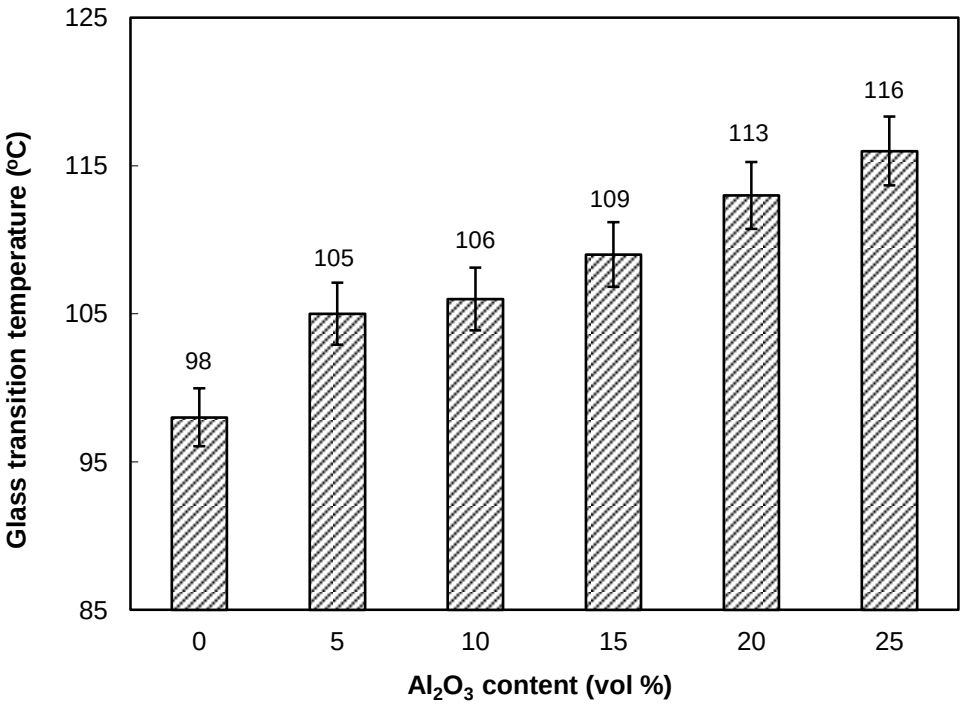

Fig 6.6 Glass transition temperatures of Set II epoxy composites

Glass transition temperature of epoxy based composites reinforced with hybrid fillers:

For multi filler composites, the glass transition temperature values of the epoxy filled with AlN in different proportions with SGM are shown in Figure 6.7 (Set III epoxy composites) and epoxy filled with Al_2O_3 in different proportions with SGM are shown in Figure 6.8 (Set IV epoxy composites).It can be seen from the figures that by increasing the content of either fillers, glass transition temperature of the respective composite system increases. For AlN premixed SGM when reinforced in epoxy resin, glass transition temperature reached maximum to 119°C for a combination of 20 vol% AlN and 10 vol% SGM whereas with a combination of 20 vol% Al_2O_3 and 10 vol% SGM this value goes higher and reaches 124°C.It can be observed that when AlN/Al_2O_3 fillers are added with SGM in the matrix body, the rate of increase of T_g accelerated which may be due to the greater affinity of SGM among all the fillers with epoxy. It is encouraging to note that the hybrid composites under present investigation exhibit improved T_g as compared to that of epoxy filled with single fillers, confirming a less mobile structure of the developed material.

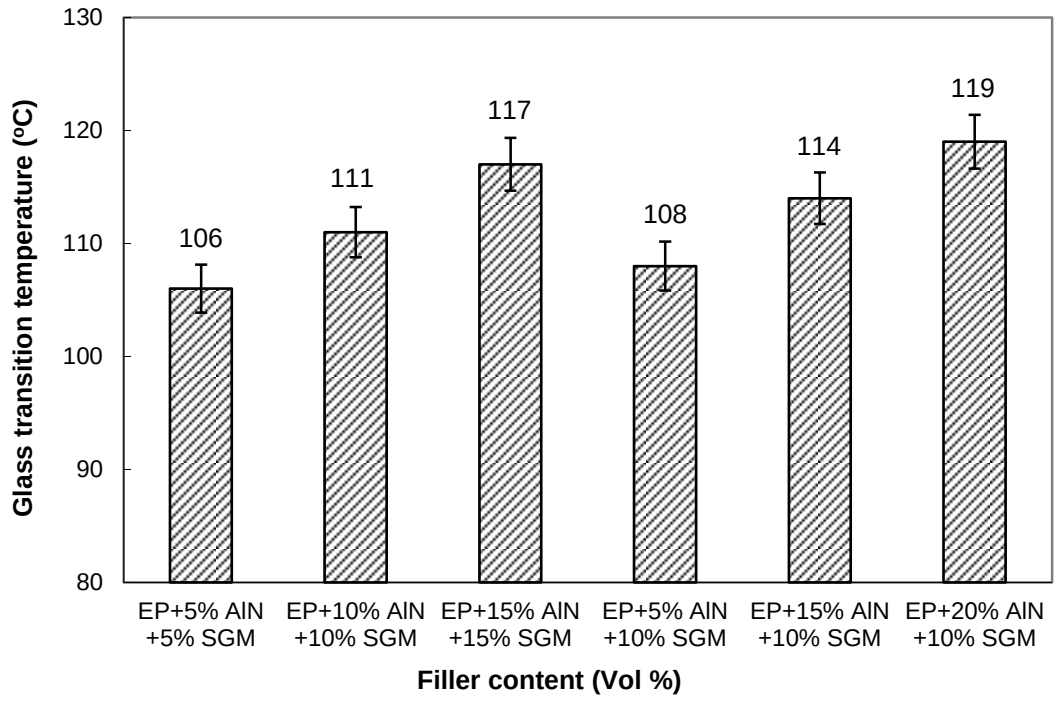

Fig 6.7 Glass transition temperatures of Set III epoxy composites

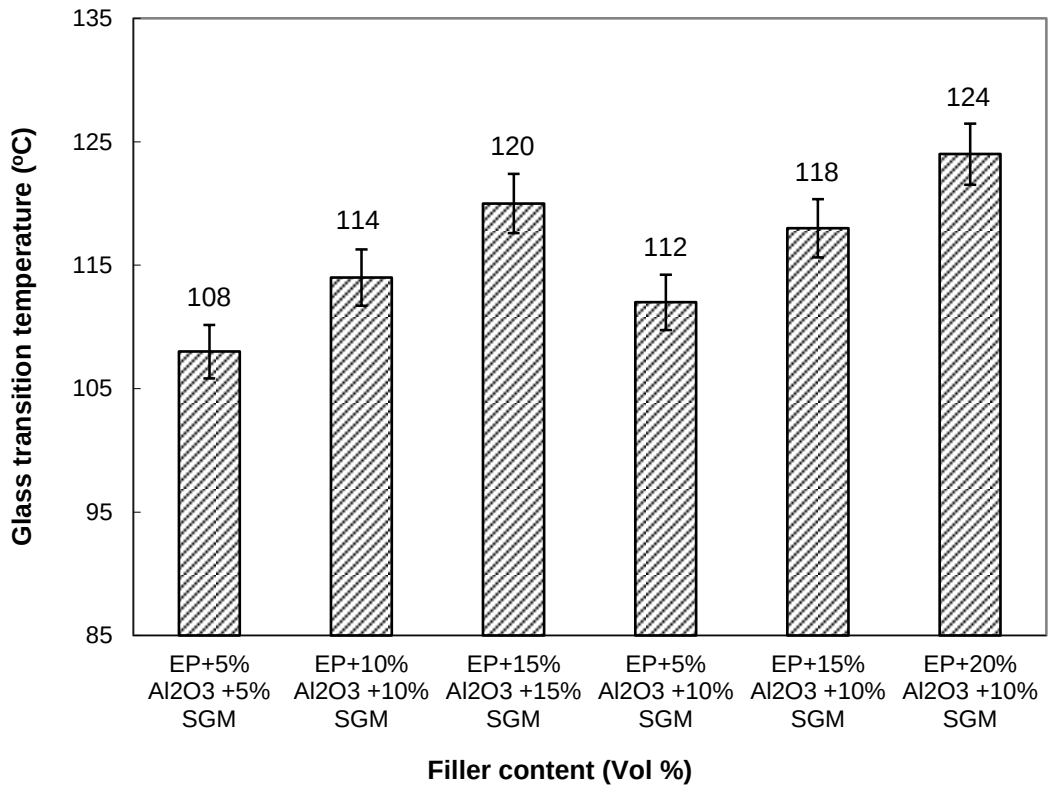

Fig 6.8 Glass transition temperatures of Set IV epoxy composites

6.1.3 Coefficient of thermal expansion

Coefficient of thermal expansion of epoxy based composites reinforced with single filler:

The intrinsic CTE values of AlN and Al_2O_3 are lower compared to that of neat epoxy. Hence, on heating, the polymer matrix will expand more as compared to these fillers. However, if the inter-phases are capable of transmitting stress, the expansion of the matrix will reduce giving rise to a reduced value of CTE for the composite as a whole. The variations in the theoretical and experimental values of CTE of the epoxy composites reinforced with micro-sized AlN (Set I epoxy composites) are shown in Figure 6.9 and epoxy composites reinforced with micro-sized Al_2O_3 (Set II epoxy composites) are shown in Figure 6.10 for different filler loading. Among the various theoretical models discussed in literature, few well established models are taken to make a comparison between the measured and the calculated values.

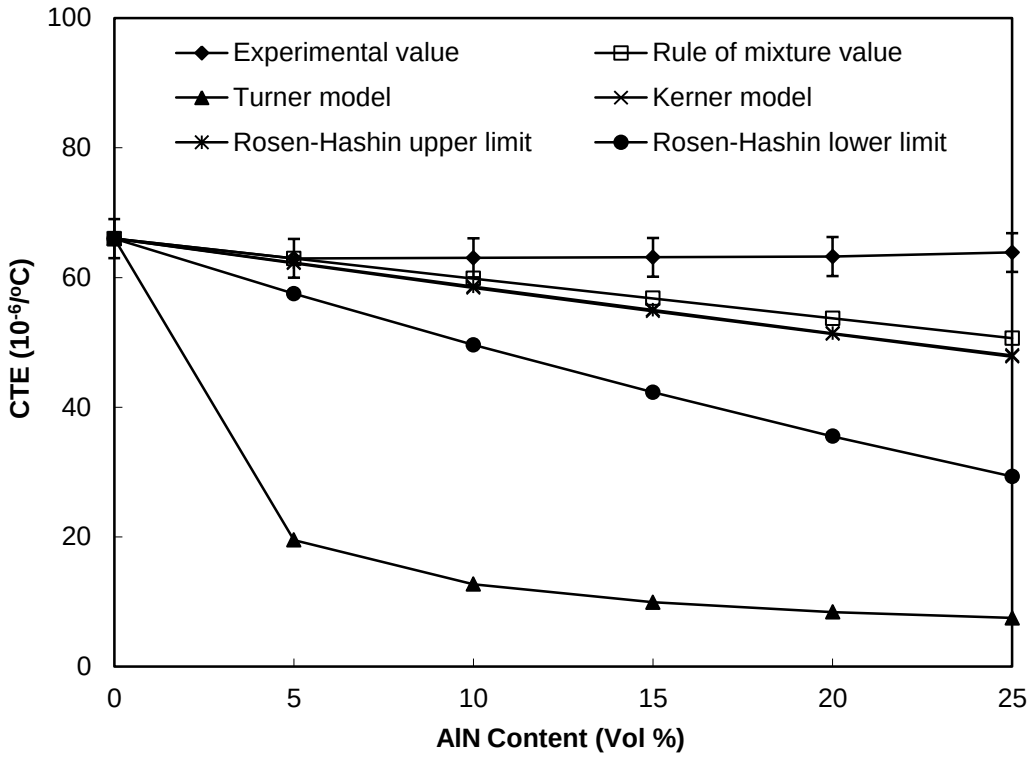

Fig 6.9 Coefficient of thermal expansion of Set I epoxy composites

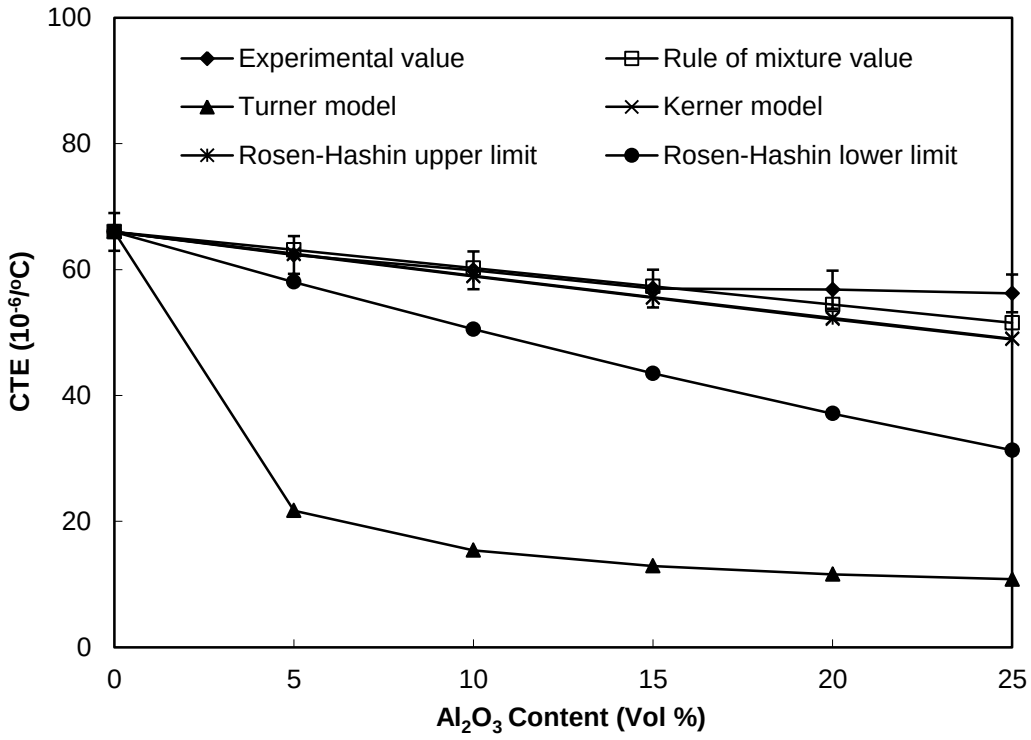

Fig 6.10 Coefficient of thermal expansion of Set II epoxy composites

The theoretical models that are considered for the sake of comparison in the present work are rule of mixture model [146], Turner model [149], Kerner model [150] and Rosen-Hashin model [155]. As expected, the incorporation of particles into the polymers results in a reduction in the value of CTE of the composites. This reduction is desirable and may be attributed to the restricted mobility of the polymer molecules arising out of adsorption of filler surfaces.

In case of epoxy/AlN composites, it is observed that, first the CTE value decreases from 66 × 10^{-6}/°C to 62.96 × 10^{-6}/°C for 5 vol% of AlN filler, and when further filler is added, a slight increase in CTE value is observed. The value of CTE is found to increase from 62.96 × 10^{-6}/°C to 63.86 × 10^{-6}/°C as the AlN content is raised from 5 to 25 vol%. The possible reason for such trend is the inevitable agglomeration of AlN particles within the matrix body at higher concentration. It is expected that the lack of uniform distribution or AlN in cluster form in some part does not provide adequate obstacles to the expansion of polymer chains.

A similar observation in case of polymer filled with clay is also reported elsewhere [292], where the addition of low clay content of 2 vol% in matrix decreased the CTE, but higher clay content of 4 vol% increased the CTE of same matrix material. Similarly, Yasmin et al. [96] reported that the addition of graphite platelets by 2.5 wt% decreases the CTE whereas addition of filler beyond 5 wt% increases the CTE of epoxy matrix.

In case of epoxy/Al_2O_3 composites, CTE decreases linearly as the filler loading increases, but for higher filler loading, not much reduction in the value of CTE is obtained after 15 vol%. The maximum decrease of about 15% in CTE is obtained at 25 vol% Al_2O_3 filled composites where the CTE reduces to a value of 56.2 × 10^{-6}/°C.

It can further be seen from both the figures that after certain filler loading, the experimental values are coming out of the range of lower and upper bound of Rosen-Hashin model and also value calculated from Kerner's model and rule of

mixture are slightly lower than the experimental value in case of epoxy/Al_2O_3 composites whereas for epoxy/AlN composites, this deviation increases to much higher values. The possible reason for such trend might be because of inevitable agglomeration in case of AlN as filler and slight agglomeration in case of Al_2O_3 as filler at higher concentration in epoxy composites fabricated by hand lay-up technique. Moreover for both sets of composites, Turner's model is far from satisfaction. This is not surprising as the Turner's model does not describe the actual stress state in the composites and consider only uniform hydrostatic stresses existing in the phases, while the stresses inside the composites are very complex.

Coefficient of thermal expansion of epoxy based composites reinforced with hybrid fillers:

For multi filler composites, the coefficient of thermal expansion values of the epoxy composites filled with AlN in different proportions with SGM (Set III epoxy composites) are shown in Figure 6.11 and epoxy composites filled with Al_2O_3 in different proportions with SGM (Set IV epoxy composites) are shown in Figure 6.12.

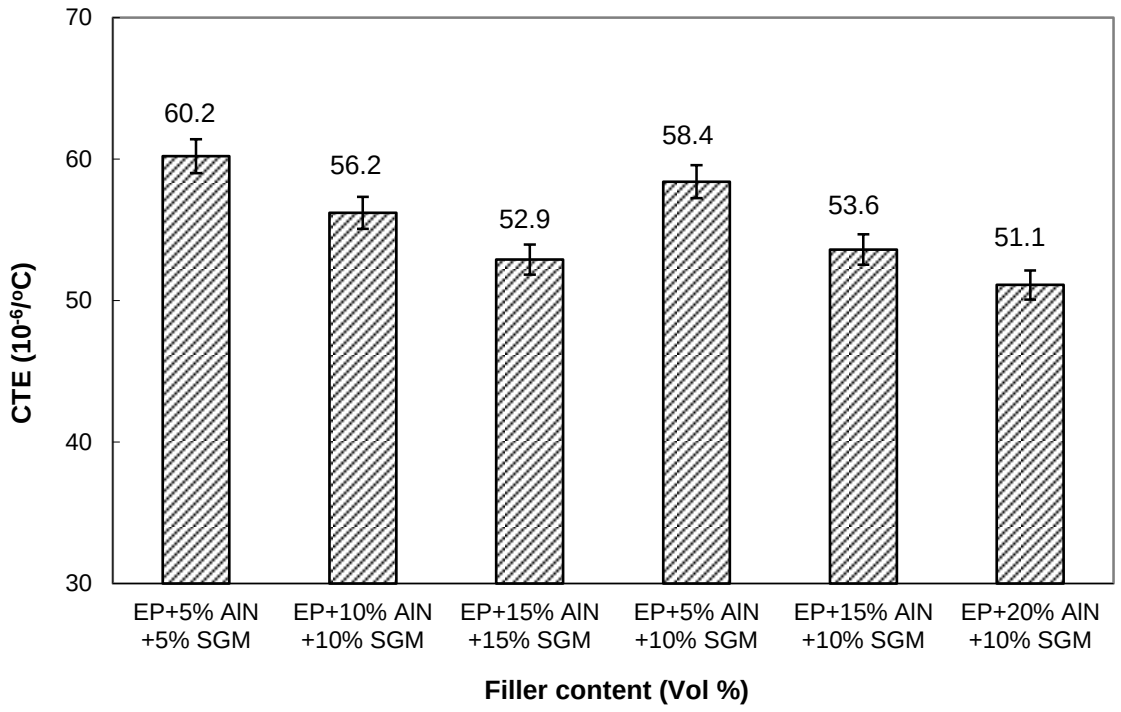

Fig 6.11 Coefficient of thermal expansion of Set III epoxy composites

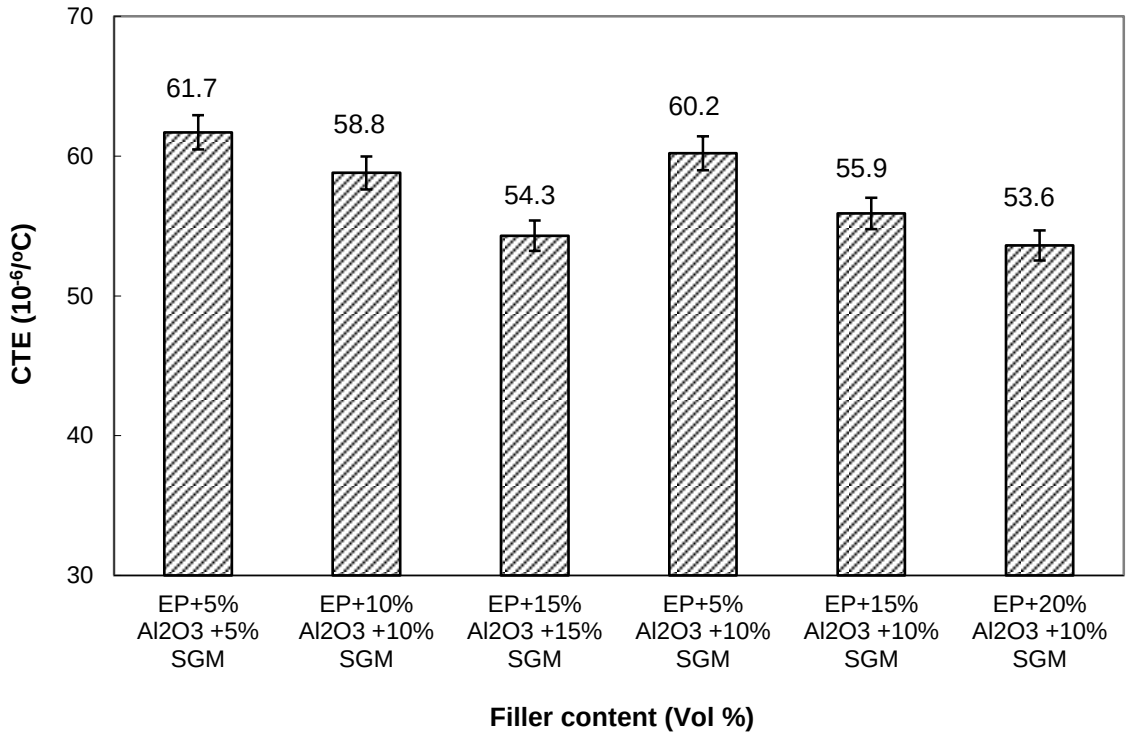

Fig 6.12 Coefficient of thermal expansion of Set IV epoxy composites

It can be seen from the figures that by increasing the content of either of the fillers, coefficient of thermal expansion of the respective composite system decreases appreciably. It can also be seen that when AlN/Al_2O_3 are premixed with SGM, an uniform decreasing trend is obtained unlike the decreasing-increasing trend in case of single filler reinforced epoxy composites.This trend of variation can be explained as; SGM restricts the formation of any cluster of micro-sized AlN/Al_2O_3 particles in the matrix body by providing uniform distribution to either filler. Also, SGM possesses low CTE value, due to which its incorporation reduces the CTE of epoxy composites remarkably. For AlN and SGM as filler, among the various samples, CTE of epoxy reduces to 51.1×10^{-6}/°C for a combination of 20 vol% AlN and 10 vol% SGM whereas with a combination of 20 vol% Al_2O_3 and 10 vol% SGM, CTE of epoxy reduces to 53.6×10^{-6}/°C. The CTE values obtained during experimentation encourages that combination of different fillers i.e. hybrid filler when reinforced in polymers provides more useful CTE values as compared to that of epoxy filled with single filler.

6.2 DIELECTRIC CHARACTERISTICS

Dielectric constant of epoxy based composites reinforced with single filler:

As already mentioned, dielectric constant is an important electrical property of any material which is defined as the ratio of the permittivity of a substance to the permittivity of free space.The materials used in integrated circuits must possess low dielectric properties for better device performance. The dielectric constant greatly influences the signal-carrying capacity and the speed of the device to propagate signals. Generally, low dielectric constant makes a high accumulation of the device itself and a high clock rate is possible. The delay in signal propagation in devices can be determined as [80]:

$$T_d = \frac{l}{c}\sqrt{\varepsilon_c} \tag{6.1}$$

where c and l are the velocity of light and transmission distance of the signal respectively. From equation 6.1, it can be seen that the time delay (T_d) caused in signal propagation is directly proportional to the square root of dielectric constant (ε_c). So a low dielectric constant is needed to reduce the delay time.

The dielectric constant variations of the Set I epoxy composites and the Set II epoxy composites with frequency in the range 1 kHz -1 MHz are shown in Figure 6.13 and 6.14 respectively. The result shows that for all sets of composites, there is a clear reduction in the value of dielectric constant within the measured frequency range. The decrease in the dielectric constant with an increase in frequency is due to the reason that the interfacial dipoles have less time to orient themselves in the direction of the alternating field when frequency rises [185]. Similar trend has been observed by Wu et al. [181] as well.

Generally in a matrix, a decrease in dipolar polarization is responsible for the reduction in the dielectric constant. But in polymer composites, the presence of fillers makes the system heterogeneous. As a result, in addition to the dipolar polarization, interfacial polarization is also present in composite materials. Thus the polymer molecules within the interphase region are restricted from dipolar

polarization compared to the molecules in the bulk matrix regions leading to the reduction in the dielectric constant [87].

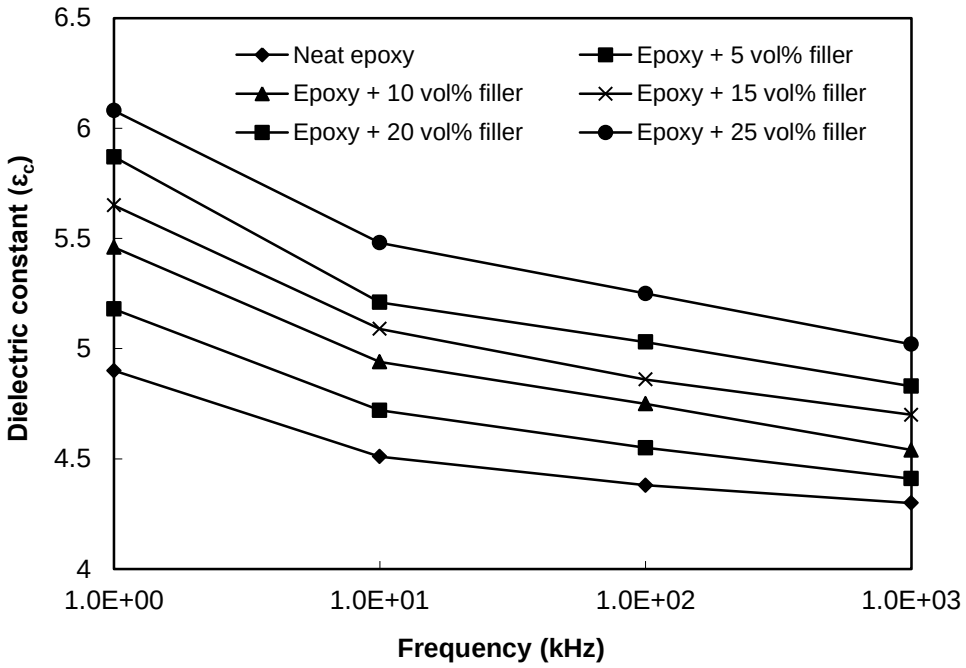

Fig 6.13 Variation of dielectric constant with frequency for Set I epoxy composites

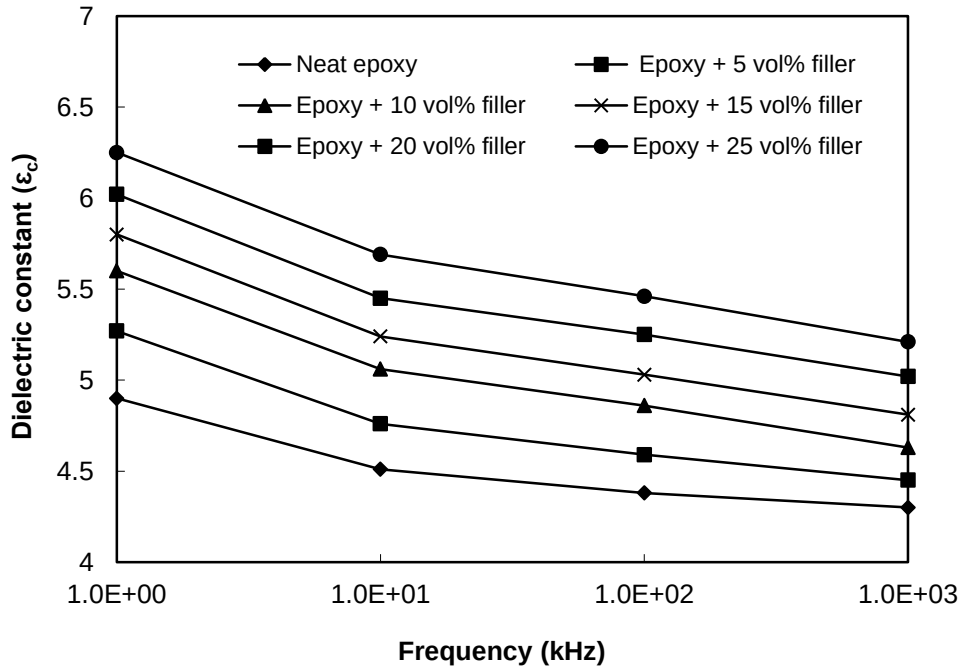

Fig 6.14 Variation of dielectric constant with frequency for Set II epoxy composites

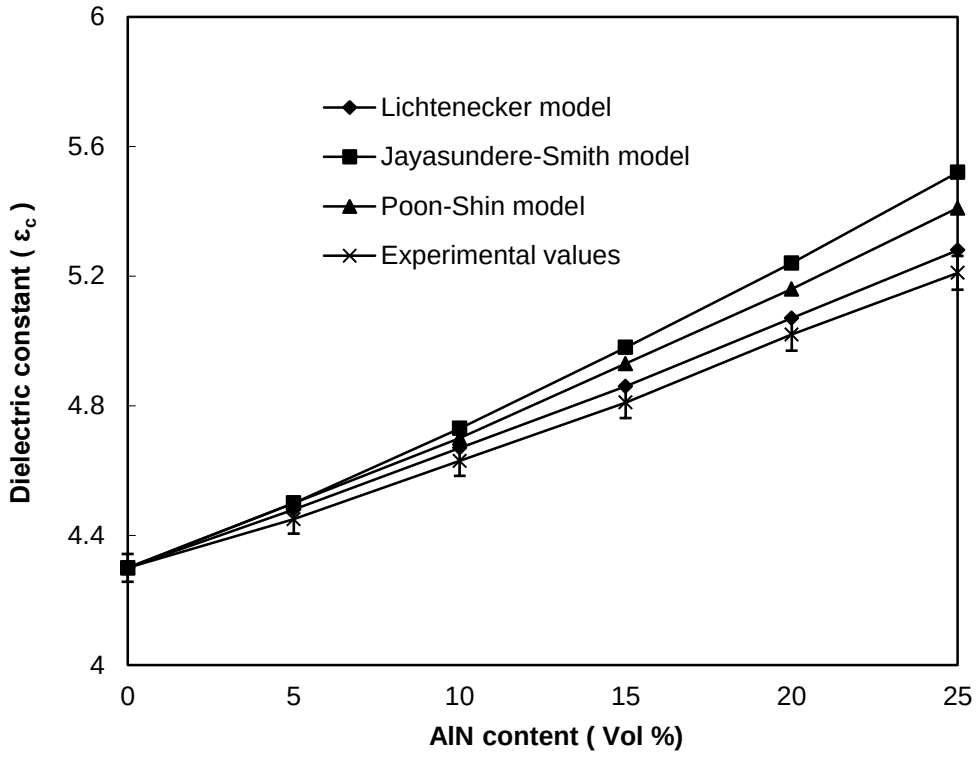

Fig 6.15 Measured and calculated dielectric constant at 1MHz for Set I epoxy composites

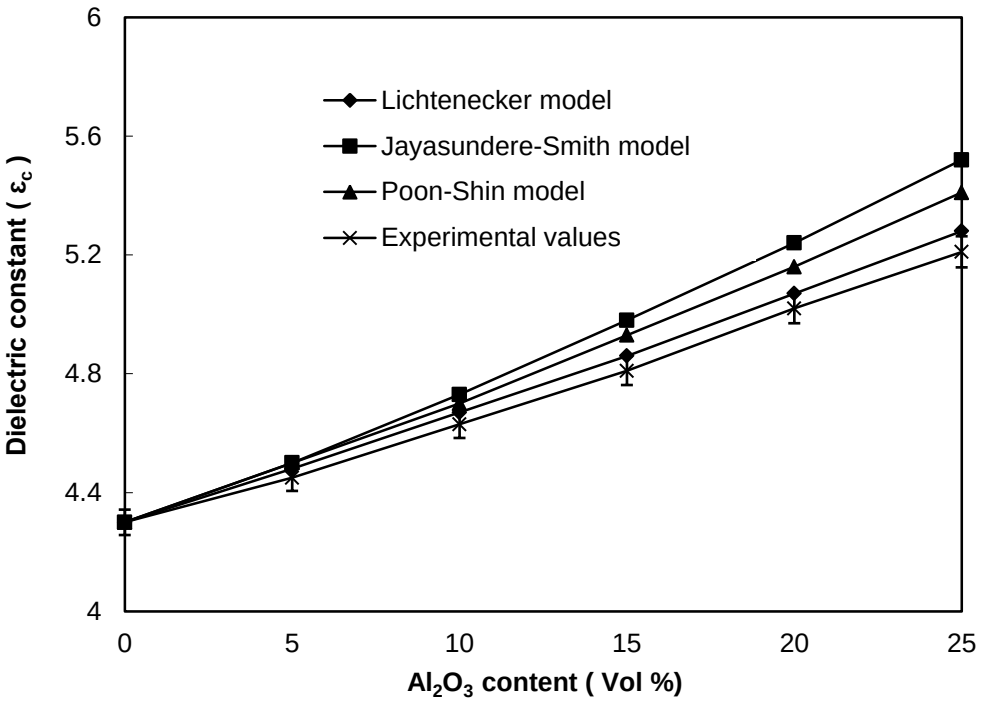

Fig 6.16 Measured and calculated dielectric constant at 1MHz for Set II epoxy composites

It can also be seen from the figures that the value of dielectric constant increases with filler content due to high dielectric constant value of AlN and Al_2O_3 compared to neat epoxy. For epoxy/AlN composites, dielectric constant reaches to 6.08 for maximum filler loading of 25 vol% at 1 kHz whereas for epoxy/Al_2O_3 composites it goes to 6.25 for similar filler loading and frequency.

Further, for two component systems, dielectric constants have been theoretically calculated by using equation 2.43, 2.48 and 2.49. These equations are the established correlations previously proposed by Lichtenecker [162], Jayasundare-Smith [166] and Poon-Shin [167] respectively. Figures 6.15 and 6.16 show the comparison between the experimental and the calculated values of dielectric constant obtained from these predictive equations at 1 MHz for epoxy/AlN and epoxy/Al_2O_3 composites respectively.

It can be seen from both the figures that the models are valid for low volume fraction and thereafter they deviate. Though Lichtenecker's model is in closest approximation to the measured values, Jayasundare-Smith and Poon-Shin models show more deviation from the experimental values. Also the measured values are always lower than the theoretical values invariably for all cases. As it is known that the dielectric constant of the composite depends on two factors i.e. the polarization associated with matrix material and filler particles, and it is also influenced by the interfacial polarization at the interface between matrix and filler. The deviations of the theoretical from the measured values are due to the reason that the equations have been developed without considering the effect of interface together with voids and defects.

It can also be seen that as the filler content increases, the experimental values deviate more from the corresponding theoretical values. It can be explained that with higher loading, the interfacial area between the matrix and filler increases and hence the influence of interface polarization on the dielectric constant also increases [183].

Dielectric constant of epoxy based composites reinforced with hybrid fillers:

For multi filler composites, when AlN /Al_2O_3 is premixed with SGM and reinforced in epoxy resin, similar trends in regard to the dielectric constant are observed as seen for single filler reinforced composites. The dielectric constant variations of the Set III epoxy composites and the Set IV epoxy composites as a function of frequency in the range 1 kHz -1 MHz are shown in Figures 6.17 and 6.18 respectively. The results show that for all sets of composites, irrespective of filler type and content, there is a slight reduction in the value of dielectric constant within the measured frequency range as experienced in case of the Set I and II epoxy composites.

Figures 6.19 and 6.20 show the measured values of dielectric constant at 1 MHz for the Set III epoxy composites and the Set IV epoxy composites respectively. It can be seen from the graph that the maximum value of dielectric constant reaches 4.63 for Set III epoxy composites and 4.75 for Set IV epoxy composites.

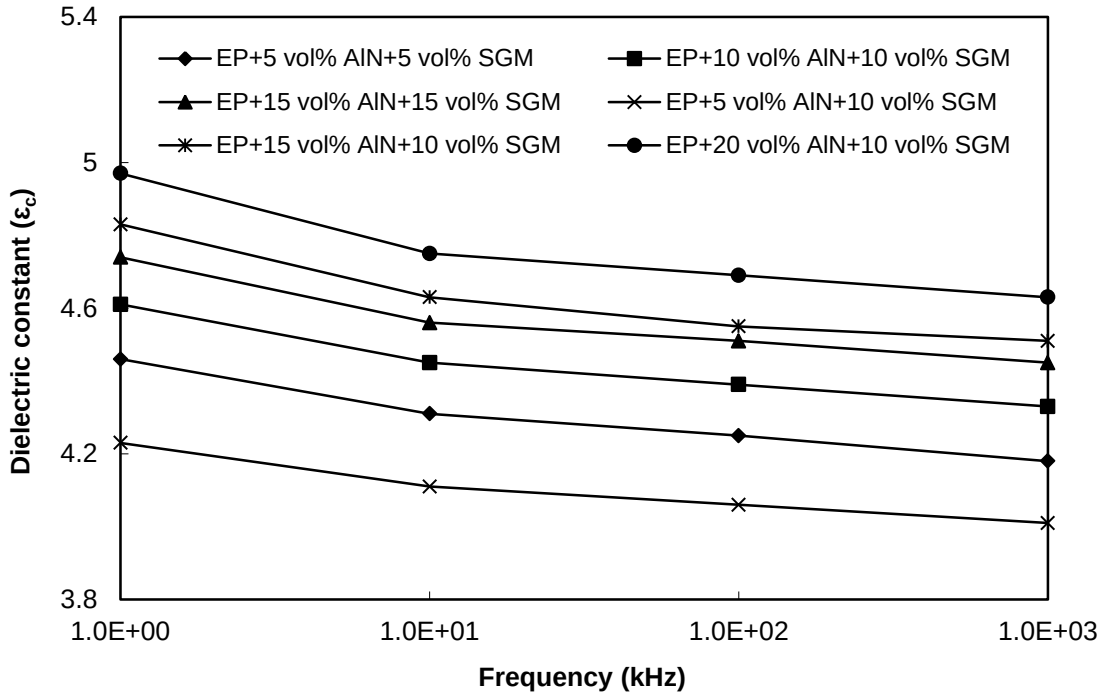

Fig 6.17 Variation of dielectric constant with operating frequency for Set III epoxy composites

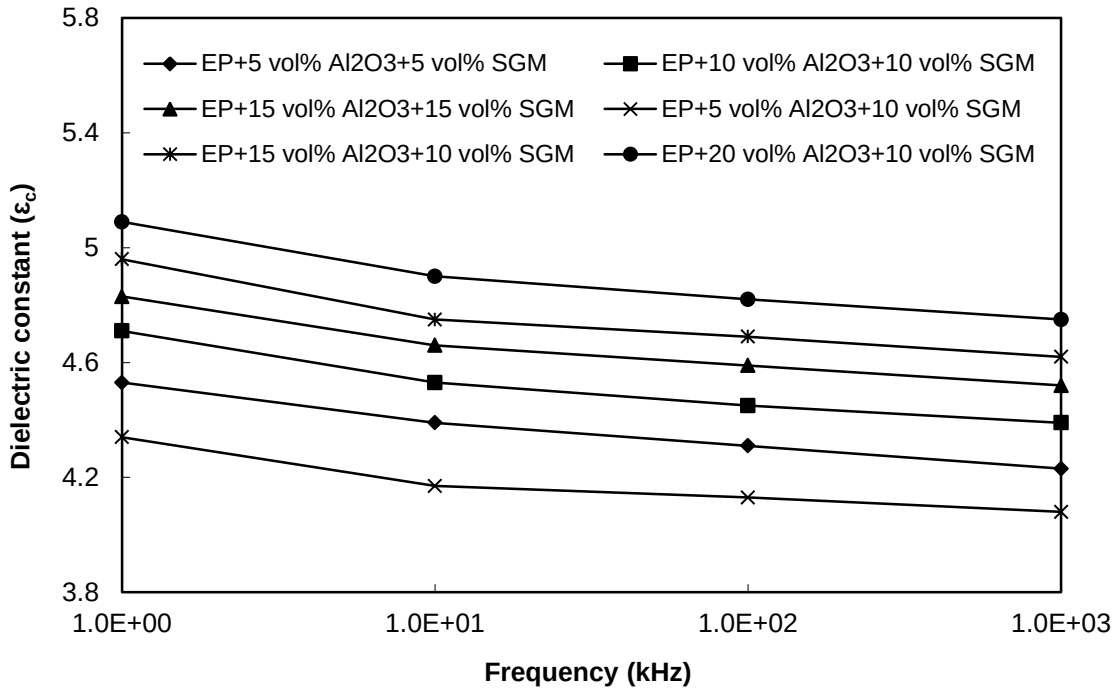

Fig 6.18 Variation of dielectric constant with operating frequency for Set IV epoxy composites

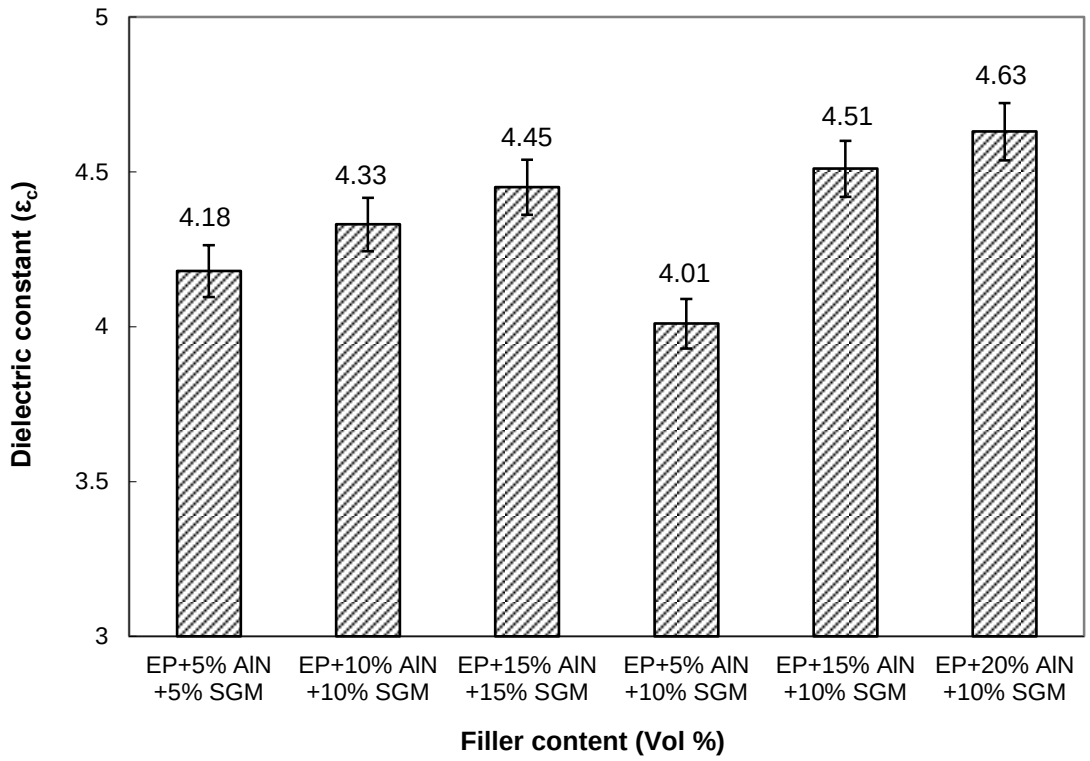

Fig 6.19 Dielectric constant at 1MHz for Set III epoxy composites

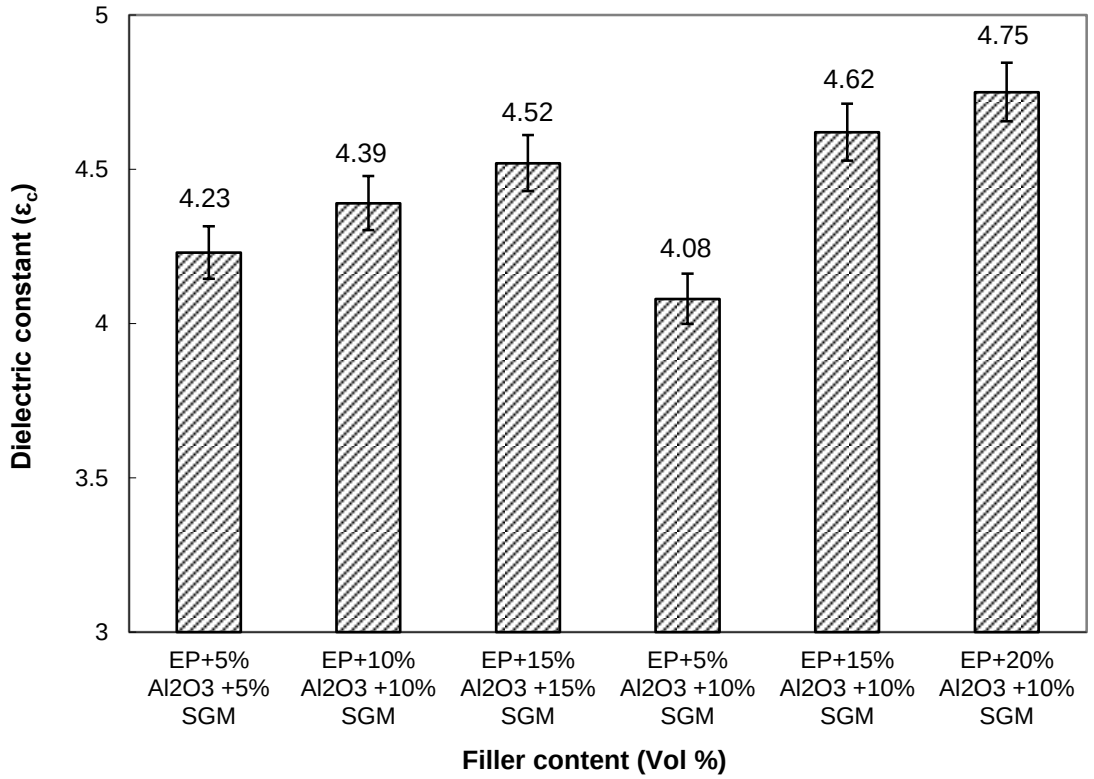

Fig 6.20 Dielectric constant at 1MHz for Set IV epoxy composites

These maximum values are obtained for composites with 20 vol% of AlN/Al_2O_3 and 10 vol% of SGM. This values increases with decrease in frequency and reaches a maximum of 4.97 and 5.09 for the Set III and IV epoxy composites respectively at lowest frequency of 1 kHz. It is clear from the graphs that as AlN/Al_2O_3 content increases; dielectric constant also increases whereas incorporation of SGM tries to bring down the value of dielectric constant. With SGM as one of the fillers, dielectric constant of epoxy based composites gets restricted to a very low value which is slightly higher than that of neat epoxy for wide range of filler content and operating frequency.

Chapter Summary

This chapter has provided:

- The results of the experiments conducted to evaluate the thermal conductivity of the epoxy based composites under study

- The validation of theoretical models developed and proposed in Chapter 3 through experimentation
- The synergistic effects of SGM and AlN/Al_2O_3 on effective conductivity of the epoxy based hybrid composites
- A complete picture on the percolation behaviour exhibited by the fillers in regard to the thermal conductivity of epoxy based composite systems
- Effects of single and hybrid fillers on glass transition temperature, coefficient of thermal expansion and dielectric constant of epoxy based composites

The next chapter presents the thermal and dielectric characteristics of polypropylene based composites under this research which would enable us to explore possible use of the composites in potential application areas.

*****

Chapter 7

Results and Discussion – III

Thermal and Dielectric Characteristics of Polypropylene Based Composites

Chapter 7

Results and Discussion – III

THERMAL AND DIELECTRIC CHARACTERISTICS OF POLYPROPYLENE BASED COMPOSITES

This chapter presents the calculated and measured values of thermal and dielectric properties of the polypropylene (PP) based composites filled with different fillers. The relative effects of different filler materials on various thermal and dielectric properties of the composites have also been discussed. It also presents the experimental validation of the proposed models (Chapter 3) related to the effective thermal conductivity of the composites.

7.1 THERMAL CHARACTERISTICS

7.1.1 Effective thermal conductivity (k_{eff})

Effective thermal conductivity of polypropylene based composites reinforced with single filler:

The effective thermal conductivities of polypropylene composites filled with micro-sized AlN particles (Set I PP composites) with filler volume fraction ranging from 0% to 25% are shown in Figure 7.1, whereas for micro-sized Al_2O_3 particles (Set II PP composites) as filler are shown in Figure 7.2. The figures show comparisons among the values of thermal conductivity calculated from some well-established theoretical models, those obtained from the proposed theoretical model (Eqn 3.20) and the measured values. The intrinsic thermal conductivity of thermoplastic polymer polypropylene is 0.11 W/m-K, which found to be improved as the conductive AlN/Al_2O_3 particles are reinforced in it and this can be clearly noted from the figures. It is again observed that the proposed model is in good agreement with the measured data whereas other established models are underestimating the value of effective thermal conductivity.

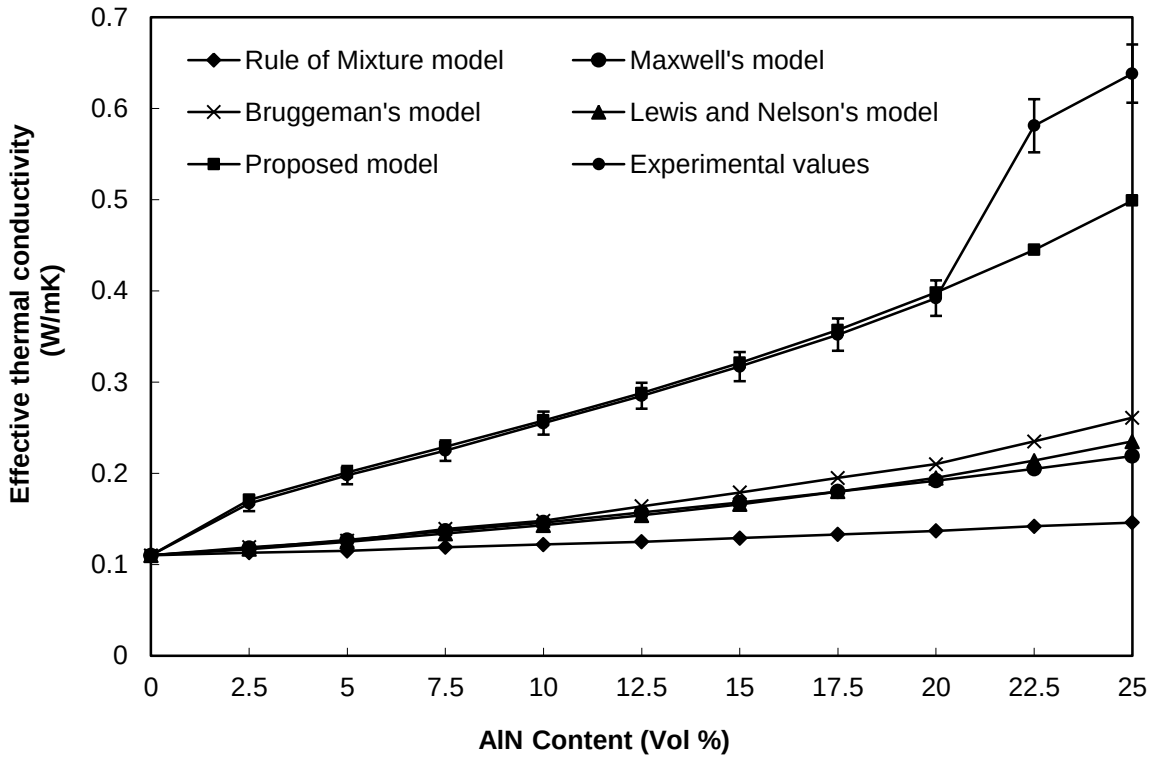

Fig 7.1 Effective thermal conductivity of Set I PP composites

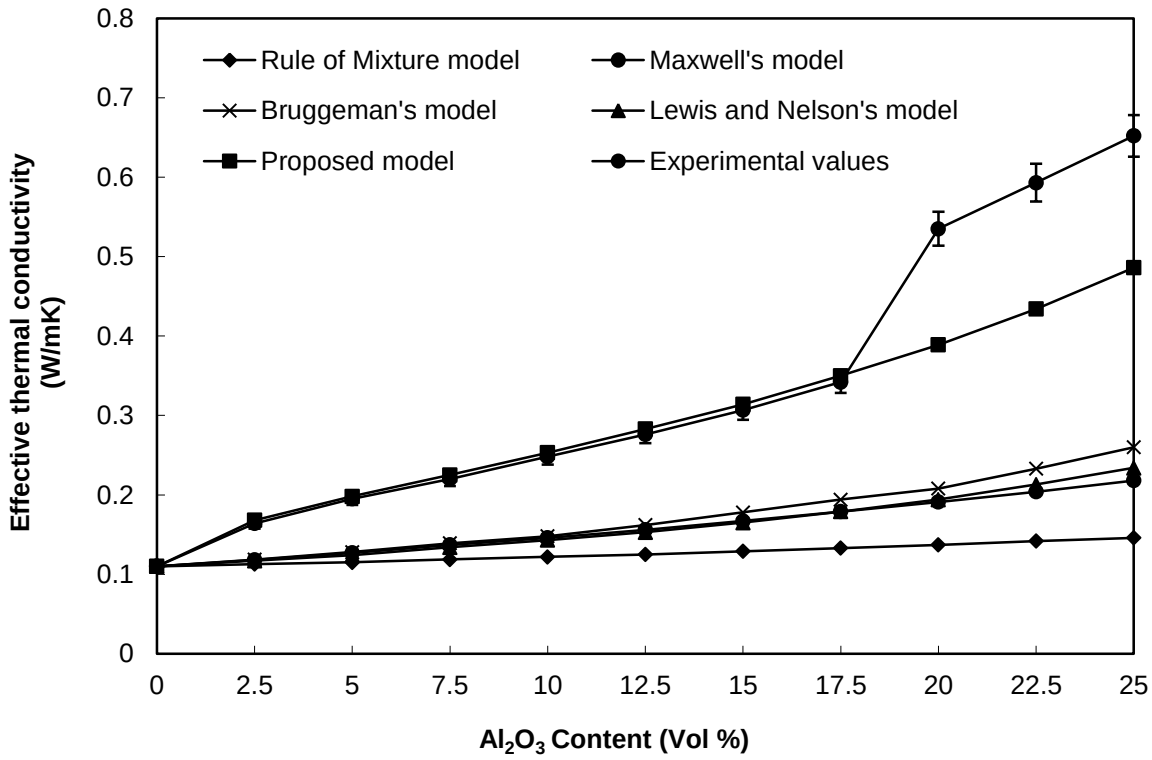

Fig 7.2 Effective thermal conductivity of Set II PP composites

This agreement between the measured k_{eff} values and the ones obtained from the proposed model is only up to the percolation threshold. Beyond this no theoretical models are estimating the conductivities value correctly. For PP/AlN composites, the percolation threshold reaches when filler content increases beyond 20 vol% and for PP/Al_2O_3 composites, the percolation threshold reaches when filler content increases beyond 17.5 vol%. It can be observed that the value of percolation threshold vary with filler as well as with matrix material. Here also like the epoxy based composites, the measured values are less than the values obtained from proposed model up to the percolation threshold for each sample.

Table 7.1 Comparison of proposed model and measured values along with associated error (For single filler PP composites)

Filler content (Vol%)	PP/AlN			PP/Al_2O_3		
	Effective thermal conductivity (W/m-K)		Absolute error (%)	Effective thermal Conductivity (W/m-K)		Absolute error (%)
	Proposed model	Measured value		Proposed model	Measured value	
2.5	0.171	0.167	2.39	0.168	0.164	2.44
5	0.201	0.198	1.51	0.198	0.195	1.54
7.5	0.229	0.225	1.77	0.225	0.220	2.27
10	0.258	0.255	1.17	0.253	0.248	2.01
12.5	0.288	0.285	1.05	0.283	0.276	2.53
15	0.321	0.317	1.26	0.314	0.307	2.28
17.5	0.357	0.352	1.42	0.350	0.342	2.34
20	0.398	0.392	1.53	0.389	0.535	27.2
22.5	0.445	0.581	23.4	0.434	0.593	26.8
25	0.499	0.638	21.8	0.486	0.652	25.5

With 25 vol% of filler content, the k_{eff} of PP/AlN composites reaches 0.638 W/m-K which is an improvement of 480% compared to neat PP and with same amount of filler loading the k_{eff} of PP/Al_2O_3 composites reaches 0.652 W/m-K

which is an improvement of about 493%. The increasing trend obtained for the value of k_{eff} in the present case is same as that obtained for epoxy based composites where the rate of increase in thermal conductivity beyond percolation is more with Al_2O_3 as the filler as compared to AlN.

Table 7.1 presents the comparison between the measured values of k_{eff} and those obtained from the proposed model for composites with different filler content. The absolute error percentages associated with each set of readings are also given. It can be seen from the error column that there is a better agreement between the experimental value and the theoretical value up to the percolation threshold and the errors are almost negligible (0-2.5%).

Effective thermal conductivity of polypropylene based composites reinforced with hybrid fillers:

For multi filler composites, the effective thermal conductivity values of polypropylene filled with AlN and SGM (Set III PP composites) in different proportions are shown in Figure 7.3 and polypropylene filled with Al_2O_3 and SGM (Set IV PP composites) are shown in Figure 7.4. It has already been seen that, incorporation of either of the AlN/Al_2O_3 fillers in the PP leads to a significant improvement in the value of k_{eff}. But when a certain amount of AlN/Al_2O_3 content is replaced by equal volume of SGM, this improvement in the k_{eff} value is reduced. This is due to the obvious reason that the intrinsic conductivity of SGM is less than that of AlN/Al_2O_3. The maximum k_{eff} among the various fabricated samples is obtained when 20 vol% AlN and 10 vol% SGM are reinforced in PP resin for the Set III PP composites. The k_{eff} values goes up to 0.397 W/mK which is an improvement of about 261% compared to neat PP (Figure 7.3). Similarly, among the Set IV PP composites, a maximum k_{eff} value of 0.382 W/mK is obtained for the composite filled with 20 vol% Al_2O_3 and 10 vol% SGM. This improvement in k_{eff} amounts to about 247% compared to the neat PP (Figure 7.4).

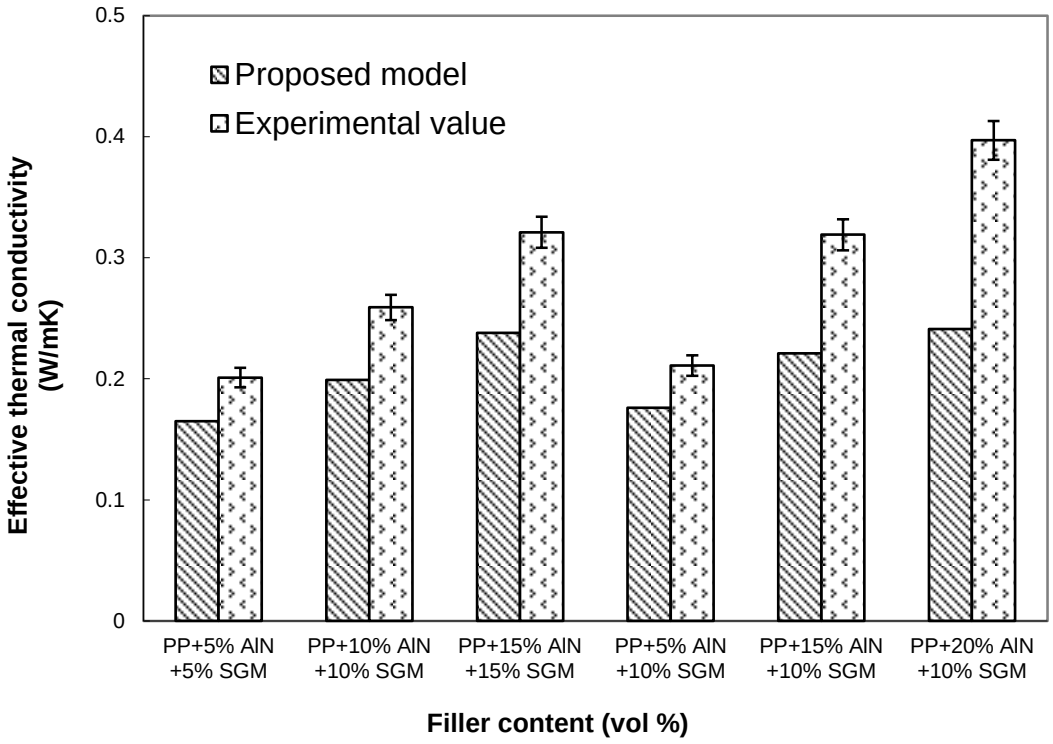

Fig 7.3 Effective thermal conductivity of Set III PP composites

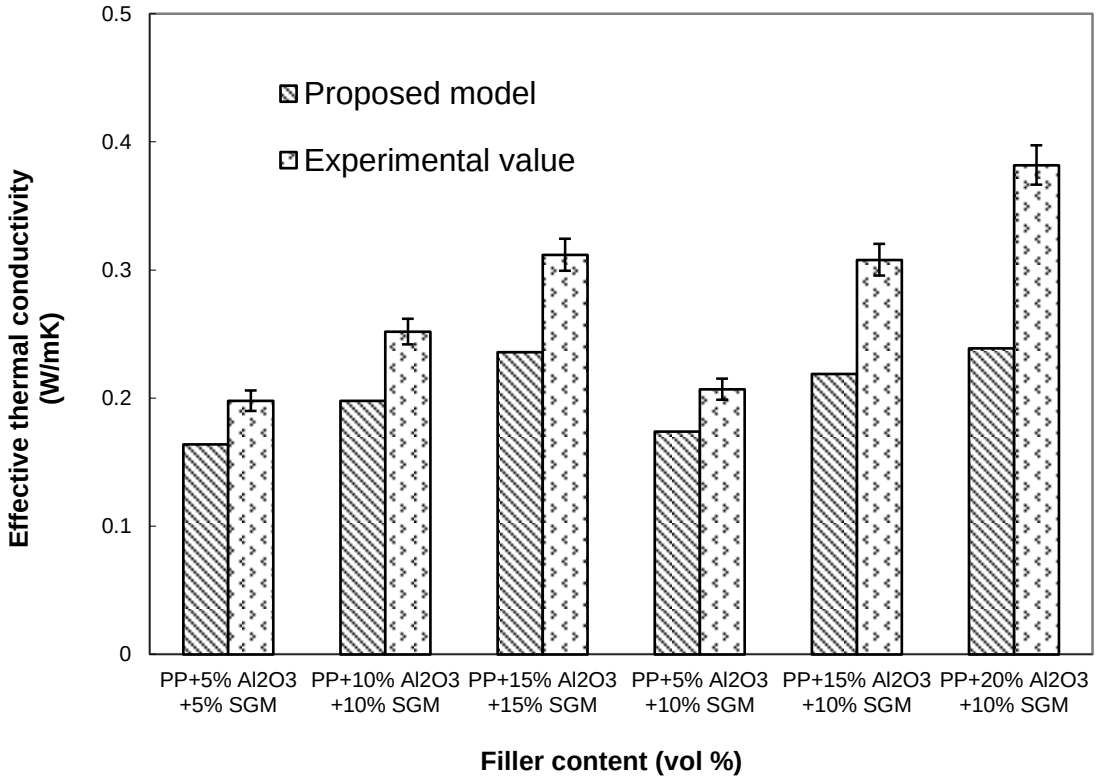

Fig 7.4 Effective thermal conductivity of Set IV PP composites

For hybrid filler composites, measured conductivity values are found to be higher compared to the proposed model values and also no sign of percolation is seen. This trend is the similar to that obtained for epoxy based hybrid composites (Chapter 6). It is further observed that, in case of PP based hybrid composites, maximum increase in the conductivity value is around 260%, which is much higher than that of epoxy based hybrid composites where a maximum increase of only around 90% has been recorded. This is because, the less conductive SGM particles which are behaving as insulative filler for epoxy resin, now start behaving as conductive filler for PP resin owing to the fact that the intrinsic conductivity value of SGM (0.238 W/mK) is higher than that of PP (0.11 W/mK). Hence, for PP as resin, both the fillers contribute towards improvement of conductivity of the composite as a whole and therefore rate of increase in conductivity for PP based hybrid composites becomes relatively higher.

7.1.2 Coefficient of thermal expansion

Coefficient of thermal expansion of polypropylene based composites reinforced with single filler:

The variations in the theoretical and measured values of CTE of the PP composites reinforced with micro-sized AlN particles (Set I PP composites) are shown in Figure 7.5 and PP composites reinforced with micro-sized Al_2O_3 particles (Set II PP composites) for different filler loading are shown in Figure 7.6. The coefficient of thermal expansion values of respective composites have been calculated theoretically using the rule of mixture model [146], Turner model [149], Kerner model [150] and Rosen-Hashin model [155] and these values are compared with the measured values. It can be seen from the figures that with increase in AlN/Al_2O_3 content in PP, CTE of the composites decreases monotonically, unlike the trend observed in case of epoxy based Set I and II composites. It can be seen from the figures that the CTE of PP reduces from 111 $\times 10^{-6}/^{o}C$ to 80.7 $\times 10^{-6}/^{o}C$ when AlN content in it reaches to its maximum of 25 vol%. On the other hand, CTE of PP reduces to 81.7 $\times 10^{-6}/^{o}C$ when 25 vol% of Al_2O_3 is added to it.

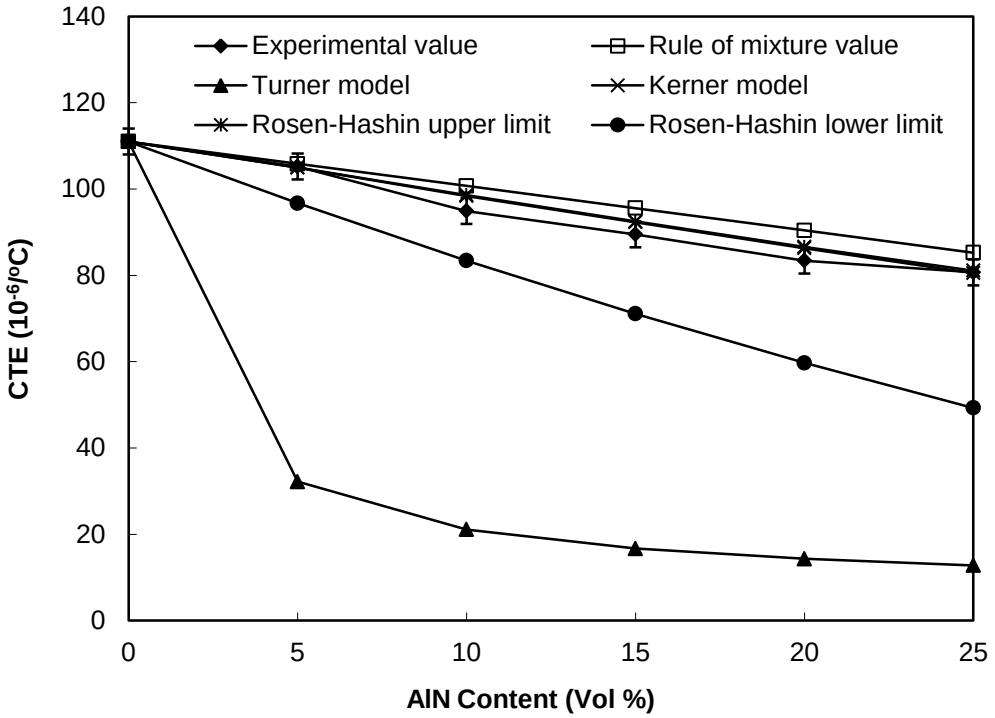

Fig 7.5 Coefficient of thermal expansion of Set I PP composites

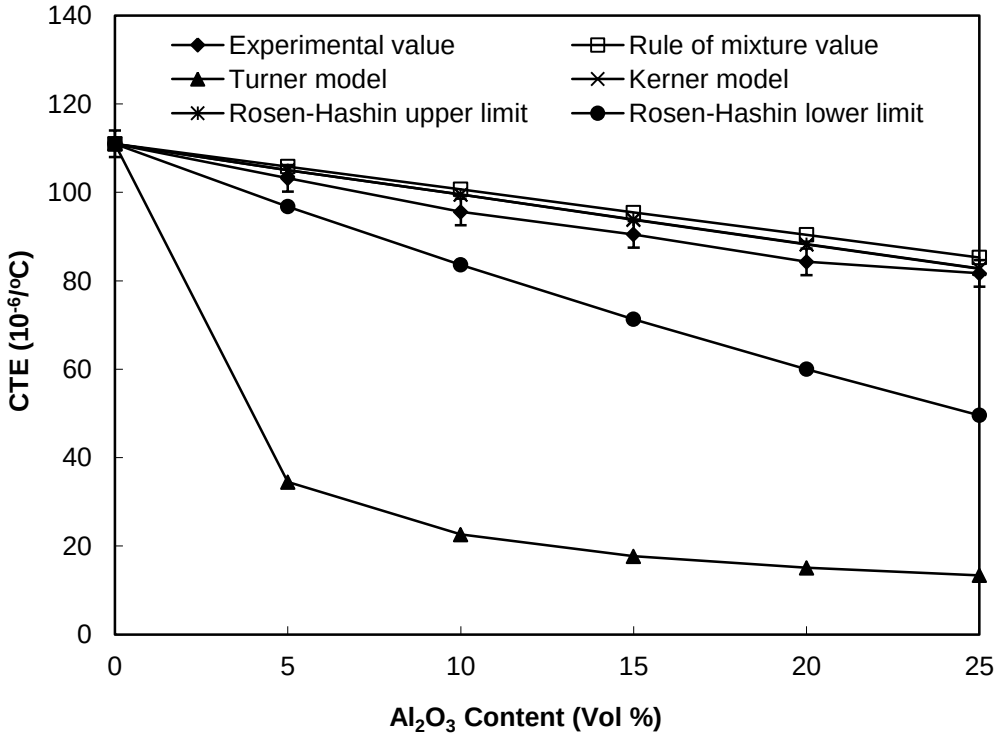

Fig 7.6 Coefficient of thermal expansion of Set II PP composites

It can be further observed from the figures that for both sets of composites, the measured CTE values lie in between the upper and lower bounds of Rosen-Hashin model for all volume fractions of filler. The measured values are close to the values obtained from upper bound of the Rosen-Hashin model as well as from the values obtained from Rule of mixture and Kerner's model whereas Turner's model is again far from satisfaction.

Coefficient of thermal expansion of polypropylene based composites reinforced with hybrid fillers:

For multi filler reinforcement, the coefficient of thermal expansion values of the PP composites filled with AlN and SGM (Set III PP composites) are shown in Figure 7.7 and those of PP composites filled with Al_2O_3 and SGM (Set IV PP composites) are shown in Figure 7.8.It can be seen from the figures that by increasing the content of either of the fillers, coefficient of thermal expansion of the respective composite system decreases appreciably. It is also worth noting that when AlN/Al_2O_3 are premixed with SGM, an uniformly decreasing trend is obtained and a much lower value of CTE is recorded with combined fillers which is because of low intrinsic CTE value of SGM.

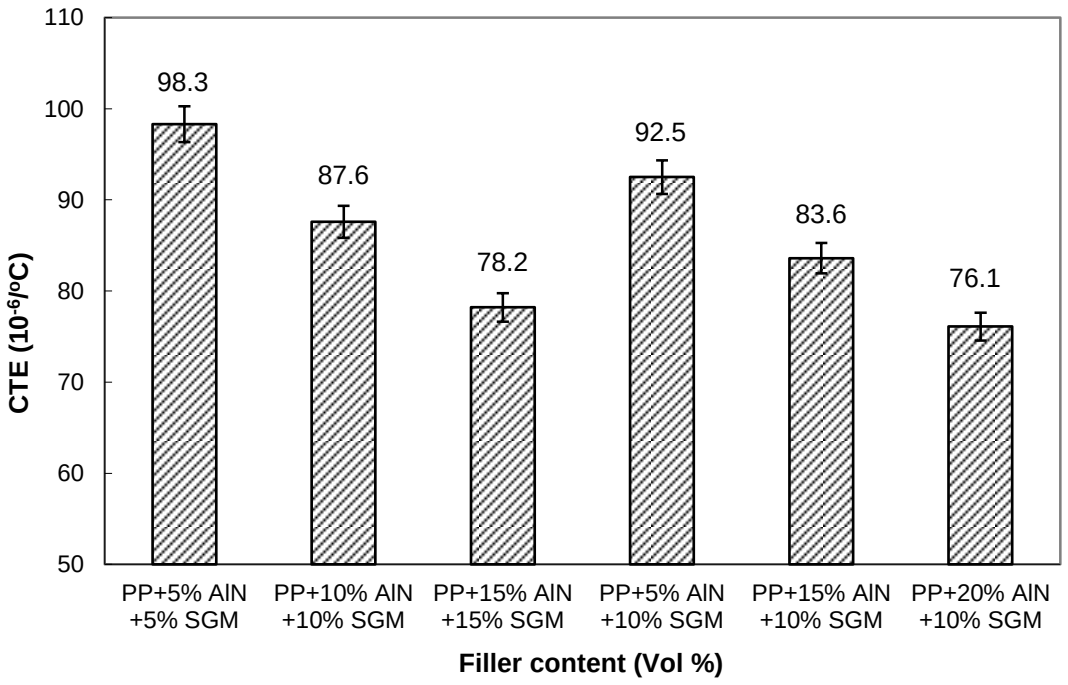

Fig 7.7 Coefficient of thermal expansion of Set III PP composites

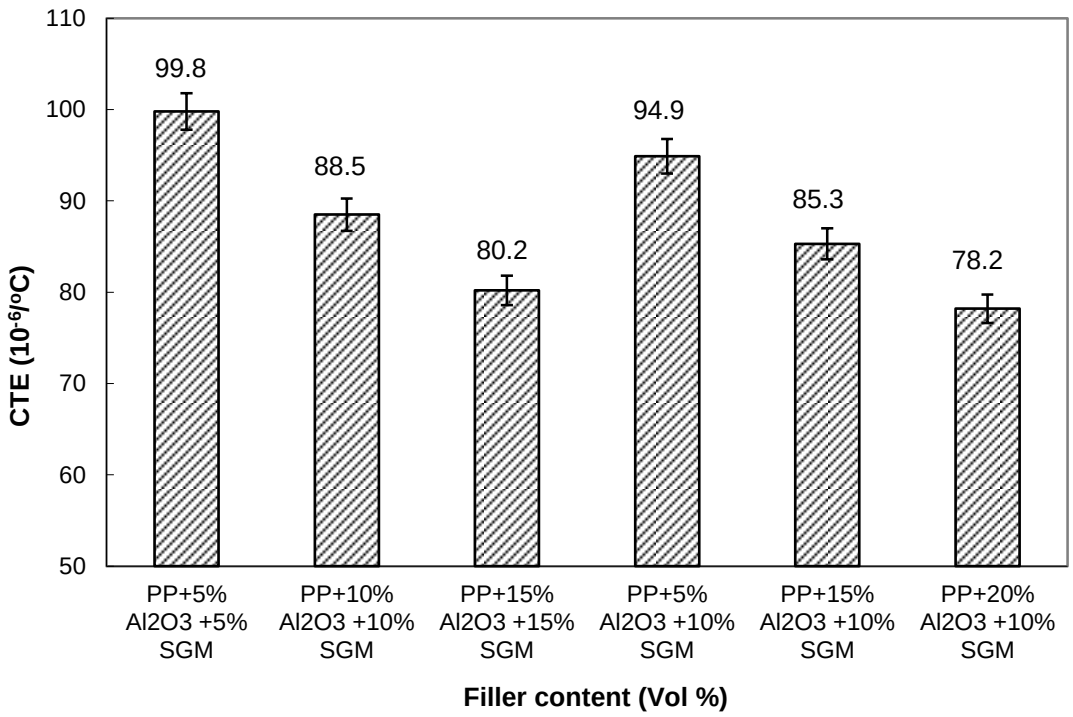

Fig 7.8 Coefficient of thermal expansion of Set IV PP composites

For AlN and SGM as filler, among the various samples, CTE of PP reduces to 76.1 × 10^{-6}/°C for a combination of 20 vol% AlN and 10 vol% SGM whereas with a combination of 20 vol% Al_2O_3 and 10 vol% SGM, CTE of PP reduces to 78.2 × 10^{-6}/°C. The CTE values obtained during experimentation encourages that combination of different fillers when reinforced in PP provides a more useful CTE as compared to that of PP filled with single filler.

7.2 DIELECTRIC CHARACTERISTICS

Dielectric constant of polypropylene based composites reinforced with single filler:

The dielectric constant variations of the Set I PP composites and the Set II PP composites with frequency in the range 1 kHz -1 MHz are shown in Figures 7.9 and 7.10 respectively. It is clear from the figures that for all sets of composites, there is a clear reduction in the value of dielectric constant within the measured frequency range. It can also be seen from the figures that the value of dielectric constant increases with filler content due to high dielectric constant value of AlN and Al_2O_3 compared to neat PP. For PP/AlN composites, dielectric constant

reaches 4.06 for a maximum filler loading of 25 vol% at 1 kHz whereas for epoxy/Al_2O_3 composites it goes to 4.28 for similar filler loading and frequency.

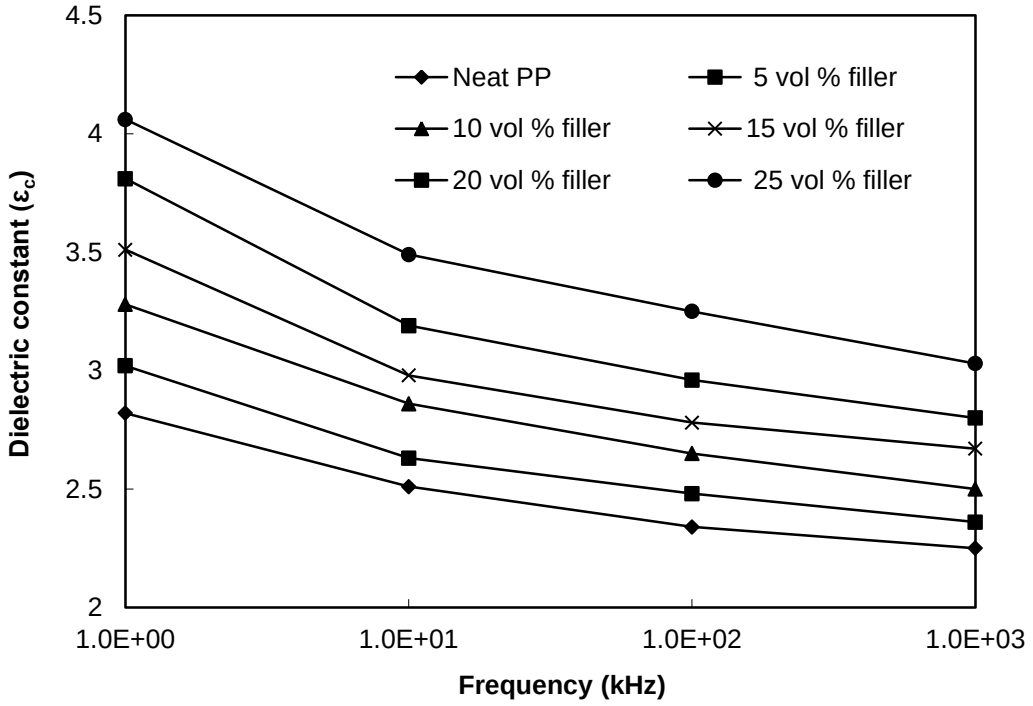

Fig 7.9 Variation of dielectric constant with frequency for Set I PP composites

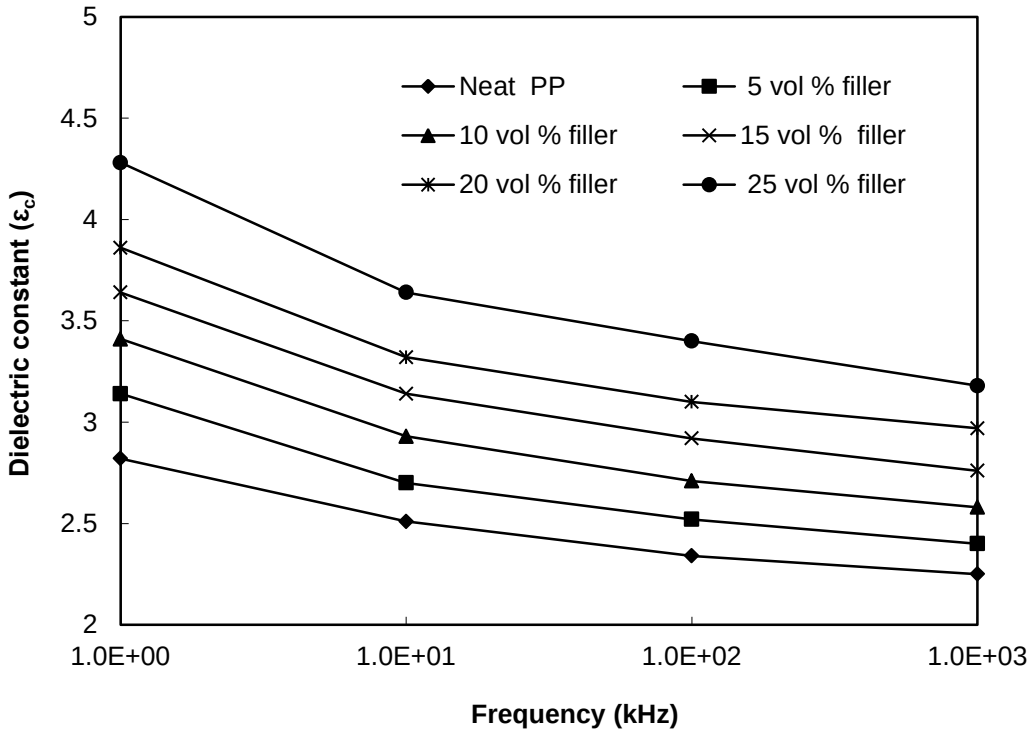

Fig 7.10 Variation of dielectric constant with frequency for Set II PP composites

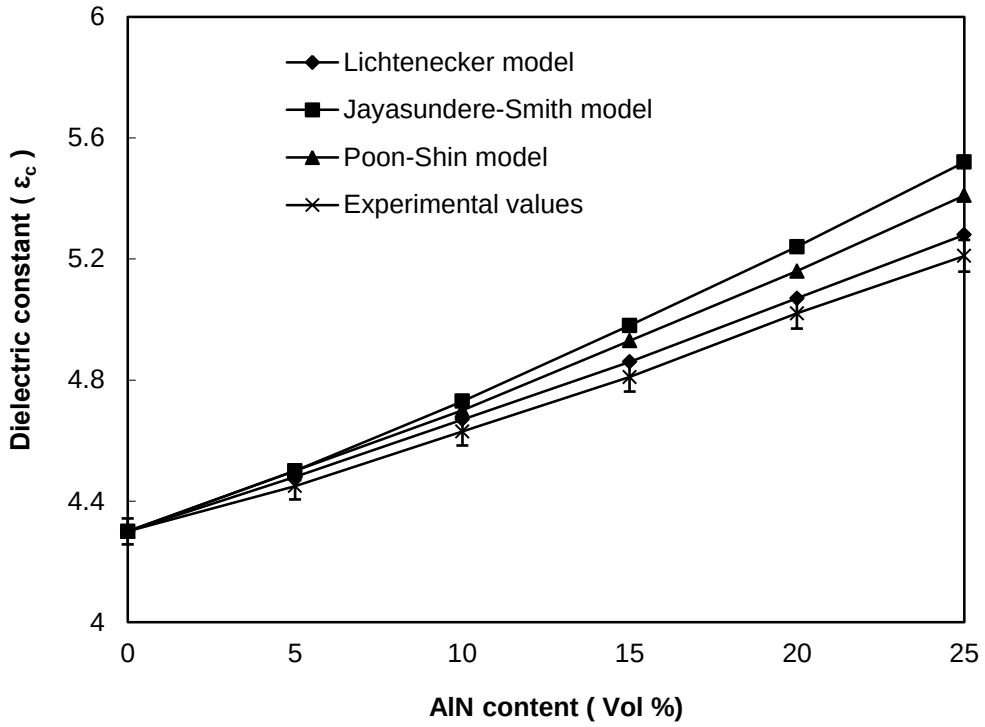

Fig 7.11 Measured and calculated dielectric constant at 1MHz for Set I PP composites

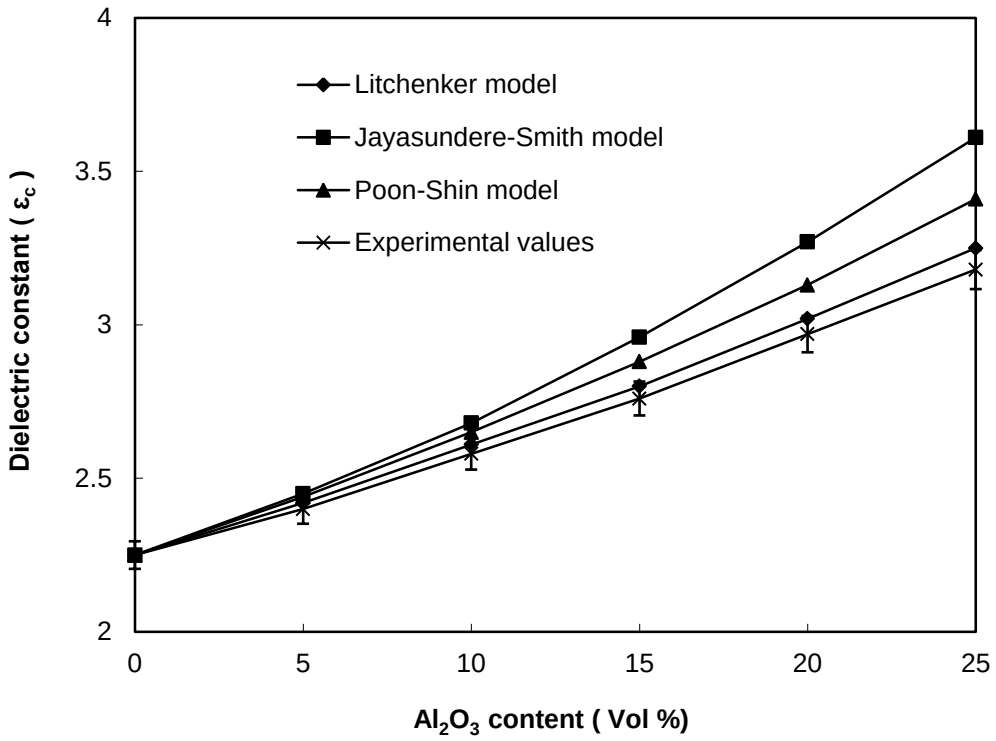

Fig 7.12 Measured and calculated dielectric constant at 1MHz for Set II PP composites

Further, for two component systems of different compositions, dielectric constants have been theoretically calculated by using few well established correlations proposed by Lichtenecker [162], Jayasundare-Smith [166] and Poon-Shin [167]. Figures 7.12 and 7.13 show the comparison between the experimental and the calculated values of dielectric constant obtained from these equations at 1 MHz for PP/AlN and PP/Al_2O_3 composites respectively. It can be seen from both the figures that the models are valid for low volume fraction and as the volume fraction increases the values obtained from the predictive correlations start deviating from the measured ones. While Lichtenecker's model is in closest approximation to the measured values, Jayasundare-Smith and Poon-Shin models show more deviation from the experimental values. It is further observed from both the figures that the measured values are always lower than the theoretical values invariably for all cases. Similar trend has also been observed when epoxy is reinforced with micro-sized AlN/Al_2O_3 (Chapter 6).

Dielectric constant of polypropylene based composites reinforced with hybrid fillers:

For multi filler composites, when AlN /Al_2O_3 is premixed with SGM and reinforced in PP resin, similar trends in regard to the dielectric constant are observed as seen for single filler reinforced composites. The dielectric constant variations of the Set III PP composites and the Set IV PP composites with frequency in the range 1 kHz -1 MHz are shown in Figures 7.13 and 7.14 respectively. The results show that for all sets of composites, irrespective of filler type and content, there is a slight reduction in the value of dielectric constant within the measured frequency range as experienced in case of Set I and II epoxy composites.

Figures 7.15 and 7.16 show the measured values of dielectric constant at 1 MHz for the Set III PP composites and the Set IV PP composites respectively. It can be seen from the graph that the maximum value of dielectric constant reaches 2.75 for the Set III PP composites and 2.86 for the Set IV PP composites. These

maximum values are obtained for composites with 20 vol% of AlN/Al_2O_3 and 10 vol% of SGM.

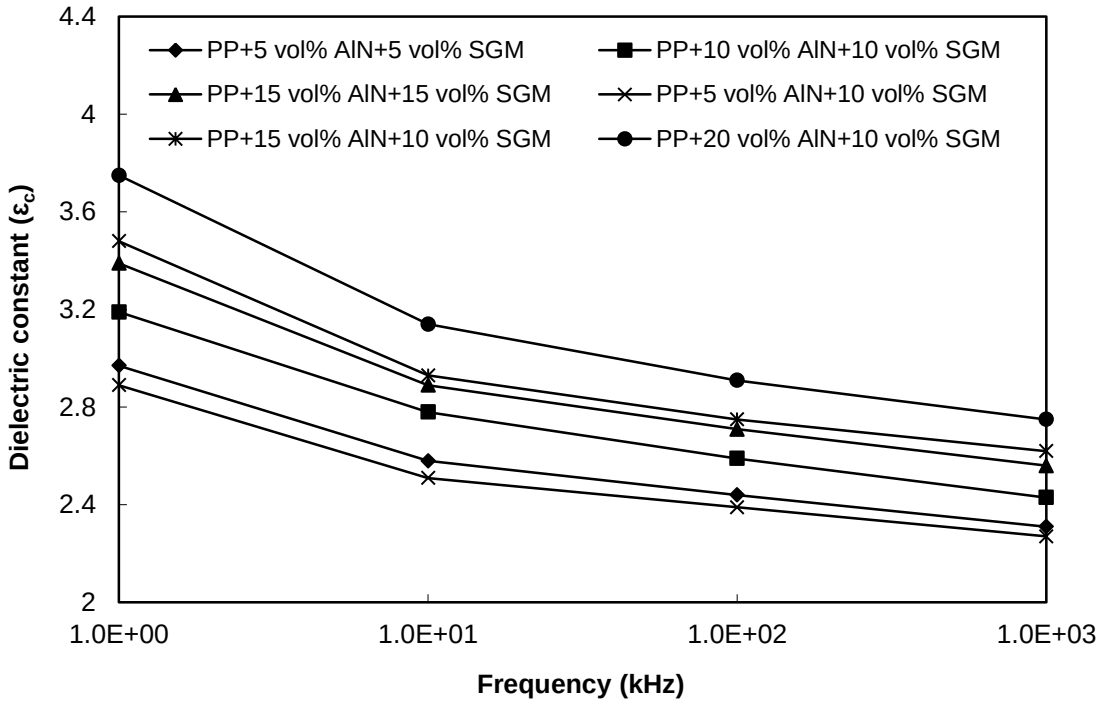

Fig 7.13 Variation of dielectric constant with operating frequency for Set III PP composites

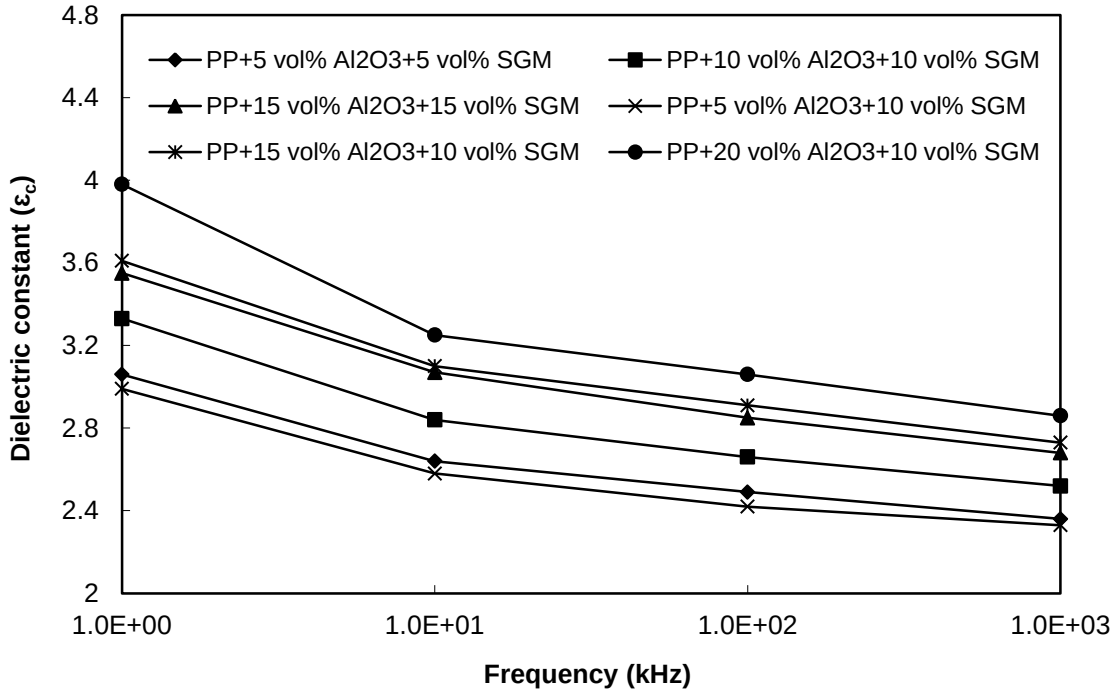

Fig 7.14 Variation of dielectric constant with operating frequency for Set IV PP composites

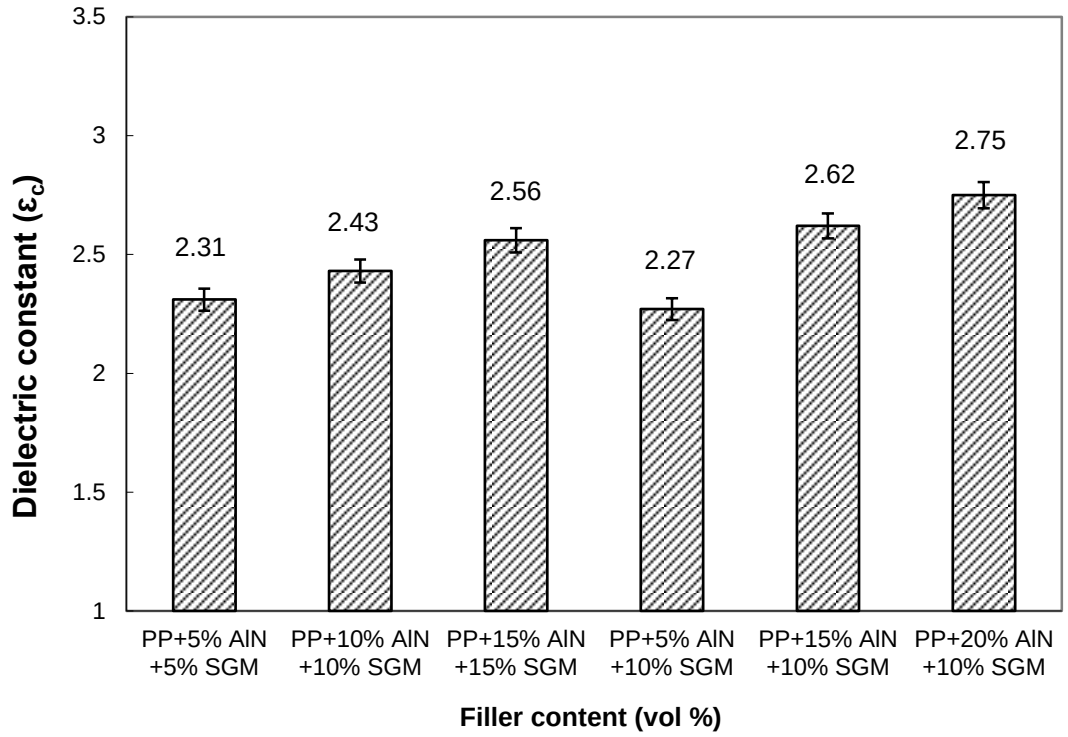

Fig 7.15 Dielectric constant at 1MHz for Set III PP composites

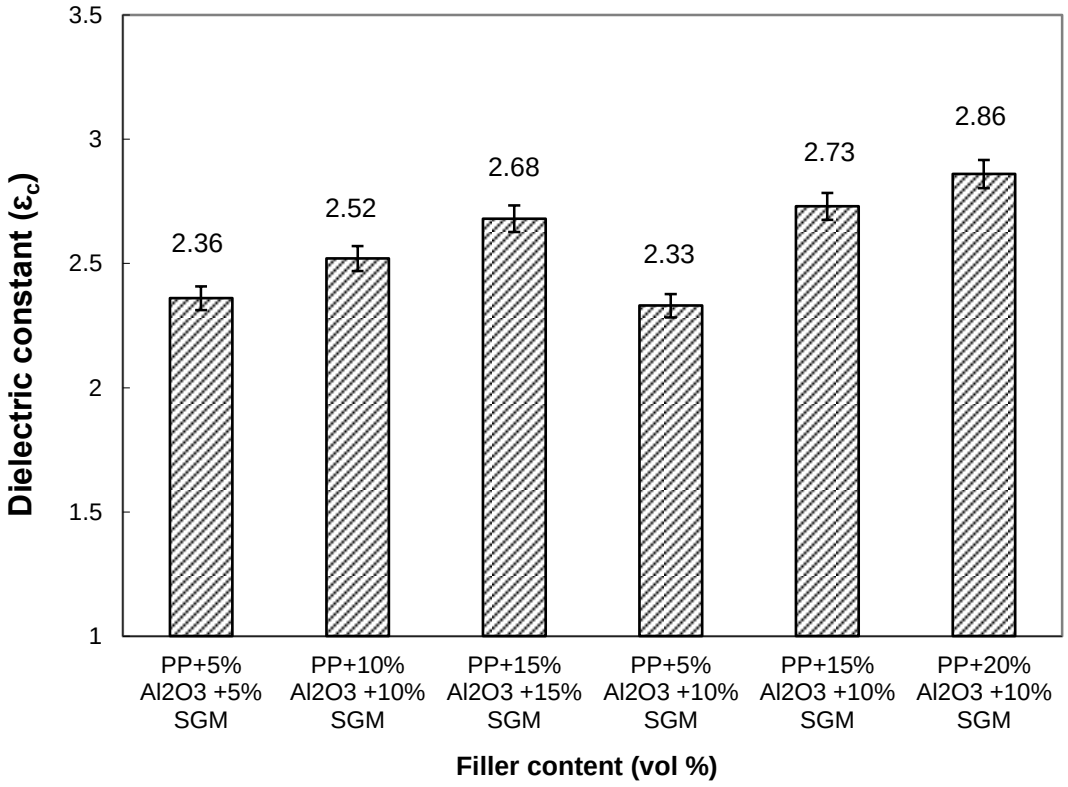

Fig 7.16 Dielectric constant at 1MHz for Set IV PP composites

These values increase with decrease in frequency and reach their maximum of 3.76 and 3.98 at frequency of 1 kHz for Set III and IV PP composites respectively. It is clear from the graphs that as AlN/Al_2O_3 content increases, dielectric constant also increases whereas incorporation of SGM contributes towards lowering the value of dielectric constant. This is because dielectric constant of SGM is much less than that of AlN and Al_2O_3. With SGM as one of the fillers, dielectric constant of PP based composites gets restricted to very low values which are almost equal to that of neat polypropylene for a wide range of filler content and operating frequency.

Chapter Summary

This chapter has provided:

- The results of the experiments conducted to evaluate the thermal conductivity of the polypropylene based composites under study
- The validation of theoretical models developed and proposed in Chapter 3 through experimentation
- The synergistic effects of SGM and AlN/Al_2O_3 on effective thermal conductivity of the polypropylene based hybrid composites
- A complete picture on the percolation behaviour exhibited by the fillers in regard to the thermal conductivity of polypropylene based composites
- Effects of single and hybrid fillers on coefficient of thermal expansion and dielectric constant of polypropylene based composites

The next chapter presents a summary of the research findings and the specific conclusions drawn from this work. Some potential applications of the fabricated composites have also been recommended in the following chapter. It also outlines various scopes for future research in the related field.

*****

Chapter 8

Conclusions and Recommendation for Future Work

Chapter 8

CONCLUSIONS AND RECOMMENDATION FOR FUTURE WORK

The research reported in this thesis broadly consists of three parts:

- The first part is about the development of theoretical heat conduction models based on which mathematical correlations have been proposed for estimation of effective thermal conductivities of polymer composites with single as well as hybrid fillers.
- The second part has provided the description of the materials used, routes adopted to fabricate the various thermoset and thermoplastic polymer composites and the details of the experiments that are conducted during this research. It also presents the test results in regard to the physical, micro-structural and mechanical characteristics of all the epoxy and polypropylene based composites filled with single filler i.e. micro-sized AlN/Al_2O_3. A comparative evaluation of the effects of premixing of SGM with micro-sized AlN/Al_2O_3 on different physical and mechanical properties of composite systems is also reported.
- The last part has reported on the thermal and dielectric characteristics of the composites under this investigation. It includes an assessment of the effective thermal conductivities of these composites using the proposed models. The results are validated by simultaneous measurement of thermal conductivity of the composites in the laboratory. Effects of inclusion of various combinations of single/hybrid fillers on the effective thermal conductivity, glass transition temperature, coefficient of thermal expansion and dielectric constant of the composites are presented.

8.1 Conclusions

The present analytical and experimental investigation on epoxy and polypropylene composites filled with different inorganic fillers (single/hybrid) has led to the following specific conclusions:

1. Micro-sized aluminium nitride, aluminium oxide and solid glass microsphere possess ample reinforcing potential to be used as functional fillers in both thermoset and thermoplastic polymers. Successful fabrication of four sets of thermoset polymer composites i.e. epoxy-AlN (Set I), epoxy-Al_2O_3 (Set II), epoxy-AlN-SGM (Set III) and epoxy-Al_2O_3-SGM (Set IV) is possible by hand lay-up technique and similar four sets of thermoplastic polymer composites i.e. PP-AlN (Set I), PP-Al_2O_3 (Set II), PP-AlN-SGM (Set III) and PP-Al_2O_3-SGM (Set IV) is possible by compression moulding route.

2. The density, porosity and morphology of these composites are greatly influenced by the type and content of filler materials, type of matrix materials and the fabrication route adopted. With increase in filler loading, density and the porosity increase invariably for all the composites. SEM micrographs reveal that by using compression moulding route, better uniformity in the distribution of filler within matrix body is obtained with relatively low amount of voids as compared to when composites are fabricated by hand lay-up technique.

3. Incorporation of micro-sized AlN/Al_2O_3 fillers in polymers alters various mechanical properties of the respective polymer. On one hand, with increase in filler content, micro-hardness and compressive strength get improved, whereas, on the other hand, a marginal reduction in the value of tensile strength of these composites is noticed. With increase in micro-sized AlN content from 0-25 vol%, micro-hardness of epoxy increases from 0.087 GPa to 0.278 GPa, its compressive strength increases from 114 MPa to 153.4 MPa and tensile strength decreases from 59 MPa to

50.3 MPa, whereas, in polypropylene composites with similar filler loading, the micro-hardness increases from 0.059 GPa to 0.208 GPa, compressive strength increases from 83 MPa to 116.4 MPa and tensile strength decreases from 45 MPa to 38.8 MPa. Similarly, with 25 vol% Al_2O_3, micro-hardness of epoxy increases to 0.331 GPa, its compressive strength increases to 159.4 MPa and tensile strength decreases to 51.4 MPa, whereas, in polypropylene composites with similar filler loading, the micro-hardness increases to 0.252 GPa, compressive strength increases to 124.2 MPa and tensile strength decreases to 40.1 MPa.

4. These mechanical properties get further improved for multi-filler composites i.e. when micro-sized AlN/Al_2O_3 particles are premixed with SGM and reinforced in polymers. For 15 vol% AlN and 15 vol% SGM as filler, micro-hardness of epoxy increases to 0.385 GPa and that of PP increases to 0.346 GPa, whereas for 15 vol% Al_2O_3 and 15 vol% SGM as filler, micro-hardness of epoxy increases to 0.419 GPa and that of PP increases to 0.382 GPa. Maximum compressive strengths of epoxy and PP are recorded as 156.7 MPa and 121.2 MPa respectively for 20 vol% AlN and 10 vol% SGM, whereas for 20 vol% Al_2O_3 and 10 vol% SGM, compressive strengths of epoxy and PP increase to 163.5 MPa and 129.9 MPa respectively. Rate of decrease in tensile strength value with filler content gets reduced when multiple fillers are used as reinforcement. Minimum values of tensile strength for hybrid filler epoxy and PP composites are recorded as 51.2 MPa and 39.9 MPa respectively for 20 vol% AlN and 10 vol% SGM, whereas for 20 vol% Al_2O_3 and 10 vol% SGM, these values are 52.3 MPa and 40.8 MPa for epoxy and polypropylene composites respectively.

5. Two correlations based on the law of minimal thermal resistance and equal law of specific equivalent thermal conductivity to estimate the effective conductivity of single filler and multi-filler composites are proposed. The proposed correlations can very well be used to estimate k_{eff}

for composites within the percolation limit for single filler composites and for the entire range of filler content for hybrid filler composites.

6. For single filler composites, with 25 vol% of micro-sized AlN particles, effective thermal conductivity of epoxy is improved by 446% and reaches 1.982 W/mK and that of PP is improved by 480% and reaches 0.638 W/mK. Similary, with 25 vol% of micro-sized Al_2O_3 particles, effective thermal conductivity of epoxy is improved by 482% and reaches 2.114 W/mK and that of PP is improved by 493% and reaches 0.652 W/mK. For multi-filler composites i.e. when AlN/Al_2O_3 is premixed with SGM, the effective thermal conductivity values are always higher than that of neat polymer. With 20 vol% AlN and 10 vol% SGM, the conductivities of epoxy and PP reach 0.684 W/mK and 0.397 W/mK respectively whereas with 20 vol% Al_2O_3 and 10 vol% SGM, the conductivities of epoxy and PP reach 0.675 W/mK and 0.382 W/mK respectively.

7. It is observed that the glass transition temperature (T_g) of epoxy gradually increases from 98°C to 112°C for epoxy-AlN composites as the AlN content increases from 0 to 25 vol% and for epoxy-Al_2O_3 composites, it goes up to 116°C as the Al_2O_3 content reaches 25 vol%. For multi-filler composites, T_g of epoxy increases to 119°C for 20 vol% AlN and 10 vol% SGM as filler. For 20 vol% Al_2O_3 and 10 vol% SGM it goes further high and reaches 124°C.

8. The coefficients of thermal expansion (CTE) of the composites decrease with the increase in filler content. While the CTE of the neat epoxy is 66 × 10^{-6}/°C, it decreases to 63.86 × 10^{-6}/°C and 56.2 × 10^{-6}/°C with 25 vol% AlN and Al_2O_3 respectively. With similar filler loading and content, CTE of PP reduces from 111 × 10^{-6}/°C to 80.7 × 10^{-6}/ °C and 81.7 × 10^{-6}/ °C respectively. For multi-filler composites, these CTE values get further reduced. With 20 vol% AlN and 10 vol% SGM, the CTE of epoxy and PP reach51.1 × 10^{-6}/°C and 76.1 × 10^{-6}/°C respectively whereas with 20

vol% Al_2O_3 and 10 vol% SGM, the CTE of epoxy and PP reach53.6 × 10^{-6}/°C and 78.2 × 10^{-6}/°C respectively.

9. It is seen that with increase in working frequency, dielectric constants of polymer composites decrease irrespective of matrix and filler type. The dielectric constant of neat epoxy is 4.3 and that of neat PP is 2.25 at an operating frequency of 1 MHz. With the addition of AlN/Al_2O_3 filler, dielectric constant of polymer composites increases. At minimum frequency of 1 kHz, for 25 vol% AlN as filler, dielectric constant of epoxy increases to 6.08 and that of PP increases to 4.06 whereas for 25 vol% Al_2O_3 as filler, dielectric constant of epoxy increases to 6.25 and that of PP increases to 4.28. For multi-filler composites, synergistic effects of AlN/Al_2O_3 and SGM fillers give reduced value of dielectric constant. At 1 kHz, with 20 vol% AlN and 10 vol% SGM, the dielectric constant of epoxy and PP get restricted to 4.97 and 3.76 whereas with 20 vol% Al_2O_3 and 10 vol% SGM, the dielectric constants of epoxy and PP composites are found to be 5.09 and 3.98 respectively.

8.2 Recommendations for Potential Applications

Composite materials show excellent performance, starting from their applications in manufacturing and electronic industries to house-hold appliances. It is mainly due to their light weight, high strength to weight ratio and potentially high resistance to environmental degradation resulting in lower lifecycle costs. The particulate filled polymer composites developed in this investigation are expected to have adequate potential for a wide variety of applications particularly in microelectronic industries. With enhanced thermal conductivity, improved glass transition temperature, reduced thermal expansion coefficient and modified dielectric characteristics, the epoxy and polypropylene composites with appropriate proportions of fillers can be used in micro-electronics applications which include printed circuit boards, substrate, interconnection, interlayer dielectrics, die attach, encapsulations, lid, heat sinks, electrical contacts, connectors, thermal interface material and housings.

8.3 Scope for Future Work

The present research work leaves a wide scope for future investigators to explore many other aspects of particulate filled polymer composites. Some recommendations for future research include:

- Development of theoretical models for filler particles of different shapes taking into account the filler-matrix interface resistance.
- Possible use of thermally conductive ceramic fillers other than aluminium nitride and aluminium oxide, polymeric resins other than epoxy and polypropylene in the development of new composite systems.
- Exploring the possibility of using natural fibers along with different ceramic particulates to fabricate such composites with improved functional properties.
- Cost analysis of these composites to assess their economic viability in industrial applications.

*****

References

REFERENCES

1. Swanson E (1998). Moore's Law. The Art and Science of Analog Circuit Design. *A volume in EDN Series for Design Engineers*, 251–261.
2. Harper CA (2004). Electronic packaging and interconnection handbook. *McGraw Hill, New York.*
3. Lau J, Wong CP, Prince JL, Nakayama W (1998). Electronic packaging: design, materials, process, and reliability. *McGraw Hill, New York*.
4. Chung DDL (2000). Polymer matrix composites for microelectronics. *Polymer and Polymer Composites*, 8: 219-229.
5. Saad GR, Ezz AA, Ahmed HA (2015).Cure kinetics, thermal stability, and dielectric properties of epoxy/barium ferrite/polyaniline composites. *Thermochimica Acta*, 599: 84-94.
6. Praveen RS, Jacob S, Murthy CRL, Balachandran P, Rao YVKS (2011). Hybridization of carbon–glass epoxy composites: An approach to achieve low coefficient of thermal expansion at cryogenic temperatures. *Cryogenics,* 51: 95–104.
7. Takei T, Hatta H, Taya M (1991). Thermal expansion behavior of particulate-filled composites i: Single reinforcing phase. *Materials Science and Engineering: A*, 131: 133-143.
8. Ranganath S (1997). A review on particulate-reinforced titanium matrix composites. *Journal of Materials Science*, 32: 1-16.
9. Ng CB, Ash BJ, Schadler LS, Seigel RW (2001). A study of the mechanical and permeability properties of nano and micron-TiO_2 filled epoxy composites. *Advanced Composite Letters*, 10: 101–111.
10. Kishore, Singh VK (1999). Studies on the variation in compression strengths of graphite powders bearing glass-epoxy composites exposed to humid conditions. *Journal of Reinforced Plastics & Composites*, 18: 224–232.
11. Bae JW, Kim W, Cho SH (2000). The properties of AIN-filled epoxy molding compounds by the effects of filler size distribution, *Journal of Materials Science*, 35: 5907–5913.
12. Sonje PU, Subramanian KN, Lee A (2004). Characterization of polymeric composites with low CTE ceramic particulate fillers, *Journal of Advanced Materials*, 36: 22–29.
13. Luyt AS, Molefi JA, Krump H (2006). Thermal, mechanical and electrical properties of copper powder filled low-density and linear low-density polyethylene composites. *Polymer Degradation and Stability*, 91: 1629-1636.

14. Xu Y, Chung DDL, Mroz C (2001). Thermally conducting aluminum nitride polymer-matrix composites, *Composite: Part A: Applied Science and Manufacturing*, 32: 1749–1757.

15. Kim HS, Khamis MA (2001). Fracture and impact behaviours of hollow micro-sphere/epoxy resin composites, *Composite: Part A: Applied Science and Manufacturing*, 32: 1311–1317.

16. Singh N, Ghildiyal N, Khelawan R, Singh RS, Venkataramani PS, Mathur GN, Shankar V (1996). Development of epoxy–metal particulate composite. *Proceedings of the Second International Conference on Advances in Composites*, IISc Bangalore.

17. Cheang P, Khor KA (2003). Effect of particulate morphology on the tensile behaviour of polymer-hydroxyapatite composites, *Materials Science and Engineering A*, 345: 47–54.

18. Ahmed S, Jones FR (1990). A review of particulate reinforcement theories for polymer composites. *Journal of Material Science*, 25: 4933-4942.

19. Cota FP, Alves RAA, Panzera TH, Strecker K, Christoforo AL, Borges PHR (2012). Physical properties and microstructure of ceramic–polymer composites for restoration works. *Materials Science and Engineering: A*, 531: 28–34.

20. Verbeek CJR, Du Plessis BJGW (2005). Density and flexural strength of phosphogypsum–polymer composites. *Construction and Building Materials*, 19: 265–274.

21. Moloney AC, Kausch HH, Kaiser T, Beer HR (1987). Review parameters determining the strength and toughness of particulate filled epoxide resins. *Journal of Materials Science*, 22: 381–393.

22. Bonner Jr WH (1962). Aromatic polyketones and preparation thereof. *U.S. Patent 3065205A*.

23. Fu SY, Feng XQ, Lauke B, Mai YW (2008). Effects of particle size, particle/matrix interface adhesion and particle loading on mechanical properties of particulate–polymer composites. *Composites: Part B: Engineering*, 39: 933–961.

24. Ou Y, Yang F, Yu ZZ (1998). A new conception on the toughness of nylon 6/silica nanocomposite prepared via in situ polymerization. *Journal of Polymer Science: Part B Polymer Physics*, 36: 789–95.

25. Liu ZH, Kwok KW, Li RKY, Choy CL (2002). Effects of coupling agent and morphology on the impact strength of high density polyethylene/$CaCO_3$ composites. *Polymer*, 43: 2501–2506.

26. Roulin-Moloney AC, Cantwell WJ, Kausch HH (1987). Parameters determining the strength and toughness of particulate-filled epoxy resins. Polymer Composite, 8: 314–23.

27. Jancar J, Dibenedetto AT (1995). Failure mechanics in ternary composite of polypropylene with inorganic fillers and elastomer inclusions. *Journal of Materials Science*, 30: 2438–2445.

28. Pukanszky B, Voros G (1993). Mechanism of interfacial interactions in particulate filled composites. *Composite Interface*, 1: 411–427.

29. Bartczak Z, Argon AS, Cohen RE, Weinberg M (1999). Toughness mechanism in semi-crystalline polymer blends: II. High-density polyethylene toughened with calcium carbonate filler particles. *Polymer*, 40: 2347–2365.

30. Cho J, Joshi MS, Sun CT (2006). Effect of inclusion size on mechanical properties of polymeric composites with micro and nano particles. *Composites Science and Technology*, 66: 1941–1952.

31. Nakamura Y, Yamaguchi M, Kitayama A, Okubo M, Matsumoto T (1991). Effect of particle size on fracture toughness of epoxy resin filled with angular-shaped silica. *Polymer*, 32: 2221–2229.

32. Nakamura Y, Yamaguchi M, Okubo M, Matsumoto T (1992). Effects of particle size on mechanical and impact properties of epoxy resin filled with spherical silica. *Journal of Applied Polymer Science*, 45: 1281–1289.

33. Buggy M, Bradley G, Sullivan A (2005). Polymer–filler interactions in kaolin/nylon 6,6 composites containing a silane coupling agent. *Composite Part A: Applied Science and Manufacturing*, 36: 437–442.

34. Levita G, Marchetti A, Lazzeri A (1989). Fracture of ultrafine calcium carbonate/polypropylene composites. *Polymer Composite*, 10: 39–43.

35. Wetzel B, Haupert F, Friedrich K, Zhang MQ, Rong MZ (2001). Mechanical and tribological properties of microparticulate and nanoparticulate reinforced polymer composites. *Proceedings of the ICCM-13, Wan Fang Digital Electronic Publisher, Beijing, ID 1021*.

36. Zhang MQ, Rong MZ, Yu SL, Wetzel B, Friedrich K (2002). Effect of particle surface treatment on the tribological performance of epoxy based nanocomposites. *Wear*, 253: 1086–1093.

37. Antunes PV, Ramalho A, Carrilho EVP (2014). Mechanical and wear behaviours of nano and microfilled polymeric composite: Effect of filler fraction and size. *Materials and Design*, 61: 50–56.

38. Anjum N, Prasad SLA, Suresha B (2013). Role of silicon dioxide filler on mechanical and dry sliding wear behaviour of glass-epoxy composites. *Advances in Tribology*, 2013: Article ID 324952.

39. Patnaik A, Satapathy A, Mahapatra SS, and Dash RR (2007). Implementation of Taguchi design for erosion of fiber-reinforced polyester composite systems with SiC filler. *Journal of Reinforced Plastics and Composites*, 27: 1093–1111.

40. Akinci A, Sen S, Sen U (2014). Friction and wear behavior of zirconium oxide reinforced PMMA composites. *Composites Part B: Engineering*, 56: 42-47.

41. Xu J, Yan H, Gu D (2014). Friction and wear behavior of polytetrafluoroethene composites filled with Ti_3SiC_2. *Materials and Design*, 61: 270-274.

42. Beecroft LL, Ober CK (1997). Nanocomposite Materials for optical applications. *Chemistry of Materials*, 9: 1302–1317.

43. Tanio N, Koike Y (2000). What is the most transparent polymer? *Polymer Journal*, 32: 43-50.

44. Maruhashi Y. Iida S (2001). Transparency of polymer blends. *Polymer Engineering & Science*, 41: 1987-1995.

45. Zhou RJ, Burkhart T (2010). Optical properties of particle-filled polycarbonate, polystyrene and Poly(methyl methacrylate) Composites. *Journal of Applied Polymer Science*, 115: 1866–1872.

46. Yuan Y, Zhang L Hu L, Wang W, Min G (2011). Size effect of added LaB_6 particles on optical properties of LaB_6/Polymer composites. *Journal of Solid State Chemistry*, 184: 3364–3367.

47. Rohsenow WM, Hartnett JR, Cho YI (1998). Handbook of heat transfer, *3rd edition, McGraw-Hill, New York*: 8.1–8.8.

48. Agari Y, Ueda A, Omura Y, Nagai S (1997). Thermal diffusivity and conductivity of PMMA–PC blends. Polymer, 38: 801–807.

49. Kurabayashi K (2001). Anisotropic thermal properties of solid polymers. International Journal of Thermophysics, 22: 277-288.

50. Mark JE (2007). Physical properties of polymers handbook. *2nd edition, Springer, New York*: 158-160.

51. Henning J, Knappe W (1964). Anisotropy of thermal conductivity in stretched amorphous linear polymers and in strained elastomers. *Journal of Polymer Science Part C: Polymer Symposia*, 6: 167-174.

52. Hansen D, Ho CC (1965). Thermal conductivity of high polymers. *Journal of Polymer Science Part A:General Papers*, 3: 659-670.

53. Peng STJ, Landel RF (1975). Induced Anisotropy of Thermal Conductivity of Polymer Solids under Large Strains. *Journal of Applied Polymer Science*, 19: 49–68.

54. Choy CL, Young K (1977). Thermal conductivity of semicrystalline polymers- a model. *Polymer*, 18: 769-776.

55. Tavman I (1991). Thermal anisotropy of polymers as a function of their molecular orientation. *Experimental Heat Transfer, Fluid Mechanics, and Thermodynamics*: 1562-1568

56. Griesinger A, Hurler W, Pietralla M (1997). A photothermal method with step heating for measuring the thermal diffusivity of anisotropic solids. *International Journal of Heat and Mass Transfer*, 40: 3049-3058.

57. Singh V, Bougher TL, Weathers A, Cai Y, Bi K, Pettes MT,. McMenamin SA, Lv W, Resler DP, Gattuso TR, Altman DH, Sandhage KH, Shi L, Henry A, Cola BA (2014). High thermal conductivity of chain-oriented amorphous polythiophene. *Nature Nanotechnology*, 9: 384–390.

58. Sofian NM, Rusu M, Neagu R, Neagu E (2001). Metal Powder-filled Polyethylene Composites. V. Thermal Properties. *Journal of Thermoplastic Composite Materials*, 14: 20–33.

59. Bjorneklett A, Halbo L, Kristiansen H (1992). Thermal Conductivity of Epoxy Adhesives Filled with Silver Particles. *International Journal of Adhesion and Adhesives*, 12: 99–104.

60. Yu YH, Ma CCM, Teng CC, Huang YL, Tien HW, Lee SH, Wang I (2013). Enhanced thermal and mechanical properties of epoxy composites filled with silver nanowires and nanoparticles. *Journal of the Taiwan Institute of Chemical Engineers*, 44: 654–659.

61. Tavman H (1997). Thermal and mechanical properties of copper powder filled poly (ethylene) composites. *Journal of Powder Technology*, 91: 63–67.

62. Mamunya YP, Davydenko VV, Pissis P, Lebedev EV (2002). Electrical and Thermal Conductivity of Polymers Filled with Metal Powders. *European Polymer Journal*, 38: 1887–1897.

63. Tavman IH (1996). Thermal and Mechanical Properties of Aluminum Powder filled High-density Polyethylene Composites. *Journal of Applied Polymer Science*, 62: 2161–2167.

64. Boudenne A, Ibos L, Fois M, Gehin E, Majeste JC (2004). Thermophysical properties of polypropylene/Aluminium Composites. *Journal of Polymer Composite: Part B: Polymer Physics*, 42: 722-732.

65. Rusu M, Sofian N, Rusu D (2001). Mechanical and thermal properties of zinc powder filled high density polyethylene composites. *Polymer Testing*, 20: 409–417.

66. Dey TK, Tripathi M (2010). Thermal properties of silicon powder filled high-density polyethylene composites. *Thermochimica Acta*, 502: 35–42.

67. Krupa I, Cecen V, Boudenne A, Prokes J, Novák I (2013). The mechanical and adhesive properties of electrically and thermally conductive polymeric composites based on high density polyethylene filled with nickel powder. *Materials and Design*, 51: 620–628.

68. Ye CM, Shentu BQ, Weng ZX (2006). Thermal Conductivity of High Density Polyethylene Filled with Graphite. *Journal of Applied Polymer Science*, 101: 3806–3810.

69. Tavman I, Aydogdu Y, Kök M, Turgut A, Ezan A (2011). Measurement of heat capacity and thermal conductivity of HDPE/expanded graphite nanocomposites by differential scanning calorimetry. *Archives of Materials Science and Engineering*, 50: 56-60.

70. Tu H, Ye L (2009). Thermal conductive PS/graphite composites. *Polymer Advance Technology*, 20: 21–27.

71. Tibbetts GG, Lake ML, Strong KL, Rice BP (2007). A review of the fabrication and properties of vapor-grown carbon nanofiber/polymer composites. *Composite Science and Technology*, 67: 1709–1718.

72. Al-Saleh MH, Sundararaj U (2009). A review of vapor grown carbon nanofiber/polymer conductive composites. *Carbon*, 47: 2–22.

73. Chen YM, Ting JM (2002). Ultra high thermal conductivity polymer composites. *Carbon*, 40: 359–362.

74. Han Z, Fina A (2011). Thermal conductivity of carbon nanotubes and their polymer nanocomposites: A review. *Progress in Polymer Science*, 36: 914-944.

75. Procter P, Solc J (1991). Improved Thermal Conductivity in Microelectronic Encapsulants. *IEEE Transaction on Components, Hybrids and Manufacturing Technology*, 14, 708–713.

76. Ishida H, Rimdusit S (1998). Very high thermal conductivity obtained by boron nitride-filled polybenzoxazine. *Thermochimica Acta*, 320: 177-186.

77. Zhou W, Qi S, An Q, Zhao H, Liu N (2007). Thermal conductivity of boron nitride reinforced polyethylene composites. *Materials Research Bulletin*, 42: 1863–1873.

78. Li S, Qi S, Liu N, Cao P (2011). Study on thermal conductive BN/novolac resin composites. *Thermochimica Acta*, 523: 111– 115.

79. Wong CP, Bollampally RS (1999). Thermal Conductivity, Elastic Modulus, and Coefficient of Thermal Expansion of Polymer Composites Filled with Ceramic Particles for Electronic Packaging. *Journal of Applied Polymer Science*, 74: 3396 –3403.

80. Zhou W, Yu D, Min C, Fu Y, Guo X (2009). Thermal, dielectric, and mechanical properties of SiC particles filled linear low-density polyethylene composites. *Journal of Applied Polymer Science*, 112: 1695-1703.

81. He H, Fu R, Shen Y, Han Y, Song X (2007). Preparation and properties of Si_3N_4/PS composites used for electronic packaging. *Composites Science and Technology*, 67: 2493–2499.

82. An Q, Qi S, Zhou W (2009). Thermal, electrical, and mechanical properties of Si_3N_4 filled LLDPE composite. *Polymer Composites*, 30: 866-871.

83. Anjana PS, Deepu V, Uma S, Mohanan P, Philip J, Sebastian MT (2010). Dielectric, thermal, and mechanical properties of CeO_2-filled HDPE composites for microwave substrate applications. *Journal of Polymer Science: Part B: Polymer Physics*, 48: 998–1008.

84. Ozmihci FO, Balkose D (2013). Effects of particle size and electrical resistivity of filler on mechanical, electrical, and thermal properties of linear low density polyethylene–zinc oxide composites. *Journal of Applied Polymer Science*, 130: 2734-2743.

85. Weidenfeller B, Hofer M, Schilling F (2002). Thermal and electrical properties of magnetite filled polymers. *Composites Part A: Applied Science and Manufacturing*, 33: 1041–1053.

86. Subodh G, Manjusha MV, Philip J, Sebastian MT (2008). Thermal properties of polytetrafluoroethylene/$Sr_2Ce_2Ti_5O_{16}$ polymer/ceramic composites. *Journal of Applied Polymer Science*, 108: 1716–1721.

87. Thomas S, Deepu V, Uma S, Mohanan P, Philip J, Sebastian MT (2009). Preparation, characterization and properties of $Sm_2Si_2O_7$ loaded polymer composites for microelectronic applications. *Materials Science and Engineering B*, 163: 67–75.

88. Tekce HS, Kumlutas D and Tavman IH (2004). Determination of the Thermal Properties of Polyamide-6 (Nylon-6)/Copper Composite by Hot Disk Method. *In Proceedings of the 10th Denizli Material Symposium*: 296–304.

89. Boudenne A, Ibos L, Fois M, Majeste JC, Gehin E (2005). Electrical and thermal behaiviour of polypropylene filled with copper particle. *Composite Part A: Applied Science and Manufacturing*, 36: 1545-1554.

90. Zhou W, Wang C, Ai T, Wu K, Zhao F, Gu H (2009). A novel fiber-reinforced polyethylene composite with added silicon nitride particles for enhanced thermal conductivity. *Composite Part A: Applied Science and Manufacturing*, 40: 830–836.

91. Weidenfeller B, Hofer M, Schilling FR (2004). Thermal conductivity, thermal diffusivity, and specific heat capacity of particle filled polypropylene. *Journal of Composites Part A: Applied Science and Manufacturing*, 35: 423–429.

92. Jiajun W, Su YX (2004). Effects of interfacial thermal barrier resistance and particle shape and size on the thermal conductivity of AlN/PI composites. *Composites Science and Technology*, 64: 1623–1628.

93. Glavchev I, Petrova K, Ivanova M (2002). Determination of the coefficient of thermal expansion of epoxy composites. *Polymer Testing*, 21: 177–179.

94. Tognana S, Salgueiro W, Somoza A, Pomarico JA, Ranea-Sandoval HF (2009). Influence of the filler content on the thermal expansion behavior of an epoxy matrix particulate composite. *Materials Science and Engineering: B*, 157: 26–31.

95. González-Benito J, Castillo E, Caldito JF (2013). Coefficient of thermal expansion of TiO2 filled EVA based nanocomposites. A new insight about the influence of filler particle size in composites. *European Polymer Journal*, 49: 1747–1752.

96. Yasmin A, Daniel IM (2004). Mechanical and thermal properties of graphite platelet/epoxy composites. *Polymer*, 45: 8211-8219.

97. Grohens Y, Brogly M, Labbe C, David MO, Schultz J (1998). Glass transition of stereoregular poly(methyl methacrylate) at interfaces. *Langmuir*, 14: 2929-2932.

98. Cai D, Song M (2009). A simple route to enhance the interface between graphite oxide nanoplatelets and a semicyrstalline polymer for stress transfer. *Nanotechnology*, 20: 3157081–3157086.

99. Ramanathan T, Abdala AA. Stankovich S, Dikin DA, Herrera-Alonso M, Piner RD, Adamson DH, Schniepp HC, Chen X, Ruoff RS, Nguyen ST, Aksay IA, Prud'Homme RK, Brinson LC (2008). Functionalized graphene sheets for polymer nanocomposites. *Nature Nanotechnology*, 3: 327-331.

100. Rimdusit S, Punson K, Dueramae I, Somwangthanaroj A, Tiptipakorn S (2011). Rheological and thermomechanical characterizations of fumed silica-filled polybenzoxazine nanocomposites. *Engineering Journal*, 15: 27-38.

101. Barabanova AI, Philippova OE, Askadskii AA, Khokhlov AR (2012). Transparent epoxy/silica nanocomposites with increased glass transition temperatures. *Procedia Chemistry*, 4: 352–359.

102. Meng G (2009). Investigations of novel high dielectric materials and new mechanisms. A dissertation submitted in partial fulfillment of the requirements for the degree of Doctor of Philosophy (Chemistry) in The University of Michigan.

103. Yung KC, Zhu BL, Yue TM, Xie CS (2010). Development of epoxy-matrix composite with both high-thermal conductivity and low-dilectric constant via hybrid filler systems. *Journal of Applied Polymer Science*, 116: 518-527.

104. O'Connor KA, Curry RD (2011). High dielectric constant composites for high power antennas. *IEEE Pulsed Power Conference*: 212 – 217.

105. Choudhury A (2009). Polyaniline/silver nanocomposites: Dielectric properties and ethanol vapour sensitivity. *Sensors and Actuators B: Chemical*, 138: 318–325.

106. Habeeb MA (2013). Effect of nanosilver particles on thermal and dielectric properties of (PVA-PVP) films. *International Journal of Applied and Natural Sciences*, 2: 103-108.

107. Rao Y, Wong CP (2002). Ultra high dielectric constant epoxy silver composite for embedded capacitor application.*52nd IEEE Electronic Components and Technology Conference*: 920 – 923.

108. Huang X, Jiang P, Xie L (2009). Ferroelectric polymer/silver nanocomposites with high dielectric constant and high thermal conductivity. *Applied Physics Letters*, 95: 242901-242903.

109. Zhou W, Zuo J, Ren W (2012). Thermal conductivity and dielectric properties of Al/PVDF composites. *Composites Part A: Applied Science and Manufacturing*, 43: 658–664.

110. Xu J, Moon KS, Tison C, Wong CP (2006). A novel aluminium filled composite dielectric for embedded passive applications. *IEEE Transactions on Advanced Packaging Conference*, 29: 295-306.

111. Zhou W, Yu D (2011). Effect of coupling agents on the dielectric properties of aluminium particles reinforced epoxy resin composites. *Journal of Composite Materials*, DOI: 10.1177/0021998310394694.

112. Sonoda K, Teirikangas M, Juuti J, Moriya Y, Jantunen H (2011). Effect of surface modification on dielectric and magnetic properties of metal powder/polymer nanocomposites. *Journal of Magnetism and Magnetic Materials*, 323: 2281–2286.

113. Saleh BAA, Ramadin Y, Zihlif AM, Elimat ZM (2014). Optical and electrical properties of polystyrene composites containing ultrafine iron particles. *Journal of Thermoplastic Composite Materials*, DOI: 10.1177/0892705714526914.

114. He F, Fan J, Lau S (2008). Thermal, mechanical, and dielectric properties of graphite reinforced poly(vinylidene fluoride) composites. *Polymer Testing*, 27: 964–970.

115. Li YC, Tjong SC, Li RKY (2010). Electrical conductivity and dielectric response of poly(vinylidene fluoride)/graphite nanoplatelet composites. *Synthetic Metals*, 160: 1912–1919.

116. Mdarhri A, Brosseau C, Zaghrioui M, Aboud IE (2012). Electronic conduction and microstructure in polymer composites filled with carbonaceous particles. *Journal of Applied Physics*, 112: 3411801-3411813.

117. Xu HP, Dang ZM, Jiang MJ, Yao SH Bai J (2008). Enhanced dielectric properties and positive temperature coefficient effect in the binary polymer composites with surface modified carbon black. *Journal of Material Chemistry*, 18: 229–234.

118. Ramajo L, Reboredo M, Castro M (2005). Dielectric response and relaxation phenomena in composites of epoxy resin with $BaTiO_3$ particles. *Composite Part A: Applied Science and Manufacturing*, 36: 1267–1274.

119. Kuo DH, Chang CC, Su TY, Wang WK, Lin BY (2004). Dielectric properties of three ceramic/epoxy composites. *Materials Chemistry and Physics*, 85: 201-206.

120. Lam KH, Chan HLW, Luo HS, Yin QR, Yin ZW, Chiy CL (2003). Dielectric properties of 65PMN-35PT/P(VDF–TrFE) 0-3 composites. *Microelectronic Engineering*, 66: 792-797.

121. Dong LJ, Xiong CX, Quan HY, Zhao G (2006). Polyvinyl-butyral/lead zirconate titanates composites with high dielectric constant and low dielectric loss. *Scripta Materialia*, 55: 835-837.

122. Yoon JR, Han JW, Lee KM, Lee HY (2009). Dielectric properties of polymer-ceramic composites for embedded capacitors. *Transactions on Electrical and Electronic Materials*, 10: 116-120.

123. Araújo MC, Costa CM, Lanceros-Méndez S (2014). Evaluation of dielectric models for ceramic/polymer composites: Effect of filler size and concentration. *Journal of Non-Crystalline Solids*, 387: 6–15.

124. Kemaloglu S, Ozkoc G, Aytac A (2010). Properties of thermally conductive micro and nano size boron nitride reinforced silicon rubber composites. Thermochimica Acta, 499: 40–47.

125. Zeng X, Yu S, Sun R (2013). Thermal behavior and dielectric property analysis of boron nitride-filled bismaleimide-triazine resin composites. *Journal of Applied Polymer Science*,128: 1353–1359.

126. Gonon P, Sylvestre A, Teysseyre J, Prior C (2001). Dielectric properties of epoxy/silica composites used for microlectronic packaging, and their dependence on post-curing. *Journal of Materials Science: Materials in Electronics*, 12: 81-86.

127. Kumlutas D, Tavman IH (2006). A numerical and experimental study on thermal conductivity of particle filled polymer composites. *Journal of Thermoplastic Composite Materials*, 19: 441-454.

128. Progelhof RC, Throne JL, Ruetsch RR (1976). Methods for predicting the thermal conductivity of composite systems: a review. *Polymer Engineering and Science*, 16: 615-625.

129. Maxwell JC (1954). A treatise on electricity and magnetism. *3rd edition, Dover, New York*: 263-269.

130. Rayleigh JW (1892). On the influence of obstacle arranged in rectangular order upon the properties of a medium. *Philosophical Magazine Series 5*, 34: 481-502.

131. Fricke H (1924). A mathematical treatment of the electric conductivity and capacity of disperse systems I. The electrical conductivity of a suspension of homogeneous spheroids. Physical Review, 24: 575-587.

132. Bruggeman DAG (1935). Calculation of various physics constants in heterogeneous substance I. Dielectricity constants and conductivity of mixed bodies from isotropic substance. *Annalen der Physik*, 416: 636-664.

133. Kanari KD (1977), Kai Nippon Dennetu Sinpojiumu Ronbuns, 14; 208-210.

134. Loeb AJ (1954). Thermal conductivity: VIII, a theory of thermal conductivity of porous materials. *Journal of the American Ceramics Society*, 37: 96-99.

135. Jefferson JB, Witzell OW, Sibitt WL (1958). Thermal conductivity of graphite-silicone oil and graphite-water suspensions. *Industrial & Engineering Chemistry Research*, 50: 1589-1592.

136. Ratcliffe EH (1968). Estimation of effective thermal conductivity of two-phase media. Journal of Applied Chemistry, 18: 25-30.

137. Progelhof RC, Throne JL (1975), Cooling of structural foam, *Journal of Cellular Plastics*, 11: 152-163.

138. Tsao GTN (1961). Thermal conductivity of two phase materials. *Industrial & Engineering Chemistry Research*, 53: 395-397.

139. Cheng S, Vachon R (1970). A technique for predicting the thermal conductivity of suspensions: emulsions and porous materials. International Journal of Heat & Mass Transfer, 13: 537–542.

140. Russell HW (1935). Principles of heat flow in porous insulators. *Journal of the American Ceramic Society*, 18: 1-5.

141. Lewis T, Nielsen L (1970). Dynamic mechanical properties of particulate-filled composites. *Journal of Applied Polymer Science*, 14: 1449-1471.

142. Agari Y, Uno T (1986). Estimation on thermal conductivities of filled polymers. *Journal of Applied Polymer Science*, 32: 5705-5712.

143. Hamilton R, Crosser O (1962). Thermal conductivity of heterogeneous two-component system. *Industrial Engineering Chemical and Fundamentals*, 1: 187-191.

144. Zehner P, Schlunder EU (1970). Thermal conductivity of granular materials at moderate temperatures. *Chemie Ingenieur Technik*, 42: 933-941.

145. Woodside W, Messner JH (1961). Thermal conductivity of porous media. I. Unconsolidated sands. *Journal of Applied Physics*, 32: 1688–1706.

146. Katz HS, Milewski JV (1987). Handbook of fillers for plastics. *Van Nostrand Reinhold, New York*: 59-60.

147. Beneto JG, Castillo E, Caldito JF (2013). Coefficient of thermal expansion of TiO_2 filled EVA based nanocomposites. A new insight about the influence of filler particle size in composites. *European Polymer Journal*, 49: 1747-1752.

148. Sun L, Kwon P (2009). ZrW_2O_8/ZrO_2 composites by in situ synthesis of ZrO_2 + WO_3: Processing, coefficient of thermal expansion, and theoretical model prediction. *Material Science and Engineering: A*, 527: 93-97.

149. Turner PS (1946). Thermal expansion stresses in reinforced plastics.*Journal of Research (National Bureau of Standards)*, 37: 239-250.

150. Kerner EH (1956). The elastic and thermo-elastic properties of composite media. *Proceeding of Physical Society Section B*, 69: 808–813.

151. Shunmugasamy VC, Pinisetty D, Gupta N (2012). Thermal expansion behavior of hollow glass particle /vinyl ester composites. *Journal of Materials Science*, 47: 5596-5604.

152. Nji J, Li G (2008). A CaO enhanced rubberized syntactic foam. *Composites Part A: Applied Science and Manufacturing*, 39: 1404-1411.

153. Gupta N, Ye R, Porfiri M (2010). Comparison of tensile and compressive characteristics of vinyl ester/glass microballoon syntactic foams. *Composites Part B: Engineering*, 41: 236-245.

154. Hashim Z, Shtrikman S (1962). A variational approach to the theory of effective magnetic permeability of multiphase materials. *Journal of Applied Physics*, 33: 3125-3131.

155. Rosen BW, Hashin Z (1970). Effective thermal expansion coefficients and specific heats of composite materials. *International Journal of Engineering Science*, 8: 157–173.

156. Levin VM (1967). Thermal Expansion Coefficient of Heterogeneous Materials. *Mechanics of Solids*, 2: 58-61.

157. Mori T, Tanaka K (1973). Average stress in matrix and average elastic energy of materials with misfitting inclusions.*Acta Metallurgica*, 21: 571-574.

158. Vo HT, Todd M, Shi FG, Shapiro AA, Edwards M (2001). Towards model-based engineering of under®ll materials: CTE modeling. *Microelectronics Journal*, 32: 331-338.

159. Chen XG, Guo JD, Zheng B, Li YQ, Fu SY, He GH (2007). Investigation of thermal expansion of PI/SiO2 composite films by CCD imaging technique from −120 to 200 °C. Composite Science and Technology, 67: 3006–3013.

160. Maxwell-Garnett JC (1904). Colours in metal glasses and in metallic films. *Philosophical Transactions of the Royal Society London A: Mathematical, Physical and Engineering Science*, 203: 385-420.

161. Skipetrov SE (1999). Effective dielectric functions of a random medium. *Physical Review B: condensed matter and materials physics,* 60: 12705-12709.

162. Goncharenko AV, Lozovski VZ, Venger EF (2000). Lichtenecker's equation: applicability and limitations. *Optics communications*, 174: 19-32.

163. Nan CW (2001). Comment on "Effective dielectric function of a random medium".*Physical Review B: condensed matter and materials physics*, 63: 1762011- 1762013.

164. Kerner EH (1956). The electrical conductivity of composite media. *Proceedings of the Physical Society of London*, B69: 802-807.

165. Tinga WR, Voss WAG, Blossey DF (1973). Generalized approach to multiphase dielectric mixture theory. *Journal of Applied Physics*, 44: 3897–3902.

166. Jayasundere N, Smith BV (1993). Dielectric constant for binary piezoelectric 0-3 composites. *Journal of Applied Physics,* 73: 2462-2467.

167. Poon YM, Shin FG (2004). A simple explicit formula for the effective dielectric constant of binary 0-3 composites. *Journal of Materials Science*, 39: 1277-1281.

168. Pal R (2007), On the Electrical Conductivity of Particulate Composites. *Journal of Composite Material*, 41: 2499-2511.

169. Yamada T, Ueda T, Kitayama T (1982). Piezoelectricity of a high-content lead zirconate titanate/polymer composite. *Journal of Applied Physics*, 53: 4328–4332.

170. Yomezava F, Cohen MH (1983). Granular effective medium approximation. *Journal of applied physics*, 54: 2895-2899.

171. Ahmad Z, Prasad A, Prasad K (2009). A comparative approach to predicting effective dielectric, piezoelectric and elastic properties of PZT/PVDF composites. *Physica B: Condensed Matter*, 404: 3637–3644.

172. Razzaq MY, Frormann L (2007). Thermomechanical studies of aluminum nitride filled shape memory polymer composites. *Polymer composites*, 28: 287–293.

173. Ling W, Gu A, Liang G, Yuan Li, Liu J (2010). Dynamic mechanical properties of aluminumnitride/cyanate ester composites for high performance electronic packaging. *Polymers Advanced Technologies*, 21: 365–370.

174. Yung KC, Zhu BL, Wu J, Yue TM, Xie CS (2007). Effect of AlN content on the performance of brominated epoxy resin for printed circuit board substrate. *Journal of Polymer Science Part B: Polymer Physics*, 45: 1662–1674.

175. Wu SY, Huang YL, Ma CCM, Yuen SM, Teng CC, Yang SY (2011). Mechanical, thermal and electrical properties of aluminum nitride/polyetherimide composites. *Composites: Part A: Applied Science and Manufacturing*, 42: 1573–1583.

176. Zhang J, Qi S (2013). Mechanical, thermal and dielectric properties of aluminum nitride/epoxy resin composites. *Journal of Elastomers & Plastics*, DOI: 10.1177/0095244313516887.

177. Yu S, Hing P, Hu X (2002). Thermal conductivity of polystyrene-aluminium nitride composite. *Composites: Part A: Applied Science and Manufacturing*, 33: 289-292.

178. Lee ES, Lee SM, Shanefield DJ, Cannon WR (2008). Enhanced thermal conductivity of polymer matrix composite via high solids loading of aluminum nitride in epoxy resin. *Journal of American Ceramic Society*, 91: 1169–1174.

179. Xie SH, Zhu BK, Li JB, Wei XZ, Xu ZK (2004). Preparation and properties of polyimide/aluminum nitride composites. *Polymer Testing*, 23: 797–801.

180. Yung KC, Zhu BL, Yue TM, Xie CS (2010). Effect of the filler size and content on the thermomechanical properties of particulate aluminum nitride filled epoxy composites. *Journal of Applied Polymer Science*, 116: 225–236.

181. Wu CC, Chen YC, Yang CF, Su CC, Diao CC (2007). The dielectric properties of epoxy/AlN composites. *Journal of the European Ceramic Society*, 27: 3839–3842.

182. Choudhury M, Mohanty S, Nayak SK, Aphale R (2012). Preparation and characterization of electrically and thermally conductive polymeric nanocomposites. *Journal of Minerals and Materials Characterization and Engineering*, 11: 744-756.

183. Zhou Y, Wang H, Wang L, Yu K, Lin Z, He L, Bai Y (2012). Fabrication and characterization of aluminum nitride polymer matrix composites with high thermal conductivity and low dielectric constant for electronic packaging. *Materials Science and Engineering B*, 177: 892– 896.

184. Peng W, Huang X, Yu J, Jiang P, Liu W (2010). Electrical and thermophysical properties of epoxy/aluminum nitride nanocomposites: Effects of nanoparticle surface modification. *Composites Part A: Applied Science and Manufacturing*, 41: 1201–1209.

185. Zhou W (2011). Thermal and dielectric properties of the AlN particles reinforced linear low-density polyethylene composites. *Thermochimica Acta*, 512: 183–188.

186. Zhou Y, Yao Y, Chen CY, Moon K, Wang H, & Wong CP (2014). The use of polyimide-modified aluminum nitride fillers in AlN@PI/Epoxy composites with enhanced thermal conductivity for electronic encapsulation. Scientific reports, 4: 4779-4783.

187. Yu H, Li L, Kido T, Xi G, Xu G, Guo F (2012). Thermal and insulating properties of epoxy/aluminum nitride composites used for thermal interface material. *Journal of Applied Polymer Science*, 124: 669–677.

188. Tilbrook MT, Moon RJ, Hoffman M (2005).On the mechanical properties of alumina–epoxy composites with an interpenetrating network structure. *Materials Science and Engineering A*, 393: 170–178.

189. Goyal RK, Tiwari AN, Mulik UP, Negi YS (2007). Dynamic mechanical properties of Al_2O_3/Poly(ether ether ketone) composites. *Journal of Applied Polymer Science*, 104: 568–575.

190. Jiang W, Jin FL, Park SJ (2012).Thermo-mechanical behaviors of epoxy resins reinforced with nano-Al_2O_3 particles. *Journal of Industrial and Engineering Chemistry*, 18: 594–596.

191. Wetzel B, Haupert F, Zhang MQ (2003). Epoxy nanocomposites with high mechanical and tribological performance. *Composites Science and Technology*, 63: 2055–2067.

192. Landel RF, Nielsen LE (1993). Mechanical properties of polymers and composites. *2nd Edition, Marcel Dekker, New York*: 131–232.

193. Schwartz CJ, Bahadur S (2000). Studies on the tribological behavior and transfer film–counterface bond strength for polyphenylene sulfide filled with nanoscale alumina particles.*Wear*, 237: 261–273.

194. Sawyer WG, Freudenberg KD, Bhimaraj P, Schadler LS (2003). A study on the friction and wear behavior of PTFE filled with alumina nanoparticles. *Wear*, 254: 573–580.

195. Xiang D, Li K, Shu W, Xu Z (2007). On the tribological properties of PTFE filled with alumina nanoparticles and graphite. *Journal of Reinforced Plastics and Composites*, 26: 331-339.

196. Wang Y, Lim S, Luo JL, Xu ZH (2006). Tribological and corrosion behaviours of Al_2O_3 /polymer nanocomposite coatings. *Wear*, 260: 976-983.

197. Tilbrook MT, Rutgers L, Moon RJ, Hoffman M (2007). Fatigue crack propagation resistance in homogeneous and graded alumina–epoxy composites. *International Journal of Fatigue*, 29: 158–167.

198. Zhao S, Schadler LS, Hillborg H, Auletta T (2008). Improvements and mechanisms of fracture and fatigue properties of well-dispersed alumina/epoxy nanocomposites. *Composites Science and Technology*, 68: 2976–2982.

199. Wetzel B, Rosso P, Haupert F, Friedrich K (2006). Epoxy nanocomposites – fracture and toughening mechanisms. *Engineering Fracture Mechanics*, 73: 2375–2398.

200. Lim SH, Zeng KY, He CB (2010). Morphology, tensile and fracture characteristics of epoxy-alumina nanocomposites. *Materials Science and Engineering A*, 527: 5670–5676.

201. Burris DL, Sawyer WG (2006). Improved wear resistance in alumina-PTFE nanocomposites with irregular shaped nanoparticles. *Wear*, 260: 915–918.

202. Guo Z, Pereira T, Choi O, Wang Y, Hahn HT (2006). Surface functionalized alumina nanoparticle filled polymeric nanocomposites with enhanced mechanical properties. *Journal of Materials Chemistry*. 2006, 16: 2800-2808.

203. Jiao W, Liu Y, Qi G (2009). Studies on mechanical properties of epoxy composites filled with the grafted particles PGMA/Al_2O_3. *Composites Science and Technology*, 69: 391–395.

204. Ji QL, Zhang MQ, Rong MZ, Wetzel B, Friedrich K (2004). Tribological properties of surface modified nano-alumina/epoxy composites. *Journal of Materials Science*, 39: 6487-6493.

205. Moreira DC, Sphaier LA, Reis JML, Nunes LCS (2011). Experimental investigation of heat conduction in polyester–Al2O3 and polyester–CuO nanocomposites. *Experimental Thermal and Fluid Science*, 35: 1458–1462.

206. Kozako M, Okazaki Y, Hikita M, Tanaka T (2010). Preparation and evaluation of epoxy composite insulating materials toward high thermal conductivity. *10th IEEE International Conference on Solid Dielectrics*, Potsdam, Germany,1-4.

207. McGrath LM, Parnas RS, King SH, Schroeder JL, Fischer DA, Lenhart JL (2008). Investigation of the thermal, mechanical, and fracture properties of alumina/epoxy composites. *Polymer*, 49: 999-1014.

208. Ash BJ, Schadler LS, Siegel RW (2002). Glass transition behavior of alumina /polymethylmethacrylate nanocomposites.*Materials Letters*, 55: 83–87.

209. Zhang C, Mason R, Stevens GC (2008). Dielectric Properties of Alumina-Polymer Nanocomposites. *IEEE Conference on Dielectrics and Electrical Insulation*, 15: 12-23.

210. Sugumaran CP (2014). Experimental investigation on dielectric and thermal characteristics of nanosized alumina filler added polyimide enamel. Journal of Electrical Engineering & Technology, 9: 978-983.

211. Liang JZ, Li RKY, Tjong SC (1997). Morphology and tensile properties of glass bead filled low density polyethylene composites. *Polymer Testing*, 16: 529–548.

212. Hasselman DPH, Fulrath RM (1966). Proposed fracture theory of a dispersion strengthened glass matrix. *Journal of the American Ceramic Society*, 49: 68-72.

213. Broutman LJ, Sahu S (1971). The effect of interfacial bonding on the toughness of glass filled polymers. *Materials Science and Engineering*, 8: 98-107.

214. Sahu S, Broutman LJ (1972). Mechanical properties of particulate composites. *Polymer Engineering and Science*, 12: 91-100.

215. Nicolais L, Drioli E, Landelt RF (1973). Mechanical behaviour and permeability of ABS/glass bead composites. *Polymer*, 14: 21-26.

216. Mallick PK, Broutman LJ (1975). Mechanical and fracture behaviour of glass bead filled epoxy composites. *Materials Science and Engineering*, 18: 63-73.

217. Ramsteiner F, Theysohn R (1984). On the tensile behaviour of filled composites. *Composites*, 15: 121-128.

218. Liang JZ, Li RKY (1999). Brittle–ductile transition in polypropylene filled with glass beads. *Polymer*, 40: 3191–3195.

219. Lee J, Yee AF (2001). Inorganic particle toughening I: micro-mechanical deformations in the fracture of glass bead filled epoxies. *Polymer*. 42: 577–588.

220. Lee J, Yee AF (2001). Inorganic particle toughening II: toughening mechanisms of glass bead filled epoxies. *Polymer*, 42: 589–597.

221. Chung H, Das S (2006). Processing and properties of glass bead particulate-filled functionally graded Nylon-11 composites produced by selective laser sintering. *Materials Science and Engineering A*, 437: 226–234.

222. Faulkner DL, Schmid LR (1977). Glass bead-filled polypropylene-1.rheological and mechanical properties. *Polymer Engineering & Science*, 17: 657-665.

223. Liang JZ, Li RKY (1998). Mechanical properties and morphology of glass bead-filled polypropylene composites. Polymer Composites, 19: 698-703.

224. Almeida JRM (1999). An analysis of the effect of the diameters of glass microspheres on the mechanical behavior of glass-microsphere/epoxy-matrix composites. *Composites Science and Technology*, 59: 2087-2091.

225. Liang JZ, RKY Li (2000). Effect of filler content and surface treatment on the tensile properties of glass-bead-filled polypropylene composites. *Polymer International*, 49: 170-174.

226. Li RKY, Liang JZ, Tjong SC (1998). Morphology and dynamic mechanical properties of glass beads filled low density polyethylene composites. Journal of Materials Processing Technology, 79: 59–65.

227. Liang JZ, Li RKY, Tjong SC (2000). Effects of glass bead size and content on viscoelasticity of filled polypropylene composites. *Polymer Testing*, 19: 213–220.

228. Xie XL, Tang CY, Zhou XP, Li RKY, Yu ZZ, Zhang QX, Mai YW (2004). Enhanced interfacial adhesion between PPO and glass beads in composites by surface modification of glass Beads via In Situ Polymerization and Copolymerization. *Chemistry of Materials*, 16: 133–138.

229. Sanchez-Soto M, Gordillo A, Maspoch MLL, Velasco JI, Santana OO, Martinez AB (2002). Glass bead filled polystyrene composites: morphology and fracture. *Polymer Bulletin*, 47: 587-594.

230. Hashemi S, Din KJ, Low P (1996). Fracture behavior of glass bead filled poly(oxymethylene) injection moldings. *Polymer Engineering and Science*, 36: 1807-1820.

231. Lim TTS (1977).Capillary extrusion of composite materials. *Polymer Engineering and Science*, 11: 240-246.

232. Lepez O, Choplin L, Tanguy PA (1990). Thermorheological analysis of glass beads-filled polymer melts. Polymer Engineering and Science, 30: 821-828.

233. Lu S, Zhu X, Qi Z, Xu H (1995). The role of creep damage in glass bead filled high density polyethylene. *Journal of Material Science Letters*, 14: 1458-1463.

234. Mishra D, Satapathy A, Paitnaik A (2012). Processing and thermal conductivity characterization of solid glass micro-sphere filled polymer composites. *Advanced Materials Research*, 445: 526-529.

235. Gupta G, Satapathy A (2014). Processing, characterization, and erosion wear characteristics of borosilicate glass microspheres filled epoxy composites. *Polymer Composites*, DOI 10.1002/pc.23079.

236. Nijenhuis K, Addink R, Van der Vegt AK (1989). A study on composites of Nylon-6 with hollow glass microspheres. *Polymer Bulletin*, 21: 467-474.

237. Ashton-Patton MM, Hall MM, Shelby JE (2006). Formation of low density polyethylene/hollow glass microspheres composites. *Journal of Non-Crystalline Solids*, 352: 615–619.

238. Liang JZ (2002). Tensile and impact properties of hollow glass bead-filled PVC composites. *Macromolecular Materials and Engineering*, 287: 588–591.

239. Liang JZ (2005). Tensile and flexural properties of hollow glass bead-filled ABS composites. *Journal of Elastomers and Plastics*, 37: 361–370.

240. Gupta N, Woldesenbet E, Kishore (2002). Compressive fracture features of syntactic foams-microscopic examination. *Journal of Material Science*, 37: 3199–3209.

241. Park SJ, Jin FL, Lee C (2005). Preparation and physical properties of hollow glass microspheres-reinforced epoxy matrix resins. *Material Science and Engineering A*, 402: 335-340.

242. Porfiri M, Gupta N (2009). Effect of volume fraction and wall thickness on the elastic properties of hollow particle filled composites. *Composites Part B: Engineering*, 40: 166–173.

243. Poveda R, Gupta N, Porfiri M (2010). Poisson's ratio of hollow particle filled composites. *Materials Letters*, 64: 2360–2362.

244. Yung KC, Zhu BL, Yue TM, Xie CS (2009). Preparation and properties of hollow glass microsphere filled epoxy-matrix composites. *Composites Science and Technology*, 69: 260-264.

245. Tagliavia G, Porfiri M, Gupta N (2010). Analysis of flexural properties of hollow-particle filled composites. *Composites Part B: Engineering*, 41: 86–93.

246. Patankar SN, Kranov YA (2010). Hollow glass microsphere HDPE composites for low energy sustainability. *Materials Science and Engineering A*, 527: 1361–1366.

247. Mutua FN, Lin P, Koech JK, Wang Y (2012). Surface Modification of Hollow Glass Microspheres. *Materials Sciences and Applications*, 3: 856-860.

248. Li J, Luo X, Lin X (2013). Preparation and characterization of hollow glass microsphere reinforced poly(butylene succinate) composites. *Materials and Design*, 46: 902–909.

249. Liang JZ (2014). Estimation of thermal conductivity for polypropylene/hollow glass bead composites. *Composites Part B: Engineering*, 56: 431–434.

250. Zhu BL, Zheng H, Wang J, Ma J, Wu J, Wu R (2014). Tailoring of thermal and dielectric properties of LDPE-matrix composites by the volume fraction, density, and surface modification of hollow glass microsphere filler. *Composites Part B: Engineering*, 58: 91–102.

251. Biswas S, Satapathy A, Patnaik A (2010). Erosion wear behaviour of polymer composites: a review. *Journal of Reinforced Plastics and Composites*, DOI: 10.1177/0731684408097786.

252. Gutans J, Tamuzs V (1987). Strength probability of unidirectional hybrid composite. *Theoretical and Applied Fracture Mechanics*, 7: 193-200.

253. Yao LN, Chou TW (1989). Analysis of hybrid effect in unidirectional composites under longitudinal compression. *Composite Structures*, 12: 27-37.

254. Hong J, Park DW, Shim SE (2010). A Review on Thermal Conductivity of Polymer Composites Using Carbon-Based Fillers: Carbon Nanotubes and Carbon Fibers. *Carbon Letters*, 11: 347-356.

255. Greef ND, Gorbatikh L, Godara A, Mezzo L, Lomov SV, Verpoest I (2011). The effect of carbon nanotubes on the damage development of carbon fiber/epoxy composites. *Carbon*, 49: 4650-4664.

256. Díez-Pascual AM, Naffakh M, Marco C, Gómez-Fatou MA, Ellis GJ (2014). Multiscale fiber-reinforced thermoplastic composites incorporating carbon nanotubes: A review. *Current Opinion in Solid State and Materials Science*, 18: 62-80.

257. Summerscales J, Short D (1978). Carbon fibre and glass fibre hybrid reinforced plastics. *Composites*, 9: 157-166.

258. Sonparote PW, Lakkad SC (1982). Mechanical properties of carbon/glass fibre reinforced hybrids. *Fibre Science and Technology*, 16: 309-312.

259. Godara A, Gorbatikh L, Kalinka G, Warrier A, Rochez O, Mezzo L, Luizi F, VanVuure AW, Lomov SV, Verpoest I (2010). Interfacial shear strength of a glass fibre/epoxy bonding in composites modified with carbon nanotubes. *Composites Science and Technology*, 70: 1346-1352.

260. Warrier A, Godara A, Rochez O, Mezzo L, Luizi F, Gorbatikh L, Lomov SV, VanVuure AW, Verpoest I (2010). The effect of adding carbon nanotubes to glass/epoxy composites in the fibre sizing and/or the matrix. *Composites Part A: Applied Science and Manufacturing*, 41: 532-538.

261. Mishnaevsky L, Dai G (2014). Hybrid and hierarchical polymer composites: Computational modelling of structure-properties relationships. *Composite Structures*, DOI: http://dx.doi.org/10.1016/j.compstruct.2014.06.027.

262. Choi S, Im H, Kim J (2012). Flexible and high thermal conductivity thin films based on polymer; aminated multi–walled carbon nanotubes/micro-aluminum nitride hybrid composites. *Composites Part A: Applied Science and Manufacturing*, DOI: http://dx.doi.org/10.1016/j.compositesa.2012.06.009.

263. Drubetski M, Siegmann A, Narkis M (2007). Electrical properties of hybrid carbon black/carbon fiber polypropylene composites. *Journal of Material Science*, 42: 1–8.

264. Panda P, Mantry S, Mohapatra S, Singh SK, Satapathy A (2013). A study on erosive wear analysis of glass fiber-epoxy-AlN hybrid composites. *Journal of Composite Materials*, DOI: 10.1177/0021998312469239.

265. Ng HY, Lu X, Lau SK (2005). Thermal conductivity, electrical resistivity, mechanical, and rheological properties of thermoplastic composites filled with boron nitride and carbon fiber. *Polymer Composites*, 26: 66–73.

266. Ferreira JAM, Capela C, Costa JD (2010).A study of the mechanical behaviour on fibre reinforced hollow microspheres hybrid composites. *Composites Part A: Applied Science and Manufacturing*, 41: 345–352.

267. Lingaraju D, Ramji K, Devi MP, Lakshmi UR (2011). Mechanical and tribological studies of polymer hybrid nanocomposites with nano reinforcements. *Bulletin of Materials Science*, 34, 705–712.

268. Zhang J, Qi S (2014). Mechanical, thermal, and dielectric properties of aluminum nitride/glass Fiber/epoxy resin composites. Polymer Composites, 35: 381–385.

269. Teng CC, Ma CCM, Chiou KC, Lee TM, Shih YF (2011). Synergetic effect of hybrid boron nitride and multi-walled carbon nanotubes on the thermal conductivity of epoxy composites. *Materials Chemistry and Physics*, 126: 722–728.

270. Im H, Kim J (2011). The effect of Al_2O_3 doped multi-walled carbon nanotubes on the thermal conductivity of Al_2O_3/epoxy terminated poly(dimethylsiloxane) composites. *Carbon*, 49: 3503-3511.

271. Patnaik A, Satapathy A, Mahapatra SS, Dash RR (2008). Erosive wear assesment of glass reinforced polyester-flyash composites using Taguchi method. *International Polymer Processing*, 13: 192–199.

272. Biswas S, Satapathy A (2009). Tribo-performance analysis of red mud filled glass-epoxy composites using Taguchi experimental design. *Materials and Design*, 30: 2841–2853.

273. Patnaik A, Satapathy A, Mahapatra SS, Dash RR (2008). Parametric optimization of erosion wears of polyester-GF-alumina hybrid composites using Taguchi method. *Journal of Reinforced Plastics & Composites*, 27: 1039–1058.

274. Leong YW, Ishak ZAM, Ariffin A (2004). Mechanical and thermal properties of talc and calcium carbonate filled polypropylene hybrid composites. *Journal of Applied Polymer Science*, 91: 3327–3336

275. Leong YW, Bakar MBA, Ishak ZAM, Ariffin A (2005). Effects of filler treatments on the mechanical, flow, thermal, and morphological properties of talc and calcium carbonate filled polypropylene hybrid composites. *Journal of Applied Polymer Science*, 98: 413–426.

276. Bakar MBA, Leong YW, Ariffin A, Ishak ZAM (2007). Mechanical, flow, and morphological properties of talc- and kaolin-filled polypropylene hybrid composites. *Journal of Applied Polymer Science*, 104: 434–441.

277. Nurdina AK, Mariatti M, Samayamutthirian P (2011). Effect of filler surface treatment on mechanical properties and thermal properties of single and hybrid filler–filled pp composites. *Journal Applied Polymer Science*, 120: 857–865.

278. Perrin FX, Nguyen V, Vernet JL (2002). Mechanical properties of polyacrylic–titania hybrids—microhardness studies. *Polymer*, 43: 6159–6167.

279. Al-Khafaji RS (2013).Mechanical and electrical behavior of polymer matrix composite and their hybrids reinforced with (carbon black–boron) particles.*Journal of Al-Nahrain University*, 16: 171-177.

280. Lee GW, Park M, Kim J, Lee JI, Yoon HG (2006). Enhanced thermal conductivity of polymer composites filled with hybrid filler. *Composites Part A: Applied Science and Manufacturing*, 37: 727–734.

281. Sanada K, Tada Y, Shindo Y (2009). Thermal conductivity of polymer composites with close-packed structure of nano and micro fillers. *Composites Part A: Applied Science and Manufacturing*, 40: 724–730.

282. Zhu BL, Ma J, Wu J, Yung KC, Xie CS (2010). Study on the properties of the epoxy-matrix composites filled with thermally conductive AlN and BN ceramic particles. *Journal of Applied Polymer Science*, 118, 2754–2764.

283. Hong JP, Yoon SW, Hwang T, Oh JS, Hong SC, Lee Y, Nam JD (2012). High thermal conductivity epoxy composites with bimodal distribution of aluminum nitride and boron nitride fillers. *Thermochimica Acta*. 537: 70– 75.

284. Ling W, Gu A, Liang G, Yuan L (2010). New composites with high thermal conductivity and low dielectric constant for microelectronic packaging. *Polymer Composites*, 31: 307–313.

285. Choi S, Kim J (2013). Thermal conductivity of epoxy composites with a binary-particle system of aluminum oxide and aluminum nitride fillers. *Composites Part B: Engineering*, 51: 140–147.

286. Sun C (2010). Controlling the rheology of polymers/silica nanocomposites. *PhD thesis, Eindhoven University of Technology, Netherlands*.

287. May CA (1988). Epoxy resins: Chemistry and technology, *2nd edition, Marcel Dekker Inc., New York and Basel*.

288. Lee H, Neville K (1957). Epoxy resins. Their applications and technology, *McGraw-Hill, New York.*

289. Behzadi S, Jones FR (2005). Yielding behavior of model epoxy matrices for fiber reinforced composites: Effect of strain rate and temperature, *Journal of Macromolecular Science, Part B: Physics*, 44: 993-1006.

290. Mishra D (2014). A study on thermal and dielectric characteristics of solid glass microsphere filled epoxy composites. *PhD Thesis*, NIT Rourkela, India.

291. Bigg DM (1986). Thermally conductive polymer compositions. *Polymer Composites*, 7: 125-140.

292. Agag T, Koga T, Takeichi T (2001). Studies on thermal and mechanical properties of polyimide-clay nanocomposites. *Polymer*, 42: 3399-3408.

*****

Appendices

Appendix A1

LIST OF PUBLICATIONS OUT OF THIS WORK

International Journals

1. **Alok Agrawal** and Alok Satapathy (2014), "Thermal and dielectric behaviour of epoxy composites filled with ceramic micro particulates*",* ***Journal of Composite Material,*** 48: 3755-3769.

2. **Alok Agrawal** and Alok Satapathy (2014), "Effects of Aluminium nitride inclusions on thermal and electrical properties of epoxy and polypropylene: An experimental investigation", ***Composite Part A: Applied Science and manufacturing***, 63: 51-58.

3. **Alok Agrawal** and Alok Satapathy (2014), "Thermal and dielectric behaviour of polypropylene composites reinforced with ceramic fillers", ***Journal of Materials Science: Materials in Electronics,*** DOI: 10.1007/s10854-014-2370-8.

4. **Alok Agrawal** and Alok Satapathy (2015), **"**Effect of Al_2O_3 addition on thermo-electrical properties of polymer composites: An experimental investigation", ***Polymer Composites,*** 36: 102-112.

5. **Alok Agrawal** and Alok Satapathy (2015), "Mathematical model for evaluating effective thermal conductivity of polymer composites with hybrid fillers", ***International Journal of Thermal Sciences***, DOI: 10.1016/j.ijthermalsci. 2014.11.006.

International Conferences

1. **Alok Agrawal** and Alok Satapathy, "Development of a heat conduction model and investigation on thermal conductivity enhancement of AlN/Epoxy composites", ***International Conference on Engineering***, 06-08th Dec, 2012, Nirma University, Ahmedabad.

2. **Alok Agrawal** and Alok Satapathy, "Development of a theoretical model for effective thermal conductivity of polymer composites filled with hybrid fillers", ***International Conference on Recent Advances in Composite Materials***, 18-21st Feb, 2013, Goa.

3. **Alok Agrawal** and Alok Satapathy, "Improved thermal conductivity of polymer composites filled with al_2o_3 particulates and solid glass microspheres", ***International Conference on Advanced Polymeric Materials***, 01-03rd March, 2013, Lucknow.

4. **Alok Agrawal** and Alok Satapathy, "Epoxy composites filled with micro-sized AlN particles for microelectronic applications", ***International Conference on Powder, Granule and Bulk Solids: Innovations and Applications***, 28-30th November, 2013, Thapar University, Patiala.

5. **Alok Agrawal** and Alok Satapathy, "Epoxy composite filled with micro sized al_2o_3 particles for microelectronic applications", ***International Conference on Functional Materials***, 5-7th Feb, 2014, IIT Kharagpur.

6. **Alok Agrawal** and Alok Satapathy, "An experimental investigation on the effects of multi fillers on thermal conductivity of polymer", ***International Conference on Advancements in Polymeric Materials***, 14-16th Feb, 2014, CIPET Bhubaneswar.

7. **Alok Agrawal** and Alok Satapathy, "Experimental investigation of micro-sized aluminium oxide reinforced epoxy composites for microelectronic applications" ***International Conference on Advances in Manufacturing and Materials Engineering***, 27-29th March, 2014, NIT Surathkal.

8. **Alok Agrawal** and Alok Satapathy, "Computational, analytical and experimental investigation of heat conduction through particulate filled polymer composites", ***International Scientific Conference on Engineering and Applied Science***, 15-17th August, 2014, Singapore.

*****

Appendix A2

Brief bio-data of the author

The author, **Alok Agrawal**, born on 30-03-1985 graduated in Mechanical Engineering from Shri Shankaracharya College of Engineering and Technology, Bhilai, India in the year 2007. He completed his Post-graduate study (M.Tech.) in Mechanical Engineering with specialization in Thermal Engineering from the National Institute of Technology, Rourkela, India in the year 2009. Immediately after completion of M.Tech programme, he joined as an Assistant Professor in the Department of Mechanical Engineering at Ashoka Institute of Technology and Management, Rajnandgaon, India and served for about 8 months. Later, in Febuary 2010, he joined Larsen and Toubro Ltd, Mumbai, India as Post-graduate Engineer Trainee and after a span of one year; he was promoted as Senior Design Engineer and became a core member of Research and Development Department. He joined National Institute of Technology, Rourkela in the year 2012 as an Institute Research Scholar in the Department of Mechanical Engineering.

The author is engaged in active research in the area of polymer matrix composite since January 2012. He has 5 research papers to his credit which have been published in various international journals with SCI index. He has also presented 8 research papers in the area of polymer composites at various international conferences held in India and abroad.

*****